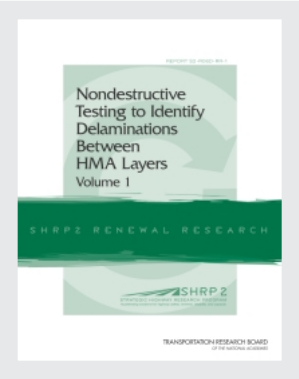

Nondestructive Testing to Identify Delaminations Between HMA Layers, Volume 1 - Summary

DETAILS

58 pages | 8.5 x 11 | PAPERBACK
ISBN 978-0-309-12938-1 | DOI 10.17226/22768

AUTHORS

Heitzman, Michae;l Maser, Kenneth; Tran, Nam H.; Brown, Ray; Bell, Haley; Holland, Steve; Ceylan, Halil; Belli, Kimberly; and Hiltunen, Dennis

The Second
STRATEGIC HIGHWAY RESEARCH PROGRAM

SHRP 2 REPORT S2-R06D-RR-1

Nondestructive Testing to Identify Delaminations Between HMA Layers

Volume 1

MICHAEL HEITZMAN
KENNETH MASER
NAM H. TRAN
RAY BROWN
HALEY BELL
STEVE HOLLAND
HALIL CEYLAN
KIMBERLY BELLI
DENNIS HILTUNEN

National Center for Asphalt Technology at Auburn University
Alabama

TRANSPORTATION RESEARCH BOARD

WASHINGTON, D.C.
2013
www.TRB.org

Subscriber Categories

Construction
Highways
Maintenance and Preservation
Pavements

The Second Strategic Highway Research Program

America's highway system is critical to meeting the mobility and economic needs of local communities, regions, and the nation. Developments in research and technology—such as advanced materials, communications technology, new data collection technologies, and human factors science—offer a new opportunity to improve the safety and reliability of this important national resource. Breakthrough resolution of significant transportation problems, however, requires concentrated resources over a short time frame. Reflecting this need, the second Strategic Highway Research Program (SHRP 2) has an intense, large-scale focus, integrates multiple fields of research and technology, and is fundamentally different from the broad, mission-oriented, discipline-based research programs that have been the mainstay of the highway research industry for half a century.

The need for SHRP 2 was identified in *TRB Special Report 260: Strategic Highway Research: Saving Lives, Reducing Congestion, Improving Quality of Life,* published in 2001 and based on a study sponsored by Congress through the Transportation Equity Act for the 21st Century (TEA-21). SHRP 2, modeled after the first Strategic Highway Research Program, is a focused, time-constrained, management-driven program designed to complement existing highway research programs. SHRP 2 focuses on applied research in four areas: Safety, to prevent or reduce the severity of highway crashes by understanding driver behavior; Renewal, to address the aging infrastructure through rapid design and construction methods that cause minimal disruptions and produce lasting facilities; Reliability, to reduce congestion through incident reduction, management, response, and mitigation; and Capacity, to integrate mobility, economic, environmental, and community needs in the planning and designing of new transportation capacity.

SHRP 2 was authorized in August 2005 as part of the Safe, Accountable, Flexible, Efficient Transportation Equity Act: A Legacy for Users (SAFETEA-LU). The program is managed by the Transportation Research Board (TRB) on behalf of the National Research Council (NRC). SHRP 2 is conducted under a memorandum of understanding among the American Association of State Highway and Transportation Officials (AASHTO), the Federal Highway Administration (FHWA), and the National Academy of Sciences, parent organization of TRB and NRC. The program provides for competitive, merit-based selection of research contractors; independent research project oversight; and dissemination of research results.

SHRP 2 Report S2-R06D-RR-1

ISBN: 978-0-309-12938-1

Library of Congress Control Number: 2013938716

Copyright Information

Note: SHRP 2 report numbers convey the program, focus area, project number, and publication format. Report numbers ending in "w" are published as web documents only.

Notice

The project that is the subject of this report was a part of the second Strategic Highway Research Program, conducted by the Transportation Research Board with the approval of the Governing Board of the National Research Council.

The members of the technical committee selected to monitor this project and review this report were chosen for their special competencies and with regard for appropriate balance. The report was reviewed by the technical committee and accepted for publication according to procedures established and overseen by the Transportation Research Board and approved by the Governing Board of the National Research Council.

The opinions and conclusions expressed or implied in this report are those of the researchers who performed the research and are not necessarily those of the Transportation Research Board, the National Research Council, or the program sponsors.

The Transportation Research Board of the National Academies, the National Research Council, and the sponsors of the second Strategic Highway Research Program do not endorse products or manufacturers. Trade or manufacturers' names appear herein solely because they are considered essential to the object of the report.

SHRP 2 Reports

Available by subscription and through the TRB online bookstore:

www.TRB.org/bookstore

Contact the TRB Business Office:
202-334-3213

More information about SHRP 2:

www.TRB.org/SHRP2

THE NATIONAL ACADEMIES

Advisers to the Nation on Science, Engineering, and Medicine

The **National Academy of Sciences** is a private, nonprofit, self-perpetuating society of distinguished scholars engaged in scientific and engineering research, dedicated to the furtherance of science and technology and to their use for the general welfare. On the authority of the charter granted to it by Congress in 1863, the Academy has a mandate that requires it to advise the federal government on scientific and technical matters. Dr. Ralph J. Cicerone is president of the National Academy of Sciences.

The **National Academy of Engineering** was established in 1964, under the charter of the National Academy of Sciences, as a parallel organization of outstanding engineers. It is autonomous in its administration and in the selection of its members, sharing with the National Academy of Sciences the responsibility for advising the federal government. The National Academy of Engineering also sponsors engineering programs aimed at meeting national needs, encourages education and research, and recognizes the superior achievements of engineers. Dr. Charles M. Vest is president of the National Academy of Engineering.

The **Institute of Medicine** was established in 1970 by the National Academy of Sciences to secure the services of eminent members of appropriate professions in the examination of policy matters pertaining to the health of the public. The Institute acts under the responsibility given to the National Academy of Sciences by its congressional charter to be an adviser to the federal government and, on its own initiative, to identify issues of medical care, research, and education. Dr. Harvey V. Fineberg is president of the Institute of Medicine.

The **National Research Council** was organized by the National Academy of Sciences in 1916 to associate the broad community of science and technology with the Academy's purposes of furthering knowledge and advising the federal government. Functioning in accordance with general policies determined by the Academy, the Council has become the principal operating agency of both the National Academy of Sciences and the National Academy of Engineering in providing services to the government, the public, and the scientific and engineering communities. The Council is administered jointly by both Academies and the Institute of Medicine. Dr. Ralph J. Cicerone and Dr. Charles M. Vest are chair and vice chair, respectively, of the National Research Council.

The **Transportation Research Board** is one of six major divisions of the National Research Council. The mission of the Transportation Research Board is to provide leadership in transportation innovation and progress through research and information exchange, conducted within a setting that is objective, interdisciplinary, and multimodal. The Board's varied activities annually engage about 7,000 engineers, scientists, and other transportation researchers and practitioners from the public and private sectors and academia, all of whom contribute their expertise in the public interest. The program is supported by state transportation departments, federal agencies including the component administrations of the U.S. Department of Transportation, and other organizations and individuals interested in the development of transportation. **www.TRB.org**

www.national-academies.org

SHRP 2 STAFF

Ann M. Brach, *Director*
Stephen J. Andrle, *Deputy Director*
Neil J. Pedersen, *Deputy Director, Implementation and Communications*
James Bryant, *Senior Program Officer, Renewal*
Kenneth Campbell, *Chief Program Officer, Safety*
JoAnn Coleman, *Senior Program Assistant, Capacity and Reliability*
Eduardo Cusicanqui, *Financial Officer*
Walter Diewald, *Senior Program Officer, Safety*
Jerry DiMaggio, *Implementation Coordinator*
Shantia Douglas, *Senior Financial Assistant*
Charles Fay, *Senior Program Officer, Safety*
Carol Ford, *Senior Program Assistant, Renewal and Safety*
Elizabeth Forney, *Assistant Editor*
Jo Allen Gause, *Senior Program Officer, Capacity*
Rosalind Gomes, *Accounting/Financial Assistant*
Abdelmename Hedhli, *Visiting Professional*
James Hedlund, *Special Consultant, Safety Coordination*
Alyssa Hernandez, *Reports Coordinator*
Ralph Hessian, *Special Consultant, Capacity and Reliability*
Andy Horosko, *Special Consultant, Safety Field Data Collection*
William Hyman, *Senior Program Officer, Reliability*
Michael Marazzi, *Senior Editorial Assistant*
Linda Mason, *Communications Officer*
Reena Mathews, *Senior Program Officer, Capacity and Reliability*
Matthew Miller, *Program Officer, Capacity and Reliability*
Michael Miller, *Senior Program Assistant, Capacity and Reliability*
David Plazak, *Senior Program Officer, Capacity*
Onno Tool, *Visiting Professional*
Dean Trackman, *Managing Editor*
Connie Woldu, *Administrative Coordinator*
Patrick Zelinski, *Communications/Media Associate*

ACKNOWLEDGMENTS

This work was sponsored by the Federal Highway Administration in cooperation with the American Association of State Highway and Transportation Officials. It was conducted in the second Strategic Highway Research Program, which is administered by the Transportation Research Board of the National Academies. The project was managed by Dr. Monica Starnes, Senior Program Officer for SHRP 2 Renewal.

The team recognizes the technical input of the research team's expert panel. In addition to providing the team with valuable comments, the highway agency team members assisted with identification and support of field evaluation sites. The members of the expert panel are Jim Musselman, the Florida Department of Transportation (DOT); Kim Willoughby, the Washington State DOT; Andrew Gisi, the Kansas DOT; Nadarajah Sivaneswaran, FHWA; John Harvey, University of California, Davis; and Harold Von Quintus, Applied Research Associates.

The team recognizes the support of the NDT technology firms that expended their own resources to provide NDT equipment and software to the study. The companies that supported the project were Geophysical Survey Systems, Inc.; MALA AB; 3d-Radar (a Curtiss-Wright Company); Geomedia Research and Development; Olson Instruments, Inc. and Olson Engineering Inc.; and Infrared Cameras, Inc. The study could not have been completed without their generous assistance.

The team especially recognizes the efforts of the hardware and software development staffs of 3d-Radar and Olson Instruments, Inc., for improving the capabilities of their NDT technologies to meet the needs of highway agencies.

FOREWORD

Monica A. Starnes, PhD, *Senior Program Officer, Renewal*

Asphalt pavements with delamination problems experience considerable early damage because delaminations provide paths for moisture damage and the development of damage such as stripping, slippage cracks, and pavement deformation. Early detection of the existence, extent, and depth of delaminations in asphalt pavements is key for determining the appropriate rehabilitation strategy and thus extending the life of the given pavement.

This report presents the findings of the first two phases of SHRP 2 Renewal Project R06D, Nondestructive Testing to Identify Delaminations Between HMA Layers. The main objective of the project was to develop nondestructive testing (NDT) techniques capable of detecting and quantifying delaminations in HMA pavements. The NDT techniques should be applicable to construction, project design, and network-level assessments.

During Phase 1 of the project, the research team evaluated NDT methods that could potentially detect the most typical delaminations in asphalt pavements. Both laboratory and field testing were conducted during this task. Based on the findings from this testing, the manufacturers of two promising technologies conducted further development of their products to meet the goals of this project in Phase 2. The two technologies advanced in this research were ground-penetrating radar (GPR) and impact echo/spectral analysis of surface waves (IE/SASW).

Additionally, the project developed guidelines and piloted both NDT technologies in collaboration with highway agencies. Once completed, the results from this additional scope of work will be published as an addendum to this report.

CONTENTS

Online version of this report: www.trb.org/Main/Blurbs/167281.aspx.

Executive Summary

The report of this study is divided into five volumes. Volume 1 is a comprehensive summary of the study. Volumes 2 through 5 provide more detailed technical information and are web-only.

Introduction

Several types of pavement surface distress can be attributed to delamination between hot-mix asphalt (HMA) layers. Longitudinal cracking in the wheel path and tearing in the surface are two common types of visual distress that are caused by delamination between layers. HMA delamination is primarily due to layer debonding or stripping. Debonding occurs when there is improper tack between paved HMA layers or between an HMA overlay and concrete pavement. Stripping develops when the aggregates and asphalt binder are incompatible, adhesion is lost, and water separates the asphalt binder from the aggregate. These conditions that cause pavement distress cannot be detected by visual inspection of the pavement, particularly in the early stages of the problem. The distress—cracking or tearing—are the first indicators that delamination may be occurring within the pavement layers.

Agencies that maintain a roadway network need a test method to detect the location and severity of delamination before the pavement deficiency causes visual pavement distress. The test method should be applicable to network-level pavement condition assessment, project-level design investigation to select the correct rehabilitation strategy, and construction quality assurance.

Coring is often used to measure the depth, type, and severity of delamination after the visual distress appears. This test method is destructive and is not suitable for effective evaluation of long lengths of pavement. Nondestructive testing (NDT) methods are needed to identify the presence, location (depth and area), and severity of delamination in a rapid, effective manner.

The objectives of this second Strategic Highway Research Program (SHRP 2) study were to determine which NDT technologies could detect delamination and further to develop the most promising methods to accomplish construction, project design, and network-level evaluations. NDT technology for construction quality assurance should have the ability to detect debonding after placement of an HMA lift. NDT technology for project-level investigation should have the ability to provide a detailed identification of the location and severity of delamination. NDT technology for network-level assessment should have the ability to detect the presence of delamination with the test equipment operating full-lane width at safe vehicle speed.

The focus of the study was to find NDT technologies that could detect the two most common causes of delamination: loss of bond and stripping. The criteria for evaluating each technology focused heavily on the ability to detect delamination, but also emphasized depth of detection, equipment availability, speed of data collection, and simplicity of data analysis. The review of literature identified four existing NDT technologies with the potential to measure loss of bond

or stripping. Ground-penetrating radar (GPR) is an established technology for finding subsurface features and is commonly used for identifying anomalies in the base and subgrade and for measuring pavement layer thickness. Infrared (IR) imaging, the second technology, is a relatively new measurement method for pavement applications and can require long periods of time to observe differences in the rate of pavement surface temperature change. The third NDT technology is a group of methods that measure mechanical waves as they travel through material from a point source impact. The final NDT technology includes devices that measure pavement surface deflection from a large dynamic mechanical load.

Findings

Each NDT technology bases its measurement on scientific principals relating the measured response to material properties. Theoretical modeling was used to predict the response for debonding and stripping in the HMA pavement. The modeling demonstrated how each test method would respond, in theory, and what aspects of the pavement were key measurements. For example, the falling weight deflectometer (FWD) model, also used for backcalculation for FWD test data, showed that the amount of pavement deflection changed as the depth of delamination changed but was not a linear relationship.

NDT vendors for each of the four technologies brought their devices to the National Center for Asphalt Technology (NCAT) Pavement Test Track and the NCAT laboratory to evaluate the equipment's potential to detect delamination under controlled conditions. The controlled conditions included ten 25-ft pavement sections constructed at the NCAT Pavement Test Track and two pavement slabs (8 ft by 4 ft by 8 in. thick) brought into the NCAT laboratory. Measurements were performed under warm-dry pavement conditions and under cool-wet pavement conditions. Each NDT device exhibited some strengths and weaknesses relative to its ability to meet the objective of the study. In general terms, NDT identifies where there is a discontinuity in the response of the pavement materials. The type of discontinuity, such as delamination or stripping, is interpreted from the NDT measurements. The list below provides a summary of the NDT technologies examined or dropped from the study. The paragraphs that follow highlight the findings for each technology.

- GPR (single antenna, single frequency)—dropped from this study;
- GPR (antenna array, frequency sweep)—developed during this study;
- IR thermography (all types)—dropped from this study;
- Mechanical wave technology [impact echo (IE)]—developed during this study;
- Mechanical wave technology [spectral analysis of surface waves (SASW)]—developed during this study;
- Mechanical wave technology [multiple impact of surface waves (MISW)]—dropped from this study;
- Mechanical deflection (FWD)—dropped from this study; and
- Mechanical deflection (lightweight deflectometer [LWD])—dropped from this study.

Three GPR vendors brought in equipment for evaluation. Their devices varied by radar frequency, number of antennae, and system operation. Three observations resulted: First, GPR technology was easily able to identify moderate and severe stripping in the pavement sections but could not detect the debonded areas unless the debonded zone contained moisture. Second, a multiple GPR antenna array that could measure across at least one-half of the pavement lane width in a single pass at speeds up to 40 mph was available. These units have a significant advantage over single-antenna systems that must make multiple passes over the pavement to achieve full lane width coverage. Third, the output data was complex. The analysis of GPR data required manual manipulation by a skilled technician to distinguish discontinuities from simple pavement changes. The vendor who demonstrated the best potential to accomplish the study's objective was selected for further NDT development and evaluation.

Two IR thermography devices were evaluated at the NCAT Pavement Test Track and in the NCAT laboratory. Artificial heating was used in the laboratory to raise the temperature of the test slabs. The degree of change in thermal response from HMA caused by delamination was so small that this technology could not practically identify the delamination within the boundaries of the objective of the study. IR-imaging NDT technology was dropped from further evaluation.

Two mechanical wave NDT vendors brought equipment to the NCAT for evaluation. In this study, two specific technologies showed promise: IE and SASW. In general, IE identified discontinuities in the pavement that were deeper than 4 in. and was most effective when the pavement was cold and the asphalt mixture was stiff. SASW identified discontinuities in the upper 5 to 7 in. of the pavement. The success of SASW testing relies heavily on the spacing between the point load and the receivers. Pavement temperature was less critical for SASW, but knowledge of the material stiffness at the test temperature is a factor in the analysis. Both technologies could find the top of a discontinuity, but neither could measure the material below that depth. This so-called "shadow" characteristic of these NDT tests conforms to the theory of the technology. Most of the commercially available equipment measures a single point and is manually moved to the next point. One device demonstrated the ability to move along a single test line and automatically measure every 6 in. This ability offers a significant improvement in testing speed over static point testing. SASW analysis is more complicated and requires more manual adjustment of each measurement. One vendor demonstrated the best potential to apply both mechanical wave technologies toward the objective and was selected for further NDT development and evaluation.

Two mechanical deflection technologies, the FWD and the LWD, were also evaluated. The FWD sensor array was modified to obtain a more detailed picture of the initial portion of the deflection basin. The LWD device was operated in a standard test configuration. Both devices measured the entire pavement response to a heavy impact load. In theory, the pavement response will exhibit a weaker structure when delamination exists between the layers. The evaluation determined that the deflection measurements from this NDT method were not suited for identifying delamination because the test measured the entire pavement response and could not determine the depth of the weakness. The study also concluded that a deeper evaluation of the test data time series might have merit. Mechanical deflection technology was dropped from further evaluation.

The second phase of the study worked with the two vendors of the most promising NDT equipment to develop their equipment and software further and then evaluate the improved systems under uncontrolled field conditions. The research team worked independently with each vendor to identify and develop hardware and software improvements. The GPR vendor had a lane-width, air-launched antenna array. The hardware improvement focused on modifying the vehicle attachment to reduce the width of the NDT equipment for safe and secure transport between testing sites. The available software processed the raw data into a three-dimensional (3-D) visual array. Software improvements were needed to analyze the processed data array to locate discontinuities in the asphalt pavement automatically. This next-step software development would flag locations in the data where the engineer could examine the GPR measurements in greater detail.

The mechanical wave vendor demonstrated a prototype device that automatically measured the pavement every 6 in. along a longitudinal path. Further development of the hardware focused on increasing the number of devices to measure the lane width in a single pass. Two software challenges needed to be addressed. The first challenge was collecting data from multiple testing devices created by the hardware improvement. The second challenge was automating the data analysis, particularly for SASW measurements. The mechanical wave data are collected as a time series of events. A skilled analyst must isolate the mechanical wave data from signal noise and input the stiffness of the pavement material. This is a time-consuming effort that examines each measurement individually.

The improved NDT equipment was evaluated at multiple sites across the country to place the equipment in realistic situations and measure different types of pavements and materials

that each exhibited unique delamination conditions. The study planned to use sites in Florida, Kansas, Maine, and Washington State. The number of locations was reduced because of weather conditions and equipment availability. The field evaluation included evaluation of GPR in Maine and of both GPR and mechanical wave in Florida and Kansas.

Both NDT vendors demonstrated improvements in their hardware and software at the field evaluations. The GPR antenna was mounted to a column and could be easily pivoted 90° to swing the lane-width device for safe and efficient transport. The GPR software demonstrated a feature that identified significant changes in the measured signal so that the data analyst was given locations to examine. The mechanical wave device was expanded to three sets of hardware to measure three longitudinal paths simultaneously. The software collected the data without any loss of testing speed, but automation of the data analysis was not ready for demonstration.

Conclusions

NDT hardware to measure changes in pavement response is available. GPR technology is the only NDT technology that is capable of testing full lane width and at moderate testing speed. Advances in mechanical wave NDT equipment significantly reduce the testing time but are limited to testing at speeds of less than 5 mph.

Software to analyze the data is available and requires a highly trained technician. The level of automated data analysis must be improved to reduce the manual time required to obtain results.

None of the NDT technologies can conclusively distinguish between types of pavement discontinuities. The measurement identifies a discontinuity, or change, in the pavement condition, but cannot determine from the measurement why the change occurred. GPR, IE, and SASW each use a unique signal measurement that is influenced by the pavement condition. The technician will need to understand how the pavement condition influences the signal. Coring will still be required to confirm the nature of the discontinuity. None of the NDT technologies is capable of identifying partial bond or no bond due to inadequate tack coat during construction.

GPR can identify variations in the pavement, isolate the depth of a discontinuity in the pavement, and provide a relative degree of severity. Severe conditions, such as stripping, can be observed with conventional analysis software. Detecting debonding between asphalt layers with current analysis methodology is possible only when there is moisture trapped in the debonded area between the layers. Software to quantify the extent of discontinuities over a large survey area is needed.

IE can identify variations in the pavement below a depth of 4 in., but confident analysis requires the HMA to be cool and stiff. The measurement has limited ability to provide the degree of severity and cannot measure pavement condition below the top of the discontinuity.

SASW can identify variations in the top 7 in. of the pavement provided that the analysis uses a reasonable value for the stiffness of the pavement. Like IE, the SASW measurement has a limited ability to provide the degree of severity and cannot measure pavement condition below the top of the discontinuity.

GPR, IE, and SASW can be valuable project-level tools used independently or in series. As the NDT industry continues to improve both hardware and software, these NDT tools will become more effective tools for pavement evaluation. For example, data analysis software development is needed to make NDT into a network-level tool for detecting delamination in HMA pavements.

Recommendations

On the basis of the results of this study, the following recommendations can be made. These recommendations are based solely on the NDT technologies available, but should not preclude other innovative approaches as they develop.

1. GPR demonstrated full lane-width testing and impact echo with spectral analysis of surface waves (IE/SASW) improved its lane width capability from a width of 2 ft to a width of 6 ft.

NDT manufacturers should continue to develop their equipment to provide testing hardware that can measure full-lane width. The hardware development must include the ability to narrow the width of the equipment during transport from site to site for the safety of both equipment and other vehicles.

2. GPR and SASW technologies require an extensive amount of manual data analysis. NDT manufacturers should continue to improve the data analysis software with the goal to provide real-time results that would be valuable for project-level and network-level pavement assessment. Software to provide real-time IE results is available.
3. Highway agencies might consider the use of GPR and IE/SASW, or both, for project-level pavement evaluation with the understanding of each NDT technology's capabilities and limitations. If highway agencies expressed an interest in applying NDT for pavement evaluation, the NDT industry would see market potential and continue to develop its equipment. A technical brief for each of these NDT technologies is provided in Appendices A through C.
4. GPR equipment should have an array of antennae and frequency sweep pattern ranging up to 3 GHz. Use GPR without a lane closure to locate discontinuities in a pavement. Operate the GPR equipment at full-lane width at moderate travel speed to perform a preliminary assessment of HMA pavement condition. The results of the GPR analysis will assist the engineer in identifying pavement sections that require more intensive evaluation.
5. IE/SASW equipment can be built as multiple unit pairs in a towing package. Use IE and SASW within a lane closure to locate the depth of pavement discontinuities. This equipment costs less than a lane-width GPR antenna full package costs, but the data collected are also less comprehensive. IE and SASW analysis together can be used to supplement GPR analysis.
6. Highway agencies might consider research funding to support development of software for project-level and network-level analysis.
7. Many highway agencies operate FWD equipment. Research funding should be considered to explore further the use of FWD time history data as an NDT tool for identifying pavement discontinuities.

CHAPTER 1

Background

Problem Statement

A pavement structure consisting of well-constructed HMA layers or HMA overlays on portland cement concrete (PCC) pavement requires a certain degree of bond at the interfaces. It has been shown that the bond between pavement layers and the integrity of each layer are necessary and that, if not present, result in shorter service life due to reduction of the total pavement strength, slippage, top-down cracking, and potential water damage (Van Dam et al. 1987; Ziari and Khabiri 2007; Leng et al. 2008; Tashman et al. 2008).

Discontinuities in HMA pavements resulting from layer debonding or stripping often cause slippage cracking and damage to the structural integrity of the pavement. Debonding occurs when there is inadequate tack between paved HMA layers. Stripping develops when the aggregates and asphalt binder are incompatible and water separates the asphalt binder from the aggregate.

Slippage (Figure 1.1) is a visible indicator of inadequate bonding between an asphalt wearing course and its binder layer in pavements where high horizontal stresses occur. This distress develops in areas where braking, accelerating, or turning wheels move and deform the surface layer of the HMA structure (West, Zhang, and Moore 2005; Romanoschi and Metcalf 2001a). Slippage can be seen on the pavement surface in the form of half-moon-shaped cracks with the ends pointing toward the traffic direction.

Severe damage to the structural integrity of the pavement occurs when two bonded pavement layers lose adhesion and separate. When this occurs, the pavement structure is quickly damaged as cracking propagates through multiple layers of the pavement (Figure 1.2) (Willis and Timm 2007). Researchers have shown that loss of bond could reduce the life of a pavement from 20 years to 7 or 8 years. A 50% reduction in fatigue life might be the result of a 10% decrease in bond strength (West, Zhang, and Moore 2005). Other studies have shown that the fatigue life reduction for a fully debonded pavement could be much more drastic and could prompt the need for repairs such as full-depth patches or complete reconstruction (Romanoschi and Metcalf 2001a, 2001b).

Delamination can propagate more quickly if water is forced along the interface between two layers (Figure 1.3) by hydrostatic pressures imposed through trafficking (Khandal and Rickards 2001).

Debonding between HMA layers typically results from poor construction practices or water damage, or both. Construction miscues, such as mixture segregation and thermal (density) segregation, are common discontinuities in pavement structures that have been linked to delamination. Other construction- or design-related issues, such as paving thin lifts of HMA, improper cleaning of surfaces, excessive or inadequate tack coat, introducing water onto an HMA lift surface, improper compacting of the upper lifts, and using water sensitive aggregate in the old pavement surface, have all been shown to reduce the bond strength of an HMA pavement (Tashman et al. 2008; Mejia et al. 2008; Canestrari et al. 2005).

Discontinuities, like delamination, in HMA pavements are difficult to detect before surface distresses and movements occur. The following conditions are typical indicators of debonding or loss of bond strength between two layers. However, it is difficult to detect these indicators without using NDT equipment.

- There is an increase in the amount of voids at the locations that have been delaminated.
- A higher level of moisture is often present in the delaminated areas.
- Lower density is recorded where the HMA layers are delaminated.
- Stiffness of the pavement material at the delaminated locations is significantly reduced.
- The measured surface deflection is higher in the delaminated areas.

Figure 1.1. Slippage failure due to poor bond between HMA layers.

- The horizontal movement of the surface layer that was delaminated from the underlying layer would be higher under heavy loads.

There are numerous NDT methods available to the highway community to help identify distress and some of the causes, but these methods have typically been applied as a forensic tool for isolated locations where premature distress was already visible. A rapid NDT method is needed to determine the existence, extent, and depth of delaminations or discontinuities during construction, and such a method is needed as part of project-level pavement monitoring. With a rapid NDT method, the appropriate pavement maintenance, repair, or rehabilitation strategy can be considered before the problem expands and affects pavement service and safety.

Source: Willis and Timm 2007.

Figure 1.2. Delamination in an HMA pavement.

Source: Khandal and Rickards 2001.

Figure 1.3. Moisture present at HMA layers interface.

Research Objective and Scope

The main objective of the second Strategic Highway Research Program (SHRP 2) Project R06D was to identify and develop rapid NDT techniques with near 100% continuous coverage that would identify and determine the extent and depth of delaminations and discontinuities in HMA pavements. To achieve this objective, this study examined NDT methods that could identify key indicators commonly associated with potential areas of delamination, including lack of bond, stripping, and segregation. This study focused on NDT technologies with the potential to measure the entire lane width in a single pass at acceptably safe operating speeds.

As recommended by the research team's expert panel, the study focused on evaluating and developing any NDT technologies for construction and postconstruction inspection and pavement forensic study applications that would be capable of identifying and determining the extent and depth of delaminations in HMA pavements. This study expanded the number of technologies investigated but did not eliminate the value of speed and full-width coverage.

The research team recognized the ultimate desire to develop equipment for network-level capability but first needed to determine that each technology could identify delamination in HMA pavements. The research fostered NDT developments by equipment manufacturers to improve the capability of each technology. The study evaluated NDT technologies for fully bonded and unbonded conditions. While degrees of bond existed in real pavements, the research focused on developing equipment that can first identify absolute conditions (i.e., bonded versus unbonded conditions). The research challenged the current state of the technology to develop NDT methods that could effectively determine the existence, extent, and depth of delamination.

CHAPTER 2

Research Approach

The research team for this study was composed of experts in the fields of nondestructive testing (NDT) and hot-mix asphalt (HMA) from multiple organizations. The organizations were the National Center for Asphalt Technology (NCAT); Infrasense, Inc.; the U.S. Army Corps of Engineers Engineering Research and Development Center (ERDC); and the Center for Nondestructive Evaluation. In addition, Infrasense used two NDT consultants from the University of Florida and Northeastern University.

This study was divided into two phases. Phase 1 was intended to identify potential NDT techniques and to prepare research programs for developing and evaluating these techniques. Phase 2 was intended to conduct the research programs and to refine the best candidate NDT technologies.

Phase 1

In the first part of Phase 1, the research team identified and assessed new and existing NDT techniques that would be capable of determining the existence, extent, and depth of delaminations and discontinuities in HMA pavements. Some of those NDT techniques would not have the potential to provide rapid results with near 100% continuous coverage of the pavement area. In addition to assessing the existing NDT methods found in the literature review, the research team also contacted manufacturers of NDT devices to discuss potential development of new or modification of existing NDT techniques for determining the delamination between HMA layers. Invitations were sent to 21 vendors based in the United States and other countries to attend an informational meeting with the research team. During the informational meeting, the research team (a) discussed the research plan and seed money that would be used to encourage the companies to develop or significantly modify the equipment and (b) requested preliminary proposals from the vendors. The research team received six preliminary proposals from the manufacturers. The research team evaluated each vendor's preliminary proposal with a vendor evaluation form (Figure 2.1) in which the evaluation criteria were based on technical, economic, and practical conditions facing highway engineering practitioners. The most important evaluation criterion was the potential of the NDT technique to identify delamination.

After completing the literature review and the evaluation of the preliminary proposals, the research team met with the panel of experts (Table 2.1), who represented the expertise and diversity critical to assist the research team with the task of selecting the most promising NDT techniques for further evaluation. At the meeting, the research team first presented an overview of the SHRP 2 research objective and work plan, a summary of the technologies under consideration, and the criteria developed to evaluate the proposals from interested vendors. Then, the six NDT equipment vendors gave brief presentations on their proposals. After the vendors' presentations, the research team shared the team's evaluation of the vendors' proposals, presented recommendations on which vendor proposals to advance into Phase 2, and shared the outline for the Phase 2 effort. The expert panel provided valuable comments to the research team.

On the basis of results of Phase 1, including the meeting with the expert panel, the following six NDT technologies, consisting of three ground penetrating radars (GPR), two mechanical wave techniques, and two infrared (IR) thermography devices, were selected for further evaluation in Phase 2.

- GPR from Geophysical Survey Systems, Inc. (GSSI), USA
- GPR from MALA AB, Sweden
- GPR from 3d-Radar AS, Norway
- Mechanical wave from Geomedia Research and Development (Geomedia), USA
- Mechanical wave from Olson Instruments, Inc. (Olson), USA
- IR camera from Infrared Cameras, Inc. (ICI), USA
- IR camera from Infrasense, manufactured by FLIR, Worldwide

Vendor: _____ **Evaluator:** Each Research Team Member

ID	Evaluation Factor	Evaluation Level	Comments	Point	Weight
	Key Indicators	Description:		na	na
A	Potential for Identifying Delamination	High (8–10 points) = high potential Medium (5–7 points) = low potential Low (<5 points) = not going to work			40%
B	Potential to Implement	High (8–10 points)= can be implemented immediately Medium (5–7 points) = may be implemented if modified Low (<5 points) = cannot be implemented			5%
	Equipment				
C	Equipment Availability	High (8 to 10 points) = commercially available Medium (5 to 7 points) = modification needed Low (<5 points)= prototype being developed			10%
D	Current Application	High (8 to 10 points)=– used for evaluating asphalt pavements Medium (5 to 7 points) = used for evaluating other pavement types Low (< 5 points) = used for other structures or have not been used			5%
E	Costs (Equipment + Operation)	High (8 to10 points)=– < $50,000 Medium (5 to7 points) = $50,000 ~ $150,000 Low (< 5 points) = > $150,000			5%
	Measurement and Analysis				
F	Speed of Data Collection	High (8 to10 pts) = highway speed greater than 45 mph Medium (5 to7 points) = speed of 5 to 45 mph Low (< 5 points) = speed less than 5 mph, point testing			10%
G	Depth of Effective Applicability	High (8 to10 points) = at least the top 5 in. Medium (5 to7 points) = top 3 in. Low (< 5 points) = top 1 in.			10%
H	Simplicity of Data Analysis	High (8 to10 points) = automated with minimum training Medium (5 to7 points) = automated but requires expertise Low (< 5 points) = manual and requires expertise			10%

Figure 2.1. Vendor evaluation form.

(continued on next page)

I	Results	High (8 to10 points) = detailed location and severity (3-D mapping) Medium (5 to7 points) = detailed location, no severity (basic map) Low (< 5 points) = general presence, no detail (tables)			5%
	Advantages and Limitations				
	Advantages	Description:		na	na
	Limitations	Description:		na	na
	Possible Modification	Description:		na	na

Note: na = not applicable.

Figure 2.1. Vendor evaluation form (continued).

In addition, the expert panel recommended that the research include deflection measurement methods. Therefore, the following two deflection measurement methods were selected for further evaluation in Phase 2. FWD with equipment from NCAT and LWD with equipment from ERDC.

Phase 2

Phase 2 was divided into three primary tasks: controlled evaluation, uncontrolled evaluation, and reporting findings. The first task in Phase 2 evaluated all eight NDT technology vendors and assessed which components of each system needed further development. Each NDT technique was evaluated under controlled laboratory conditions (except for the FWD) and controlled field conditions. The controlled testing was performed under both warm-dry and cold-wet environmental conditions to observe the change (if any) in the NDT measurement. The controlled laboratory evaluation was carried out by using two slabs with built-in delaminated interfaces, and the controlled field evaluation was conducted with test sections built at the NCAT Pavement Test Track to simulate full-scale, real-world pavement conditions.

The first round of controlled testing was conducted under warm and dry environmental conditions. The layout of the delaminated areas for both controlled laboratory and field evaluation sections was withheld from the equipment

Table 2.1. Panel of Experts

Name	Affiliation	Expertise Area
Jim Musselman	the Florida DOT	Pavement material and construction
Kim Willoughby	the Washington State DOT	Pavement material, research, and NDT
Andrew Gisi	the Kansas DOT	Pavement design, geotechnical, and research
Nadarajah Sivaneswaran	Federal Highway Administration	Pavement management, design, and research
John Harvey	University of California, Davis	Pavement design, material, and NDT research
Harold Von Quintus	Applied Research Associates	Pavement design, evaluation, and NDT

Note: DOT = Department of Transportation.

technicians who conducted the testing and analyzed the data. There were no identifying marks on the test slabs or test sections. After evaluating results of the first controlled evaluation, the research team shared the evaluation results with each NDT equipment manufacturer. The team discussed potential refinement of existing NDT hardware and software to improve the device's ability to measure delamination between HMA layers. The second round of controlled evaluation was conducted under cool and wet pavement conditions. The procedure for evaluating each NDT technique was the same as that conducted in the first round of testing. However, the starting location for measurements was changed slightly to alter the location of the delamination during the test and water was injected into the delamination. Plastic standpipes were installed at several locations and filled with water to apply hydrostatic pressure into the delaminated layer interfaces. It was anticipated that the presence of water at the delaminated interfaces would change the GPR's ability to detect the delamination.

At the completion of the controlled evaluations, the research team assessed the controlled testing results and the proposed improvements of hardware and software from the manufacturers to select the most promising NDT methods for further evaluation. The selection criteria were based on technical, economic, and practical conditions facing highway engineering practitioners. The parameters evaluated included the ability to measure the extent and depth of the delaminated area, accuracy, repeatability, area of coverage, speed of data collection, and speed and sophistication of data analysis. The research team also met with the SHRP 2 staff and panel of experts to review the evaluation and selection results. Two NDT techniques, GPR from 3d-Radar and mechanical wave technique from Olson Instruments, Inc., were selected for further refinement and uncontrolled field evaluation later in the study. Seed money was distributed to the two NDT vendors to encourage them to refine the equipment and software.

After the vendors had refined their equipment and analysis software, the uncontrolled field evaluation was conducted to measure the effectiveness of the NDT technologies under field conditions. Each evaluation site included uncontrolled pavement sections that had been identified as having delamination problems. Validation sites were selected in Florida, Kansas, Maine, and Washington State. Cores were extracted from areas identified as delamination by NDT techniques to verify the NDT results.

At the conclusion of Phase 2, all testing results were analyzed and summarized, and two reports were prepared to document the study. This volume summarizes the study and highlights the findings. Volumes 2 through 5 provide more detailed information for readers with specific interests. See Appendix D for a list of the topics in these volumes.

CHAPTER 3

Findings and Applications

Controlled Evaluation of NDT Techniques

Test Slabs and Pavement Sections for Controlled Testing

This chapter provides brief information about the test slabs and pavement sections. More detailed information about the design and construction of the slabs and pavement sections is presented in Volume 3, Chapter 1.

Test Slabs

Figure 3.1 illustrates the design of the delamination conditions of the two test slabs. Two types of delamination—lack of bond and stripping—were simulated at two depths. Three interface treatments were used to achieve bonded and debonded conditions at the interfaces: (a) optimum amount of tack coat to the receiving surface for achieving full bond, (b) baghouse fines from the HMA plant to the receiving surface to achieve no bond, and (c) placement of a separate 1-in.-thick, uncompacted, coarse-fractionated reclaimed asphalt pavement (RAP) to the receiving surface to represent a stripping condition.

To construct the two slabs, a short pavement section was built at the National Center for Asphalt Technology (NCAT) Pavement Test Track. After the construction was completed, the two slabs were cut out of the pavement section. The locations of stripped and debonded interfaces were examined and confirmed. Finally, the two slabs were boarded and transported to the main NCAT laboratory for testing. Extreme care was used to lift and transport the slabs without creating tensile and/or bending stress cracks.

Pavement Sections at NCAT Pavement Test Track

Ten controlled asphalt pavement test sections were built in the inside lane at the NCAT Pavement Test Track for controlled field testing. There was no bond or good bond (control) at the interfaces between dense-graded asphalt layers. The research team ensured the good bond by using a tack coat and bad bond by using bond breakers, including baghouse fines and two layers of heavy kraft paper. A 1-in.-thick, uncompacted, coarse-fractionated RAP material was used to simulate a stripping condition.

The design for the controlled field test sections is illustrated in Figure 3.2. The test sections were designed to simulate 10 different bonded and debonded conditions that represent a majority of situations encountered in the top 5 in. of HMA pavements. Both full-lane-width and partial lane debonding conditions were constructed for evaluating the NDT methods. The partial lane debonding condition included wheel path and two 3-ft by 3-ft squared areas. Each test section was 12 ft wide (full paving width) and 25 ft long. To achieve compaction, the full-lane-width debonded areas were only 10 ft wide. The outer 1 ft on either side of the section was fully bonded to confine the experimental debonded areas for compaction.

The 10 pavement test sections were built in the inside lane adjacent to Section N5 between Stations 0+15 and 2+65 (Figure 3.3). The old pavement section built between these stations was constructed in 2000 with a 24-in.-thick HMA layer on top of a 6-in.-thick aggregate base. Because of deep cracks between Stations 0+50 and 0+75, repairs were done before the construction of the delamination test sections. The asphalt and a portion of the aggregate base layers were milled at the beginning of the old pavement section. For the second half of the experimental section, the old asphalt layer was milled down approximately 6 in. to accommodate leveling and the delamination test sections. After the milling and backfilling work was completed, a 6-in.-thick concrete slab was constructed from Station 0+15 through Station 0+65. Layers of HMA leveling were paved from Station 0+65 through Station 2+65 to prepare the surface for the delamination test sections. The 10 pavement test sections, designed as described

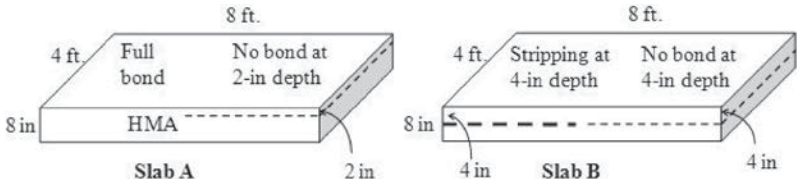

Figure 3.1. Design of two HMA slabs for controlled laboratory evaluation.

in Figure 3.2, were then built on top of the concrete slabs and asphalt leveling course.

Three lessons were learned from the construction of the controlled test sections. First, kraft paper was not strong enough to resist tensile forces generated by HMA paving screed as the screed passed over the paper. A heavier or stronger type of paper should be used for the upper layer. Second, after the RAP is placed, the material should be allowed to soften from solar heating and compacted with one pass of a rubber tire. This tightens the material in place and reduces the potential for the paver screed to move the material ahead. Third, paper was picked up by paver tires. To avoid that problem, the paper should be covered with loose mix ahead of the paver.

After the first round of controlled laboratory and field testing in late October and early November 2009, the research team extracted five cores to verify the interface conditions of the field test sections, as follows:

- Two portions of Core 1 (cut from Section 1) broke at a depth of approximately 5 in. from the pavement surface during coring. This result confirmed that the baghouse fines placed on top of the concrete slab (at a depth of approximately 5 in. from the surface) caused the debonding problem at the interface as anticipated.
- Core 2 was extracted from Section 2 (one of the control sections), and this core showed no signs of delamination as expected.
- Core 3 was extracted from Section 5. An interface of baghouse fines (the debonding material) was observed between the lifts at the 2-in. depth, as expected. The layers did not separate during coring, indicating that some degree of partial bond was present at that location.
- Core 4 was extracted from Section 8. The interface at a depth of approximately 5 in. broke during coring. This interface was delaminated with an approximately 1-in.-thick, uncompacted RAP layer.
- Core 5 was cut from Section 9. The core broke at the 5-in. interface where two layers of brown paper were used as a bond breaker.

In addition, before the second round of controlled laboratory and field testing started, a plastic standpipe was installed

	Section 1	Section 2	Section 3	Section 4	Section 5	Section 6	Section 7	Section 8	Section 9	Section 10
Top 2-in. lift	Full bond	Full bond	Full bond	Partial bond	No bond	Partial stripping	Full bond	Full bond	Full bond	Full bond
Bottom 3-in. lift	No bond	Full bond	Full bond	Full bond	Full bond	Full bond	Full bond	Partial stripping	Partial bond	No bond
Existing surface	PCC	PCC	HMA	HMA	HMA	HMA	HMA	HMA	HMA	HMA

Note: Section 1 contains no bond between 5-in. HMA overlay and PCC pavement. Section 2 contains full bond between 5-in. HMA overlay and PCC pavement (control section). Section 3 contains full bond between 5-in. HMA overlay and HMA pavement (Control Section 1 of 2). Section 4 contains partial bond between 2-in. HMA overlay surface lift and 3-in. HMA overlay leveling lift. Section 5 contains no bond between 2-in. HMA overlay surface lift and 3-in. HMA overlay leveling lift. Section 6 contains simulated stripping in the wheel path between 2-in. HMA surface lift and 3-in. HMA leveling lift. Section 7 contains full bond between 5-in. HMA overlay and HMA pavement (Control Section 2 of 2). Section 8 contains simulated stripping in the wheel path between 3-in. HMA overlay leveling lift and HMA pavement. Section 9 contains partial bond between 3-in. HMA overlay leveling lift and HMA pavement. Section 10 contains no bond between 3-in. HMA overlay leveling lift and HMA pavement.

Figure 3.2. Layout of controlled field test sections.

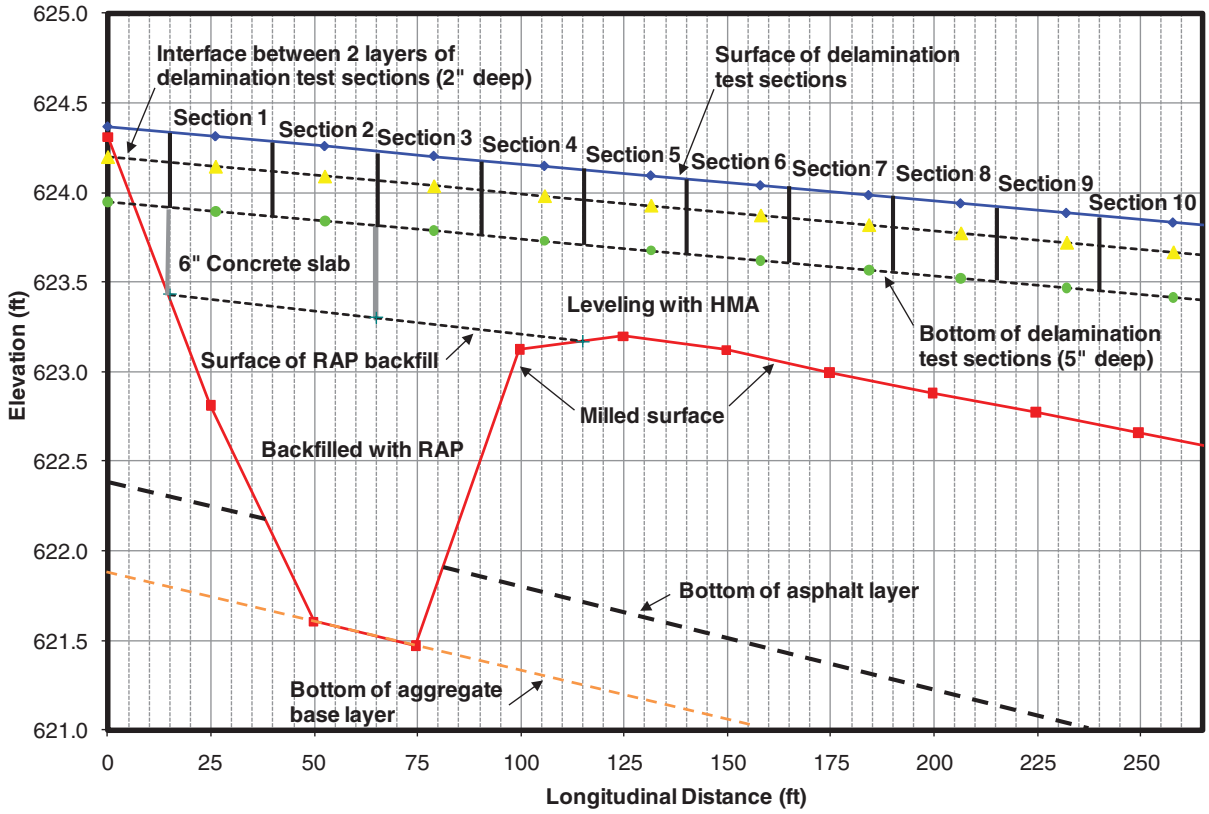

Figure 3.3. Pavement test section profile: Stations 0+00 to 2+65.

at each of the following locations. The pipe was filled with water to apply hydrostatic pressure to inject water into the delaminated layer interfaces. This was done to investigate the NDT's ability to detect the delamination when water was present at the delaminated seams.

- Section 1 at Station 0+15 and 2 ft from the inside edge to inject water into the delaminated interface constructed by using baghouse dust at a depth of approximately 5 in.;
- Section 4 at Station 1+03 and 2 ft from the inside edge to inject water into the bonded interface at a depth of approximately 2 in.;
- Section 5 at Station 1+28 and 2 ft from the inside edge to inject water into the delaminated interface constructed by using baghouse dust at a depth of approximately 2 in.;
- Section 6 at Station 1+46 and 2 ft from the inside edge to inject water into the stripped layer constructed by using RAP at a depth of approximately 2 in.;
- Section 8 at Station 2+03 and 2 ft from the inside edge to inject water into the stripped layer constructed by using RAP at a depth of approximately 5 in.;
- Section 9 at Station 2+28 and 9 ft from the inside edge to inject water into the delaminated interface constructed by using baghouse dust at a depth of approximately 5 in.; and
- Section 10 at Station 2+53 and 7 ft from the inside edge to inject water into the delaminated interface constructed by using baghouse dust at a depth of approximately 5 in.

Ground-Penetrating Radar

Background

Delamination can potentially be identified in radar profiles by the pulse reflected from the delamination boundary, or by the change in the overall transmission characteristics caused by the delamination. In asphalt pavements, if two layers of HMA are well bonded, the only detectable effect in the GPR signal would be caused by the difference in properties between the two layers. When delamination occurs, the damage and water infiltration at the debonded area can produce anomalous reflections beyond those that would normally occur, and the anomalous reflections can potentially be detected with GPR.

GPR can be used at any speed up to normal driving speeds with air-coupled antennae. Lane closures are not required, and traffic is not interrupted. Thus, personnel are not exposed to safety hazards. GPR can detect subsurface anomalies down to 24 in. in HMA with a 1-GHz horn antenna and down to 15 in. with a 2-GHz horn antenna.

Surveys carried out by the Departments of Transportation (DOTs) in Montana and South Dakota showed that the

primary state DOT applications of GPR were for measurement of pavement thickness (ASTM D 4748-06), bridge deck delamination, and depth of reinforcing steel (Maser and Puccinelli 2009; Maser 2005). While the use of GPR for measuring pavement thickness and bridge deck delamination is fairly routine (Hammons et al. 2005; Maser 1999; Scullion and Rmeili 1997; Hammons et al. 2006; Manning and Holt 1987; Maser 2008), GPR has been used only on a case-by-case basis for identifying moisture damage ("stripping") in asphalt pavement (Hammons et al. 2006; Scullion and Rmeili 1997). For example, the Texas A&M Transportation Institute studied the use of GPR to detect stripping in a section of asphalt over concrete. The study showed that GPR was successful in accurately identifying areas where stripping occurred but was not particularly sensitive to severity (Scullion and Rmeili 1997). The Georgia DOT and Applied Research and Associates carried out one study in 2006 with a 1-GHz air-coupled antenna along with infrared thermography (IR), falling weight deflectometer (FWD), and mechanical wave methods. The study found that GPR was not a stand-alone solution but was helpful in focusing the efforts of the more accurate point tests (Manning and Holt 1987).

Theory and Modeling

GPR transmits electromagnetic energy and receives reflections from the pavement layers. Dielectrics of each layer are then determined and can be used to determine the delamination boundary. For example, areas where there is a high dielectric constant indicate the presence of moisture due to water's relatively high dielectric constant of 81 versus typical pavement material constants ranging from 4 to 12. Other contributors to a pavement's varying dielectric constant are the conductivity of the pavement and air void content.

As part of this project, an analytical simulation study was carried out to investigate the ability of GPR systems to detect asphalt pavement delamination. The study investigated an 8-in.-thick pavement radiated by both 1- and 2-GHz antennae. The delamination was modeled as a 1-mm-thick air- or water-filled gap in the asphalt structure, located at depths of 2 and 4 in. from the surface. Later-stage delamination (stripping) was modeled as a 1-in.-thick granular material with higher void ratio and moisture content than would be expected of a properly constructed asphalt mixture. Single monostatic and bistatic antenna configurations were considered in the modeling study.

In all cases, the 2-GHz antenna provided better results than those of the 1-GHz antenna. Both frequencies provided adequate resolution down to the bottom of the pavement (8 in. or 200 mm). Changing the height of the transmission and receiving antenna pair from zero to 0.12 in. (3 mm) above the surface seemed to have little discernible impact on the results. As expected, water-filled delaminations were much more evident in the simulation results than were air-filled delaminations of the same size.

A bistatic move-out simulation showed that a spacing between transmit and receive antennae was often desirable. However, the ideal separation was governed by a variety of factors, including depth of damage and the electromagnetic properties of the materials—both of which affected the angle of reflection. For this reason, an array configuration with a single transmitter and multiple receivers may be beneficial. From the move-out results, it appears that spacing between 100 and 170 mm (3.9 and 6.7 in.) is optimal for detecting delamination. More details are presented in Volume 2, Chapter 1.

Equipment

A typical GPR system consists of an antenna, a control cable, and a data acquisition, control, and display unit. Some GPR systems are able to run multiple antennae simultaneously. The frequency and type of GPR antenna generally control the depth of penetration and the level of detail. Low-frequency antennae (200 to 400 MHz) can penetrate deeper (6 to 8 ft) but do not provide the level of detail required to distinguish pavement layers. Higher-frequency antennae (1 to 3 GHz) provide the pavement layer detail but have penetration limits of 1 to 3 ft. Ground-coupled antennae provide good penetration into the pavement but must be operated at low speeds, while air-coupled horn antennae can collect data at normal driving speeds.

For the pavement delamination application, it is appropriate to focus on high-frequency antennae to obtain the detail required for delamination detection. Also, it is of interest to look at arrays of multiple antennae, so that the full width of the pavement can be investigated and the horizontal extent of delamination can be distinguished. With these objectives in mind, the following equipment systems were considered.

- A 3-GHz "horn antenna" (Figure 3.4a) and a 2.6-GHz "ground-coupled" antenna (Figure 3.4b) provided by GSSI. The GSSI system focused on the implementation of new high-frequency antennae that would have the resolution to detect the small changes associated with pavement delamination. The specific advantage of the horn antenna is that it is noncontact and can be used to survey a pavement at much higher speeds than can a ground-coupled antenna, which requires contact with the pavement. The horn antenna tested as part of this work was a prototype. The ground-coupled antenna is a currently manufactured product.
- A 1.3-GHz ground-coupled antenna array (MIRA) (Figure 3.5a) and a 2.3-GHz ground-coupled antenna (Figure 3.5b) provided by MALA AB. The MIRA system from MALA is a 16-channel array that has the advantage of obtaining greater

(a) (b)

Figure 3.4. GSSI GPR equipment at NCAT Pavement Test Track: (a) prototype 3-GHz horn antenna and (b) 2.6-GHz ground-coupled antenna.

coverage with multiple paths from the array of transmitters and receivers. The MIRA's disadvantage is that it is a ground-coupled system that is deployed at a relatively low (walking) speed, and the antenna frequency (1.3 GHz) is not optimal for delamination detection. To address those concerns, MALA also tested a 2.3-GHz ground-coupled antenna for which a high-speed deployment arrangement was available.

- A swept frequency (150 MHz to 3 GHz) noncontact antenna array provided by 3d-Radar (Figure 3.6). The 3d-Radar system uses a 29-channel array (14 transmitters and 15 receivers) producing 29 channels of data. The system is operated in a swept frequency mode from 150 MHz to 3 GHz, thus producing data over a wide range of depths. The array has the coverage advantages described above for the MIRA system. In addition, the antenna elements are housed in a single unit that operates about 6 to 12 in. above the pavement surface.

Controlled Laboratory and Field Testing

Controlled laboratory and field testing were conducted in two rounds. For the first round of testing, the GSSI and

(a) (b)

Figure 3.5. MALA GPR equipment at NCAT Pavement Test Track: (a) 1.3-GHz ground-coupled antenna array (MIRA) and (b) 2.3-GHz ground-coupled antenna.

(a) (b)

Figure 3.6. 3d-Radar swept frequency (150 MHz to 3 GHz) noncontact array: (a) rear view and (b) side view.

3d-Radar systems were evaluated on November 8–9, 2009, and the MALA system was tested on November 22, 2009. The second round of testing took place on March 7–8, 2010, for all the systems.

The first round of laboratory and field testing was carried out in an "as-is" condition. In the second round of testing, water was introduced into the delaminated areas by using standpipes to see whether the presence of water would affect their detection.

Controlled Laboratory Testing

The three GPR technologies were evaluated in the NCAT laboratory by using two slabs with intact and delaminated interfaces as described previously. More information about the laboratory testing of the GPR technologies is provided in Volume 3, Chapter 2.

The data analysis was presented as "time-depth slices," showing amplitude variations for the multiple antenna data lines within a particular time range (slice). The time slice was converted to a depth slice by using an assumed dielectric constant, which for asphalt is typically between 5 and 6. The depth slices presented by each organization were accompanied by supporting B-scan samples for individual lines of data.

The results of the first and second rounds of testing on Slab A are shown in Figure 3.7. Only the GSSI 3-GHz horn antenna depth slice for Round 1 was able to detect a significant anomaly in the delaminated area. After the water was introduced in Round 2, however, each of the three systems detected an anomaly in this area.

Figure 3.8 shows the results obtained for Slab B. In the results of the first round of testing, both the GSSI and 3d-Radar systems detected an anomaly near the debonded interface at a depth of 4 in. No anomaly was detected in the stripped area. This is surprising because (a) the debonded interface at a depth of 4 in. in Slab B should be harder to detect than the debonded at a depth of 2 in. in Slab A, and (b) the stripped area should be much easier to detect with GPR than the debonded interface. This observation suggested that the property discontinuity at the debonded interface at a depth of 4 in. was more pronounced than one would expect. As with the debonded interface at a depth of 2 in. in Slab A, the detection of the debonded interface at a depth of 4 in. in Slab B was enhanced by introducing moisture.

Controlled Field Testing at NCAT Pavement Test Track

All testing was conducted on the pavement sections with simulated no-bond and good-bond conditions. A brief description of the field evaluation of each GPR technology is presented in this section. More information about the field evaluation of the GPR technologies is presented in Volume 3, Chapter 2.

GSSI tested the 2.6-GHz ground-coupled antenna pair and the prototype 3-GHz horn antenna, and each system was deployed from a survey vehicle as shown in Figure 3.4. The first round of field testing evaluated both systems, but the second round of testing focused on the 3-GHz horn. The tests were carried out by using a series of parallel survey lines spaced initially at 1 to 1.5 ft apart and ultimately at 6 in. apart. Data were collected at rates ranging from 4 to 12 scans/ft. The position of the data was registered by using a distance encoder mounted to the wheel of the test vehicle. Data collection speed ranged from 3 to 5 mph. The 2.6-GHz ground-coupled antenna pair was placed end-to-end on a skid plate, while the horn antenna was suspended about 12 in. above the

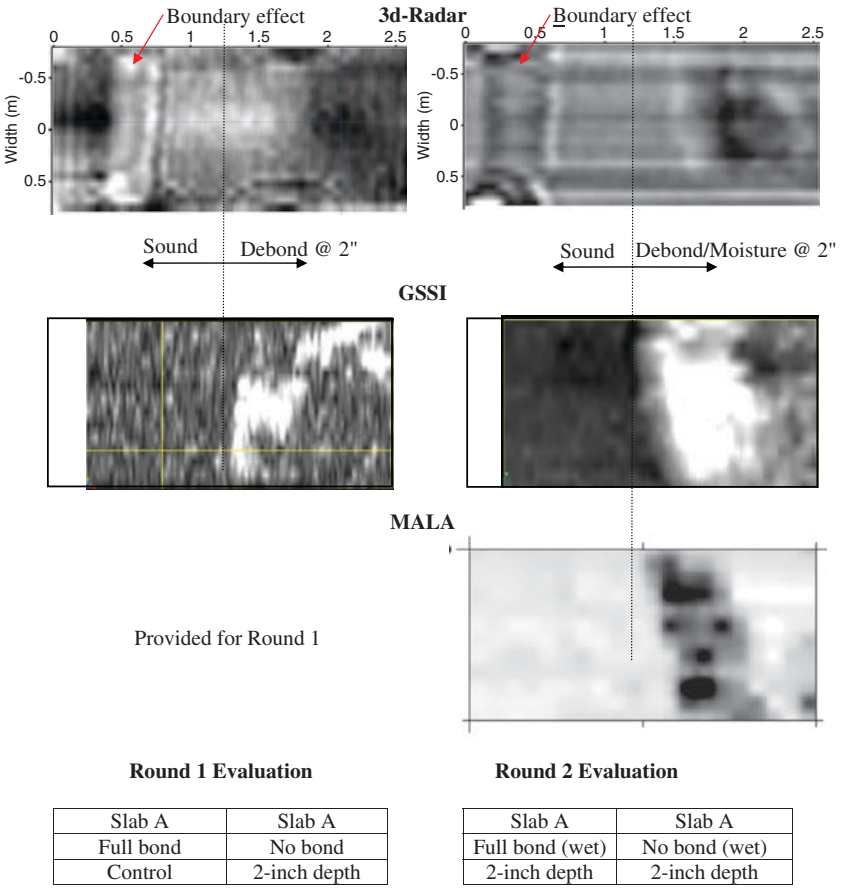

Slab A	Slab A
Full bond	No bond
Control	2-inch depth

Slab A	Slab A
Full bond (wet)	No bond (wet)
2-inch depth	2-inch depth

Figure 3.7. Time-depth slices at 2 to 3 in. for first and second rounds of testing of Slab A.

pavement surface with a wooden support beam. The alignment of the data lines was visually maintained by the vehicle driver by using spacing markers painted on the pavement surface every 100 ft.

For the first round of field testing of the MALA equipment, the conditions were rainy, and the pavement was wet at the test track. Testing included a pair of 2.3-GHz ground-coupled antennae and a 16-channel MIRA system using 1.3 GHz antennae (Figure 3.5). At the test track, the 2.3-GHz antennae were attached end-to-end, and data was collected as a series of parallel survey lines spaced 1 ft apart. The MIRA system (covering about 30 in. in width) covered the full width of the test lane by using six overlapping passes. The MIRA data were collected by using three transmit-receive antenna configurations, including standard (monostatic), end-fire array, and common midpoint (CMP). The MIRA system was deployed by using a wheeled cart, and position of the data was obtained by using a total station. The 2.3-GHz antennae were deployed by using a wheeled cart, and position was recorded with a linear distance encoder. The second round of testing was conducted under more favorable field conditions by using the same antenna systems. However, the 2.3-GHz antenna cart deployed four antennae side-by-side.

In the first round of field testing, 3d-Radar used a 7.5-ft (2.3-m)-wide antenna unit housing 29 antenna elements and producing 29 channels of data. The horizontal coverage of this array was approximately 7.4 ft (2.25 m). The elements produced data by using a swept frequency with a range of 150 MHz to 2.69 GHz. Signal generation and data acquisition were controlled by a unit called the "GeoScope," which was mounted in the bed of the test vehicle. Data location was registered by using a linear distance encoder mounted to one of the antenna support wheels. Three acquisition configurations were evaluated by varying the density of the data in the *x* and *y* directions and the corresponding speed of data collection. Full coverage of the test section was obtained with two overlapping longitudinal runs of the system, one on the left half of the lane and one on the right half. For the second round of testing, 3d-Radar used a smaller, 29-channel unit (Figure 3.6) that had a frequency-sweep range of 140 MHz to 3 GHz and a lateral coverage width of approximately 4.9 ft (1.5 m). The test area was scanned with five parallel overlapping longitudinal runs.

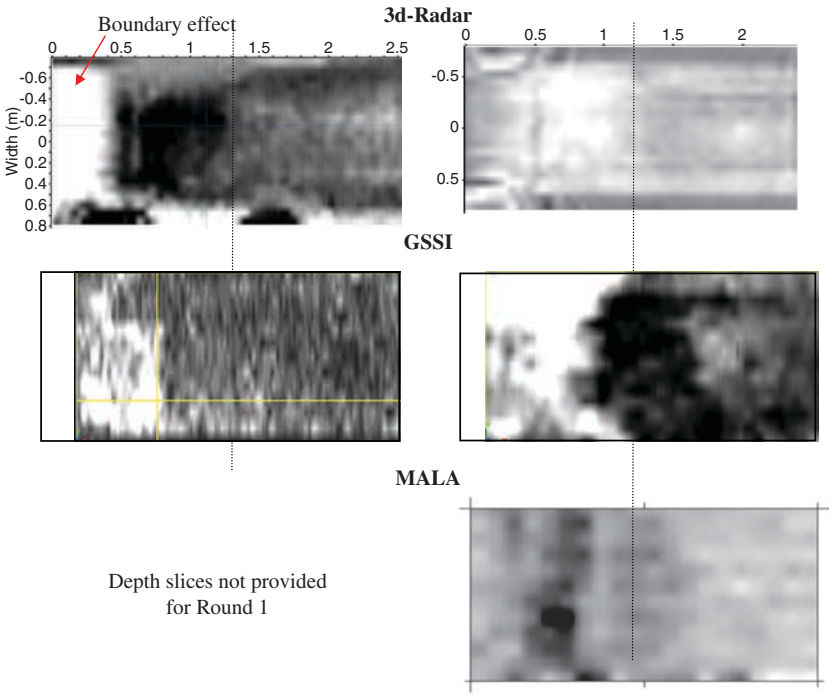

Figure 3.8. Time-depth slices at 4 to 5 in. for first and second rounds of testing of Slab B.

The GPR data for each system were analyzed by using a time-depth slice technique, which is a representation of the reflection activity in a horizontal plane at a particular time and depth interval. Time-depth slice data obtained for each GPR system in Sections 4, 5, 6, and 7 (Figure 3.9) show that all systems were sensitive to the stripping condition located in Section 6, and to the presence of moisture in debonded areas, as noted by the standpipe locations. Other than where moisture was present, the GPR systems are not able to detect the extensive presence of debonding at a depth of 2 in. in Sections 4 and 5.

Time-depth slices for Sections 8, 9, and 10 (Figure 3.10) also show that all systems were able to detect the stripping condition located in Section 8 at a depth of 5 in., as well as the presence of moisture in the debonded areas at a depth of 5 in. in Sections 9 and 10. None of the systems appeared to be capable of detecting the extensive areas of debonding in Sections 9 and 10 when moisture was not present. The 3d-Radar system was tested at three different speeds: 5, 10, and 30 km/h. In order to achieve the higher speeds, the sampling grid was progressively increased in size from 7.5 × 10 cm to 15 × 30 cm. The higher collection speeds provided the same stripping information as did the lower collection speeds, but the detailed boundaries of the damaged areas for higher speeds were less clear.

Infrared Thermography

Background

The use of IR thermography for detecting delamination is based on the disruption in heat flow caused by the delamination. In the presence of a heat source, the disruptions in heat flow lead to temperature differences on the surface, which can be detected by an IR camera. In manufacturing and aerospace industries, the heat source is generally provided by heat lamps or other controllable power sources. For large structures such as bridge decks and pavements, the heat source has generally been solar energy. When the pavement surface is exposed to solar radiation, the temperature above a delaminated interface increases relative to neighboring intact areas as a result of the disruption in vertical heat flow caused by the delamination. In bridge decks, for example, delaminated areas can be as much as 5°C hotter during daytime hours than the surrounding sound areas (Holt and Eckrose 1989). At night, the delaminated interfaces cause the surface above them to dissipate heat faster than the surrounding solid areas, so the surfaces above the interfaces register cooler. These temperature differentials are normally detected by using an IR camera. In order to enable the IR camera to detect the pavement temperature differences, certain environmental conditions

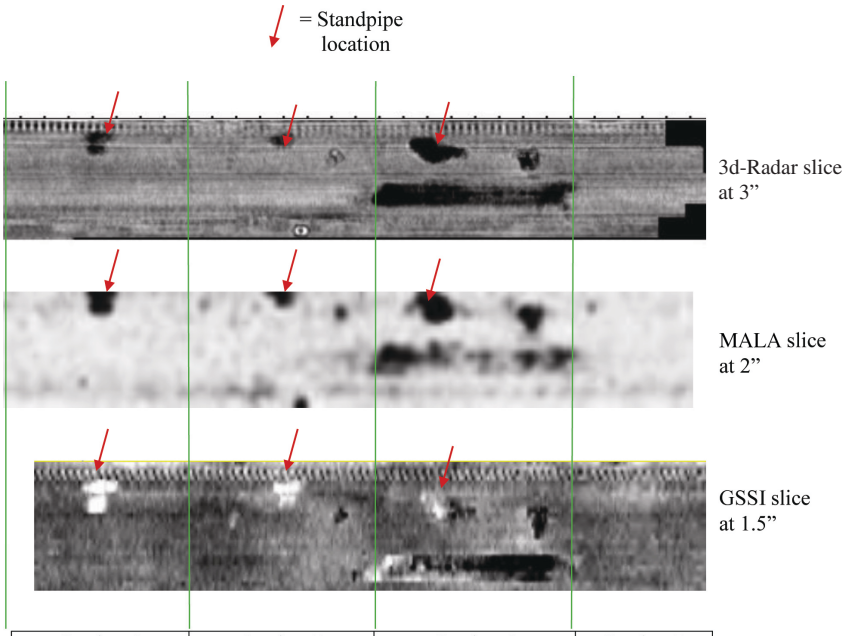

Section 4	Section 5	Section 6	Section 7
Partial bond	No bond	Partial stripping	Full bond
2-inch depth	2-inch depth	2-inch depth	control

Figure 3.9. GPR time-depth slices for Sections 4, 5, 6, and 7.

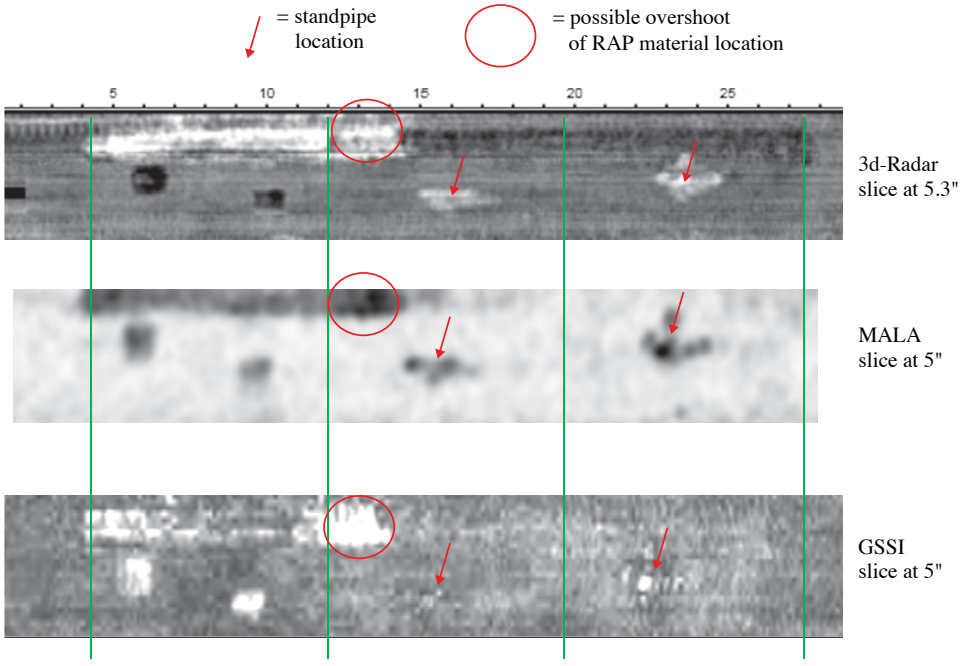

Section 8	Section 9	Section 10
Partial stripping	Partial bond	No bond
5-inch depth	5-inch depth	5-inch depth

Figure 3.10. GPR time-depth slices for Sections 8, 9, and 10.

are required, including a minimum temperature difference of 0.5°C and a wind velocity of less than 30 mph (ASTM D4788-03).

Interpretation of the IR image should be done with some field confirmation data, such as taking cores. Also, the IR data are generally accompanied by a visual image to ensure that the observed anomalies are not related to surface blemishes or stains. Typically, the confirmation testing consists of coring the pavement in locations determined during the IR survey. These locations include both delaminated and sound areas. This procedure will establish what the delaminated areas look like in the IR image. Under favorable conditions for bridge decks, 80% to 90% of the existing delaminations can be detected with the IR camera (Manning and Holt 1987). The main limitation of the IR thermography technique is its lack of ability to determine the exact dimensions (depth and size) of the localized defects.

IR thermography has been used routinely by state highway agencies for detecting delamination bridge decks. This application has been carried out as part of the Wisconsin DOT's statewide deck inspection program, and by the Illinois DOT on a case-by-case basis. The use of IR thermography in HMA pavements has been primarily for detecting segregation in newly placed HMA (Stroup-Gardiner and Brown 2000). In this latter application, the hot asphalt provides the heat source, and segregation produces the detectable temperature changes. This application has been implemented primarily by the Washington State DOT and the Texas DOT. The Washington State DOT uses hand-held IR cameras for quality control to image the newly placed pavement and to locate potential problem areas. The Texas DOT has pursued the use of an array of IR sensors mounted behind the paver to provide feedback on problem areas during the paving process.

Theory and Modeling

The use of IR thermography is based on the detection of surface thermal anomalies associated with subsurface defects. These anomalies develop under the influence of solar heating and cooling. To evaluate the potential effectiveness of this method, thermal models were used to calculate the magnitude of surface thermal anomalies associated with delamination. In the model, solar radiation was modeled as a triangular input radiation pattern from sunrise to sunset, with a maximum value of 800 W/m^2 and with radiational cooling and convection to ambient temperature taking place when there was no sunshine. Two types of solar inputs were considered. The first type was a continuous solar input assuming that the pavement was continuously exposed to the sun. The second type assumed that the solar input was blocked for a period of time.

An 8-in.-thick pavement was modeled, with delamination at a depth of 2 in. The thickness of the delamination was 0.04 in. (1 mm), and the delamination was filled with either air or water. The delamination was considered as either continuous or intermittent. A stripped layer 0.6 in. (15-mm) thick at a depth of 2 in. was also modeled, as both dry and wet. This layer was assigned lower density than the surrounding asphalt and thermal properties associated with its composition.

The results of each analysis were presented as a temperature difference between the delaminated case and the intact case. If this difference exceeds the detectability limits of a typical commercial IR camera, the condition can be detected in the field. On the basis of the results, it appears that the temperature differentials produced by a dry, stripped pavement layer were below the threshold of detectability. On the other hand, the temperature differentials for an air-filled delamination area were up to 3°C, which was within the detectable range. Considering intermittent or partial contact, the maximum temperature differential decreases to half, and the likelihood of detection reduces. Unlike with GPR, the presence of moisture in the delamination or stripped area reduces the detectability with IR thermography. More details of this modeling work are presented in Volume 2, Chapter 2.

Equipment

IR thermography equipment is produced by a number of manufacturers, and numerous models are available for different applications. IR temperature measurements can be made at a point by using spot radiometer, or imaged over an area by using an IR camera. The imaging cameras are most commonly used for IR thermography, since the cameras visually reveal the thermal anomalies of interest. The cost of an IR camera can range from $1,000 to $100,000, depending on the camera's features and capabilities. A typical camera has an array of sensors that emit voltage proportional to incoming IR radiation. The incoming radiation focuses on the array by using a lens, and calibration data are used to convert radiation to temperature. In order to detect the levels of incoming radiation accurately, the detector array must not be sensitive to the internal temperature of the camera. Some cameras are electronically cooled to achieve this purpose, while others do not require cooling. An IR camera can provide a real-time thermal image and record the image in a format similar to a standard video file.

Two IR cameras were made available for this testing: an Infrared Cameras, Inc. (ICI) 7320 camera and a FLIR Systems A40M camera with a wide-angle lens. The ICI 7320 camera has a resolution of 320 × 240 pixels and a frame rate of 30 Hz. The FLIR A40M camera also had the same pixel resolution but a maximum frame rate of 60 Hz. The wide-angle lens was used in conjunction with the FLIR camera so that a full lane width could be captured from a mounting platform about 13 ft above the pavement surface. The ICI camera has a similar wide-angle

lens, but this lens was not available at the time of testing. The primary difference between the two cameras is size. The FLIR camera weighs about 3 lbs and measures 3 in. × 3 in. × 6 in., and the ICI camera is about the size of a pocket digital camera.

Controlled Laboratory Testing

For each test slab, the IR cameras were operated from a ladder to provide sufficient height to allow a complete IR image view of the entire test slab. A series of still IR images were recorded at specified times during the heating/cooling cycle of the test slab. The slabs were heated by using an array of eight high-intensity heat lamps, and the surface and bottom slab temperatures were continuously monitored during the heating process. During the heating process, the area around the heated slab was enclosed to contain the heat.

After the slabs were heated, thermal anomalies are observed on both slab images. For Slab A, one of the anomalies was located in the intact section, and thus was apparently caused by factors other than subsurface delamination (for example, uneven heating). The anomalies in Slab B could be related to the debonding and stripping at 4 in. depth, but the results of Slab A suggest that these anomalies could also be due to other factors. Therefore, the laboratory IR tests were inconclusive. More details of the controlled laboratory testing of IR thermography techniques are presented in Volume 2, Chapter 3.

Controlled Field Testing at the NCAT Pavement Test Track

For controlled field testing, an IR camera mounting and recording system was provided, as shown in Figure 3.11. Testing with this system was carried out continuously for both the FLIR and ICI cameras by using a vehicle speed of approximately 3 mph. During each test, IR images were collected at 1-ft intervals and sequentially stored on the laptop hard drive. Simultaneously, a visual video image was recorded through a digital video recorder. The distance traveled was encoded with a counter and superimposed on the video image using a video overlay device. The first round of IR system tests was carried out on November 8, 2009. Two series of tests were carried out: the first from 1 to 2 p.m. and the second from 3 to 4 p.m. The temperature conditions on the pavement were relatively the same during each series of tests. The weather conditions were sunny with temperatures in the 60°F range.

The second round of controlled field testing was carried out on March 7–8, 2010. One of the objectives of this second series was to explore a larger range of temperatures. During this second round, tests were carried out with ambient temperatures ranging from 34°F to 62°F and with pavement temperatures ranging from 35°F to 105°F.

The IR images from the test track test section were spliced together to produce a single composite strip IR image for the entire test section. One such image was produced for each test. The images were evaluated visually, in conjunction with the visual video data, to identify IR anomalies that could be associated with subsurface debonding, delamination, and stripping.

Figure 3.12 shows an example of the analysis of the IR data. The figure shows a portion of the composite IR image representing Sections 4, 5, 6, and 7 at the test track. The image shows some anomalies in Section 6 in the area where 0.75 in. of RAP was placed 2 in. down from the surface to simulate stripping. However, examination of the surface video shows those anomalies to correspond with surface features

Figure 3.11. Infrared thermography setup for testing at the NCAT Pavement Test Track.

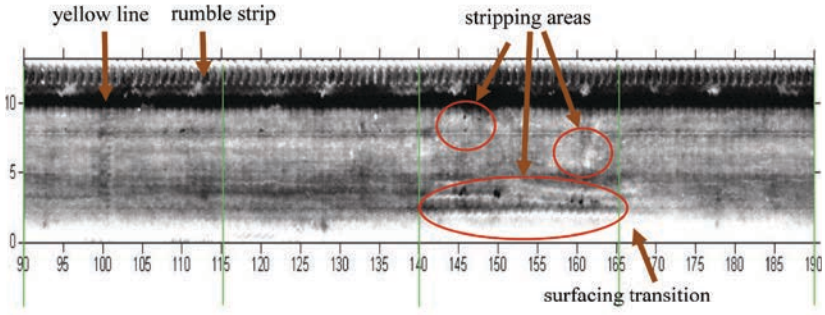

Section 4	Section 5	Section 6	Section 7
Partial bond	No bond	Partial stripping	Full bond
2-inch depth	2-inch depth	2-inch depth	control

Figure 3.12. Infrared strip image of Sections 4 through 7.

and tire marks, rather than subsurface features. In general, the IR image anomalies did not clearly correlate with the known subsurface defects placed in the test sections.

Mechanical Wave Methods

Background

Mechanical energy wave methods are used for determining material properties and detecting defects based on the principles of elastic wave propagation. The methods are conducted by striking the surface of a material, generating elastic waves, and receiving the waves propagating to two or more locations at some distance from the source impact. There are two types of elastic waves: body waves (i.e., P-waves or S-waves) and surface waves (R-waves). Surface waves have higher amplitudes and lower frequencies than do body waves (Mejia et al. 2008).

Two mechanical wave methods—impact-echo (IE) and spectral analysis of surface waves (SASW)—have been used for evaluating bonding condition between HMA layers. More commonly, IE has been used in bridge deck evaluations and pavement evaluations. High-frequency mechanical waves (ultrasound) are used in railroad engineering for detecting small fractures and flaws in rail. IE identifies body-wave reflections in the surface response, and SASW determines the changes in surface wave dispersion characteristics and elastic properties (Mejia et al. 2008).

Theory and Modeling

Munoz (2009) conducted an extensive evaluation of the capabilities of mechanical wave testing methods to characterize pavements containing delaminations. The evaluation utilized finite element simulations and included IE, impulse response, and ultrasonic surface waves (USW) methodologies. The study concluded that (a) IE can detect totally and partially debonded defects and can determine defect depth for depths greater than 4 in. (100 mm), (b) impulse response can detect defects for delamination depths less than 6 in. (150 mm), and (c) USW technology can detect totally debonded defects, but not partially debonded defects and not for depths greater than 4 in. (100 mm).

In a study carried out as part of this project, the use of surface waves with one source and up to 20 receivers was considered. This was an enhancement over SASW, which typically uses only two receivers. The study also used a finite element model, in which the delamination was represented both as a thin layer with low modulus and by an interface element that allowed sliding between layers. Both representations yielded similar results. The study concluded that delaminations are detectable by measuring surface waves and showed how the detectability increased as the delamination became closer to the surface and as the area of the delamination increased. More details of this modeling are presented in Volume 2, Chapter 3.

Equipment Availability

Mechanical wave testing devices from Geomedia and Olson were evaluated by the research team. Geomedia manufactures the portable seismic pavement analyzer (PSPA). Olson manufactures several pavement testing devices, including the scanning IE/SASW device and the multiple impact of surface waves (MISW) device.

The PSPA (Figure 3.13) can automatically conduct both IE and SASW tests simultaneously. SASW tests measure the stiffness, and IE tests measure the thickness of the bound layer. The PSPA is used to estimate the in-situ modulus of asphalt and concrete pavements and determine relevant strength parameters to a depth of 12 in. for use in pavement evaluations. Moduli estimated with the PSPA are low-magnitude, high-frequency values.

The PSPA is operated from a laptop computer connected by a cable to an electronics box that transmits power to the

Figure 3.13. PSPA Testing at NCAT Test Track.

receivers and the source. The source strikes the pavement surface and generates stress waves that are detected by the receivers. The measured signals are returned to the data acquisition board in the computer. The system measures the velocity of the propagated surface wave and computes the material modulus. Testing duration is typically 1 min per test. This duration includes three test replicates at one location.

The scanning IE/SASW device was initially developed for IE testing on concrete bridge decks while being towed behind a truck at a speed of 1 to 2 mph. The system consists of two transducer wheels made of high-density polyethylene with six embedded receiver sensor heads from Olson Instruments around the circumference of each wheel at 6-in. intervals. Each sensor head is paired with a small steel solenoid impactor. The wheels are coupled together with a rubber isolated axle, which provides alignment for SASW testing or misalignment for IE testing. Figure 3.14 shows a photo of the scanning IE/SASW system.

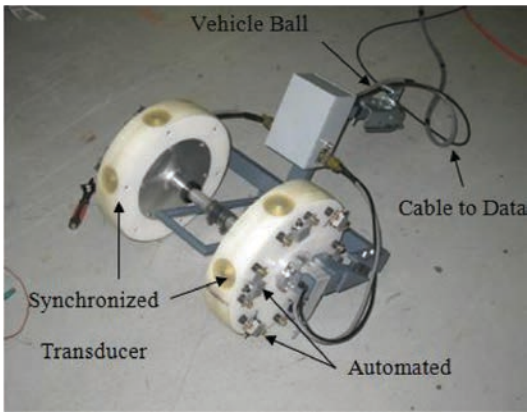

Figure 3.14. Scanning IE/SASW System Used for Controlled Testing.

The MISW method collects data similar to that collected with the SASW method but involves multichannel data-processing techniques to determine pavement modulus and thickness information. Hence, the amount of data collected with the MISW method is significantly greater than that collected with the SASW method. An accelerometer is placed on the pavement surface, and several impactors are triggered at various distances from the accelerometer to measure the surface wave responses.

Controlled Laboratory and Field Evaluation

Portable Seismic Pavement Analyzer

Data obtained from testing the test sections on the test track were analyzed by evaluating the shapes of the time and frequency domain plots and by determining the average vector distances. Then, probabilities of the pavement to be bonded were determined for each testing location. The worst case (a 5% probability of being bonded) was determined based on the average vector distances of the shallow delaminated portion of the laboratory slab. The best case (100% probability of being bonded) was determined d on the basis of the average vector distances of Section 3 (one of the control sections) on the test track. Probabilities of being bonded for other test points on the test track were determined d on the basis of the worst and best conditions.

Figure 3.15 shows the probabilities of being bonded for all the test points on the test track d on the basis of average vector distances. The probabilities are given for the data collected in October and February along with the pavement temperature at the time of testing. Section 2, consisting of bonded HMA over portland cement concrete (PCC), had a more abnormal and sensitive power distribution because the PCC layer may have provided additional reflected energy to confound the analysis method.

On the basis of design of the test sections, most test locations with probability of 0.6 or more were in bonded areas, while most of those test locations with probability of 0.5 or less were in delaminated areas. On the basis of the above probability levels, the PSPA was able to detect approximately 69% and 78% of delamination in the warm and cool temperature conditions, respectively. The PSPA did a better job of identifying the delamination in the cooler pavement temperature conditions.

Overall, the PSPA was able to identify the bonded sections. The nondestructive device had a difficult time detecting the delamination at 2-in. depth when the baghouse dust was used. However, the PSPA was able to detect the delaminated areas at 5-in. depth by using the baghouse dust, particularly in the cooler pavement temperature conditions. This test does not provide continuous measurement of the bond, but the test does identify bond for each test location. More details of the controlled evaluation are in Volume 3, Chapter 4.

Test Date October 2009

Test location (ft) >	Section 1					Section 2				
	17.5	22.5	27.5	32.5	37.5	42.5	47.5	52.5	57.5	62.5
Test Line 1 >	0.1	0.2	0.2	0.2	0.1	0.4	0.9	0.6		0.5
Test Line 2 >	0.2	0.3	0.2	0.1	0.1	0.9	0.8	0.9	0.9	1.0
Test Line 3 >	0.2	0.2	0.2	0.3	0.5	1.0	1.0	0.7	1.0	0.8
Test Line 4 >	0.4	0.2	0.1	0.1	0.1	0.8	1.0	0.9	0.9	0.9
Pavement Surface Temperature (F) >	63°	64°	65°	64°	66°	69°	70°	70°	71°	70°

Test Date February 2010

Test Line 1 >	0.1	0.2	0.2	0.5	0.2	0.7	0.3	0.3	0.7	0.6
Test Line 2 >	0.3	0.2	0.3	0.2	0.3	0.7	0.6	0.6	1.0	1.0
Test Line 3 >	0.2	0.2	0.2	0.3	0.7	0.6	0.6	0.7	0.7	1.0
Test Line 4 >	0.6		0.1	0.1	0.2	0.7	1.0	0.9	0.6	1.0
Pavement Surface Temperature (F) >	41°	42°	41°	41°	40°	42°	44°	47°	49°	51°

Section 3					Section 4					Section 5				
67.5	72.5	77.5	82.5	87.5	92.5	97.5	102.5	107.5	112.5	117.5	122.5	127.5	132.5	137.5
1.0	1.0	0.8	1.0	0.8	0.9		0.6	0.5	0.4	0.0	0.6	0.3	0.9	0.8
1.0	0.8	1.0	0.7	1.0	0.9	0.9	0.9	1.0	0.8	0.1	0.3	0.8	0.8	0.7
1.0	1.0	0.9	1.0	1.0	1.0	0.4	0.8	0.2	1.0	1.0	0.4	0.1	1.0	0.3
1.0	0.9	0.7	1.0	0.7	0.9	1.0	0.9	0.8	0.9	0.7	1.0	0.7	0.7	0.6
70°	71°	71°	70°	71°	72°	74°	81°	81°	84°	85°	85°	86°	86°	86°
0.9	1.0	1.0	0.9	1.0	1.0	1.0	0.5	0.8	0.3	0.1	0.3	0.2	0.5	1.0
1.0	1.0	1.0	1.0	0.8	0.9	1.0	1.0	1.0	1.0	0.1	0.2	1.0	1.0	1.0
1.0	0.8	0.8	1.0	1.0	0.8	0.7	1.0	0.2	1.0	1.0	0.4	0.1	1.0	0.7
1.0	0.9	1.0	1.0	0.9	0.9	1.0	1.0	1.0	1.0	1.0	1.0	0.8	0.1	0.8
52°	52°	53°	53°	54°	55°	56°	57°	59°	59°	58°	53°	51°	51°	52°

Section 6					Section 7					Section 8				
142.5	147.5	152.5	157.5	162.5	167.5	172.5	177.5	182.5	187.5	192.5	197.5	202.5	207.5	212.5
0.8	0.3	0.8	0.7	0.6	0.8	0.7	0.8	0.7	0.8	0.5	0.5	0.6	0.5	0.3
0.9	0.6	1.0	0.8	0.8	0.7	0.9	0.5	0.7	0.5	0.6	0.6	0.7	0.7	0.2
0.8	0.6	0.8	0.8	0.8	0.9	1.0	1.0	0.7	0.9	0.8	0.7	0.7	0.8	0.4
0.2	0.1	0.8	1.0	0.9	0.6	0.7	0.9	0.6	0.7	0.6	0.7	0.7	0.4	0.6
87°	86°	86°	87°	84°	84°	83°	82°	52°	84°	85°	84°	84°	85°	52°
1.0	0.1	0.6	1.0	1.0	1.0	1.0	0.3	0.1	1.0	1.0	0.2	0.4	0.5	0.3
0.7	0.9	0.8	1.0	1.0	1.0	1.0	1.0	1.0	0.7	0.3	0.4	1.0	1.0	0.3
1.0	1.0	0.8	0.9	1.0	1.0	1.0	1.0	1.0	1.0	1.0	1.0	0.5	0.6	0.8
0.2	0.1	0.1	0.2	0.6	1.0	1.0	0.9	1.0	0.5	0.5	1.0	0.6	0.3	1.0
53°	53°	51°	51°	51°	51°	51°	51°	51°	51°	51°	51°	52°	53°	53°

Section 9					Section 10				
217.5	222.5	227.5	232.5	237.5	242.5	247.5	252.5	257.5	262.5
0.3	0.7	0.6	0.1	0.1	0.5	0.3	0.0	0.8	0.2
0.8	0.9	1.0	0.6	0.9	0.2	0.3	0.6	0.6	0.3
1.0	0.7	0.7	0.5	0.6	0.7	0.6	0.5	1.0	0.6
0.6	0.6	0.5	0.6	0.8	0.7	0.8	0.7	0.5	0.4
52°	52°	52°	52°	52°	53°	54°	55°	58°	58°
0.4	0.4	0.6	0.4	0.5	0.3	0.4	0.3	0.5	0.2
0.5	0.5	0.9	0.3	0.3	0.1	0.4	0.1	0.3	0.2
0.6	0.2	0.4	0.4	0.3	0.3	0.5	0.4	0.5	0.7
0.6	0.4	0.2	0.6	0.3	0.4	0.6	0.8	0.5	0.3
53°	54°	54°	55°	57°	58°	58°	58°	57°	58°

Sect 1 – no bond at 5-in. depth
Sect 2 – full bond (control)
Sect 3 – full bond (control)
Sect 4 – partial bond at 2-in. depth
Sect 5 – no bond at 2-in. depth
Sect 6 – partial stripping at 2-in. depth
Sect 7 – full bond (control)
Sect 8 – partial stripping at 5-in. depth
Sect 9 – partial bond at 5-in. depth
Sect 10 – no bond at 5-in. depth

0.1	0.3	0.5	0.7	1.0

>> increasing bond >>

Figure 3.15. Probabilities of test track test points to be bonded.

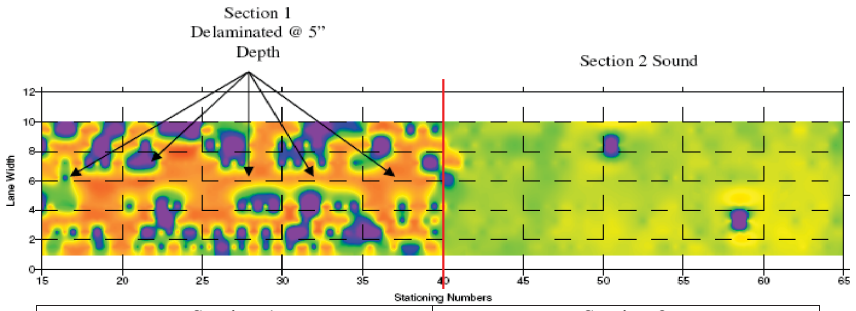

Section 1	Section 2
No bond	Full bond
5-inch depth	control

Figure 3.16. Scanning IE thickness plots for Sections 1 and 2.

Scanning IE/SASW and MISW Devices

Figures 3.16 and 3.17 show examples of detailed results of the scanning IE test in the form of resonant frequencies during the second round of testing on Sections 1, 2, 9, and 10. The resonant frequency shown in the figures is directly related to the pavement structure's thickness. The thicker areas shown in blue, purple, and green, which represent low-frequency flexural resonances, indicate delamination. The areas in orange and yellow are considered to be bonded. The results show that the scanning IE identifies the bonded areas well and does a fair job of identifying the delaminations simulated with paper at a depth of 5 in. and the stripping simulated with RAP at a depth of 2 in.

It was important to try to quantify the results of the scanning IE device to compare with the PSPA results. The same analysis procedure used for the PSPA was used with the scanning IE device; however, only the February results (with cooler pavement temperature) were analyzed. On the basis of the results, it appears that the scanning IE device was able to detect approximately 74% of the delaminated areas on the test track.

The MISW accurately predicted bonding or delamination for six of the 10 tests conducted on the test track during the October testing (with warmer pavement temperature). The test method had the ability to determine the delamination depth; however, the measurements were not accurate. The amount of testing with the MISW was minimized because of the test time required with this equipment. The MISW testing was performed at 12 locations on the test track during the February testing (with cooler pavement temperature). The MISW test accurately identified the bonded or delaminated areas for 10 of the 12 tests performed. No tests were conducted on the areas that had delaminations at a depth of 2 in. Therefore, it was difficult to judge the test method's potential for accurately identifying shallow HMA delamination.

The scanning IE/SASW and MISW methods demonstrated ability for measuring delamination, but the MISW method was time-consuming and not very practical for rapid testing. It was difficult to judge the potential for the MISW method to identify HMA delamination accurately on the basis of a few data points. The scanning IE/SASW device was quicker and easier to use, and it showed some potential for measuring delamination. The shallow delaminations (at a depth of 2 in. or less) appeared to be difficult to observe with the IE testing alone. It was concluded that testing at colder temperatures was a significant advantage for relatively high frequency (500

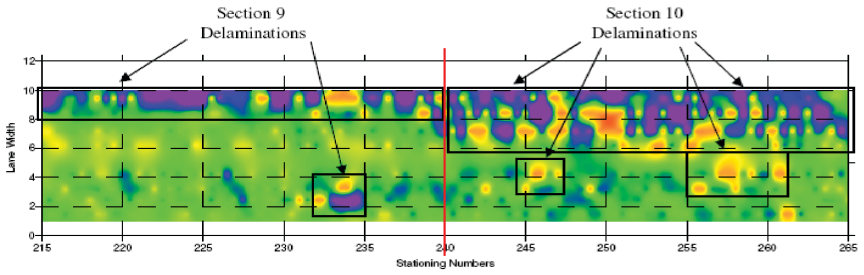

Section 9	Section 10
Partial bond	No bond
5-inch depth	5-inch depth

Figure 3.17. Scanning IE thickness plots for Sections 9 and 10.

to 200,000 Hz) wave propagation–based test methods, such as the PSPA, the scanning IE/SASW device, and the MISW device. More details of the controlled evaluation are in Volume 3, Chapter 4.

Deflection Measurement Methods

Background

Deflection measurement methods are conducted by applying an impulse load on the pavement surface. The applied force and the pavement deflections are measured and used in a backcalculation program to estimate the moduli of each pavement layer. For this study, two deflection measurement methods, the lightweight deflectometer (LWD) and FWD, were evaluated.

There have been several investigations regarding the use of the FWD to detect delamination of HMA at layer interfaces. Past experience with using the FWD for detecting delamination has shown mixed results (Mejia et al. 2008). The majority of the literature studied pointed out that a decrease in bituminous stiffness or an unexpected lower backcalculated asphalt concrete modulus was an indication of HMA layer debonding (Mejia et al. 2008; Hammons et al. 2006; Sangiorgi et al. 2003; Gomba 2004; Al Hakim, Armitage, and Thom 1998). The surface deflections measured with the FWD are influenced by delaminated HMA.

Advantages of using the FWD for detecting HMA delamination are that the tests are simple to run and the equipment is available to most agencies. Disadvantages include that the impulse duration at a frequency of 25 Hz is too long to focus on the top thin layers, and the variability in thickness and modulus of underlying layers may mask the detection of delamination (Mejia et al. 2008; Al Hakim, Armitage, and Thom 1998). In addition, the geophone spacing used for routine applications may not be appropriate for the top thin HMA layers.

Theory and Modeling

The BISAR (BItumen Structures Analysis in Roads) software developed by Shell Global Solutions (DeJong 1973) for computing stresses, strains, and displacements at any position in an elastic layered system under surface loading was used to investigate the effect of the delamination condition on HMA pavement responses. All interfaces between layers have an interface friction factor that can vary from 0 (fully bonded) to 1 (no bond) between layers.

Two case scenarios of HMA pavement structure under 9-kip FWD loading were modeled. Case 1 represents a 12-in.-thick HMA pavement structure with delamination at different depths (at 2, 6, and 10 in. below the surface). Case 2 represents a 6-in.-thin HMA pavement structure with delamination at different depths (at 2, 3, and 4 in. below the surface). For both cases, differences in the predicted vertical deflections were observed. In both cases, greater deflections were observed in the HMA pavement structure with delamination at the mid-depth of the HMA layer. The results indicated that vertical deflection measurement methods can be analyzed to detect delamination in HMA pavements. More details of the modeling are in Volume 2, Chapter 4.

Equipment Availability

LWD is an NDT device that provides a structural evaluation of pavements by using a drop weight and one to three sensors (D1, D2, and D3) (Figure 3.18). The drop weights for the LWD are selected from 22, 33, or 44 lb. The loading plate diameter can be adjusted to 3.8, 7.8, or 11.8 in. The height of the drop is adjustable. The weight is dropped onto a rubber buffer located on top of a load cell. The results are presented as a plot of the time history of the measurements from the load cell and the geophones. Peak deflection and surface deflection measurements of each sensor are recorded.

Figure 3.18. LWD testing at NCAT test track.

FWD is an impact load device that applies a single-impulse transient load of approximately 25- to 30-ms duration. With this trailer-mounted device, a dynamic force is applied to the pavement surface by dropping a weight onto a set of rubber cushions. This results in an impulse loading on an underlying 11.8-in. diameter circular plate in contact with the pavement. The applied force is measured with a load cell, and the pavement deflections are measured with velocity transducers. The drop heights of the weights can be varied from 6 to 15.7 in. to produce a force varying from 6,000 to 27,000 lb. Velocities are measured and deflections are computed at seven locations from the center of the load plate.

Controlled Laboratory and Field Evaluation

LWD Testing

The drop weight used for the LWD testing on the test track was 22 lb. The distances from the center of the loading plate to the three geophones (D1, D2, and D3) were 0 (underneath the loading plate), 6 in., and 12 in., respectively. The 7.8-in.-diameter load plate was used. During both rounds of testing, accelerometer D3 did not appear to provide much information. The measured deflections for D3 were close to 0 mils in the field and in the lab. A closer inspection of geophone D3 after the Round 2 evaluation was completed proved that the accelerometer was not working properly during Round 1 and Round 2 testing.

There were significant differences with the LWD data collected between the test sections on the test track. Similar trends were seen with the Round 1 testing in October and the Round 2 testing in February. The average measured deflections from Round 2 testing were typically lower than those in Round 1 testing, as shown in Figure 3.19. The measured deflections from Round 2 were approximately 45% lower than the measured deflections from Round 1, particularly in Sections 5 through 10. This result was expected because of the lower pavement temperatures. The test pavement from Station 0+00 to approximately Station 1+00 was backfilled with RAP, which explains the higher measured deflections of Sections 1 through 4 compared to those of Sections 5 through 10.

The 10 sections were also analyzed separately. The data points were analyzed to determine the differences in measured deflection between each of the sections and to compare the measured deflections of a fully bonded area to a debonded area. The measured deflections for each type of simulated delamination and bonded area were compared to each other for Sections 7 through 10. Sections 1 through 6 were left out of the comparison because of concern about the effect of the backfilled RAP on deflections in these sections. Figure 3.20 shows the results of the comparisons for Round 1 testing.

As shown in Figure 3.20, the fully bonded areas provided similar deflection measurements to those areas with RAP and baghouse dust. Simulated debonding using paper had much higher deflections compared to the baghouse dust, RAP, and fully bonded areas. It seems that using the paper created a loss in bond and possibly some loss in friction between the two layers, while the baghouse dust may have resulted in a higher bond than when the paper was used. The higher measured deflections with paper may have been an indication of loss of friction between the layers under loading, resulting in more relative movement at the interface between the two layers. As the load from the LWD was applied, the HMA layers were able to slide along the paper, resulting in increased movement and deflection. Some friction most likely existed within the

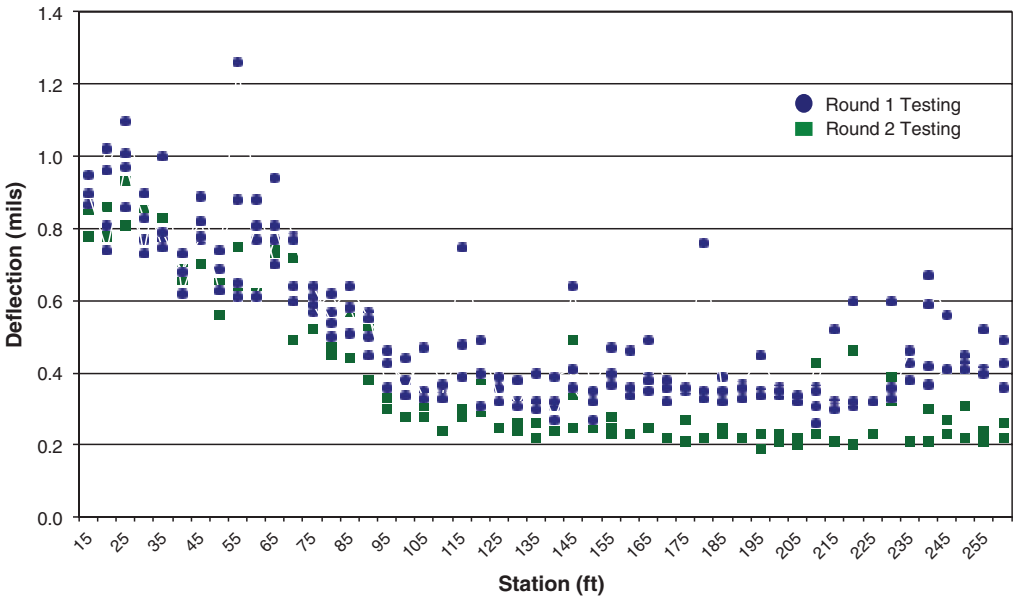

Figure 3.19. Average D1 measurements from controlled field evaluations.

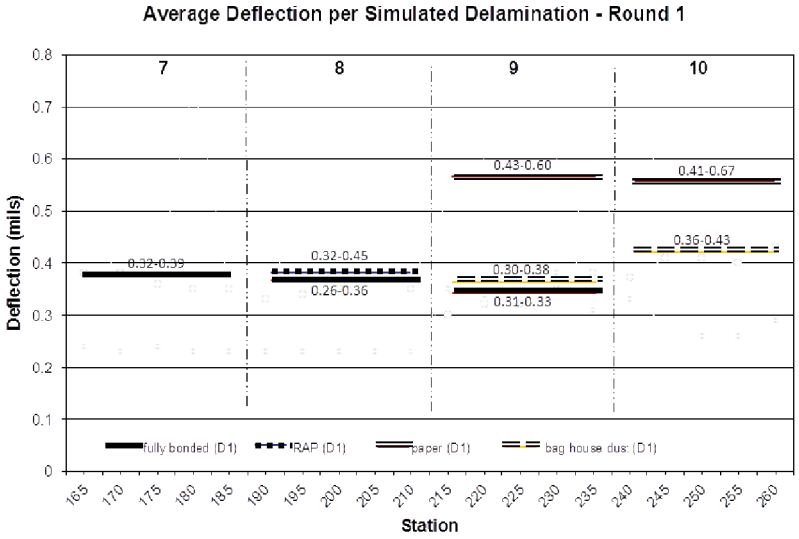

Section 7	Section 8	Section 9	Section 10
Full bond	Partial Stripping	Partial bond	No bond
control	5-inch depth	5-inch depth	5-inch depth

Figure 3.20. Round 1 average deflections of each delamination type (Sections 7 through 10).

delaminated areas simulated with baghouse dust because of the texture provided by the baghouse dust.

On the basis of field testing results, the LWD does not appear to be able to show differences in deflection between the various sections. It is difficult to identify what causes this lack of change in deflection, but a section that is delaminated should have higher deflection than a section that is not delaminated. Although the LWD can detect changes in the pavement structure, it is doubtful that the LWD can be used to identify the cause of the change in deflection and the depths at which the delaminations occur.

The research team used its LWD on the controlled test sections containing good bond and delamination. Since the LWD equipment could be included at no additional cost to the project, LWD equipment was used in the uncontrolled field testing to measure pavement response at suspected delamination areas. More details of the controlled evaluation are in Volume 3, Chapter 6.

FWD Testing

The FWD testing was carried out at four load levels: approximately 6, 9, 13, and 18 kips. The locations of nine geophones were at 0 in. (D0), 8 in. (D8), 12 in. (D12), 16 in. (D16), 20 in. (D20), 24 in. (D24), 28 in. (D28), 32 in. (D32), and 36 in. (D36) from the center of the FWD loading plate. Seventeen locations representing all interface bonding conditions in the 10 test sections were selected for this testing. At each location, two FWD tests were conducted at each load level. For each test, both the maximum deflection information and time-history data were collected for analysis.

Two methods were used to analyze the FWD data. The first method compared the maximum deflections measured by each geophone and the deflection basin parameters, including the area under the deflection basin curve (AREA), area under pavement profile (AUPP), impact stiffness modulus (ISM), surface curvature index (SCI), base curvature index (BCI), and base damage index (BDI). The differences in the maximum deflections and deflection basin parameters between the intact and delaminated sections were not significant. This result may have been due to the thick and strong layers built under the test sections.

The second method evaluated delamination behavior on the basis of FWD deflection time history. Figure 3.21 shows an example of deflection time history measured under the center of the loading plate for the 18-kips load level of FWD Test 6 in Section 4. FWD Test 6 in Section 4 was conducted on the inside wheelpath (IWP) with partial delamination and on the outside wheelpath (OWP) with full delamination. As seen in Figure 3.21, peak deflections of both locations under loading show no significant difference, but deflections of OWP (delamination) under unloading are recovered more quickly and higher. This behavior was observed in some of the FWD test results in delaminated sections. More details of the controlled evaluation are in Volume 3, Chapter 7.

Selection of Most Promising NDT Technologies for Field Evaluation

On the basis of results of the controlled evaluations, the research team followed the same set of evaluation factors

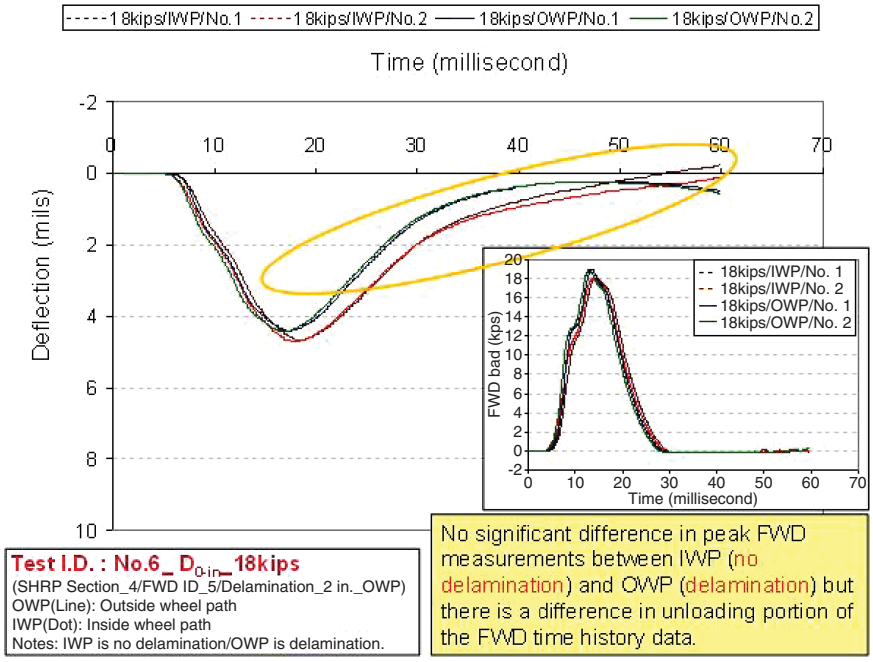

Figure 3.21. D_0 Time history under 18-kip loading for FWD Test 6 in Section 4.

used in Phase 1 to rank the evaluated NDT techniques. Nine factors were rated on a scale of 1 (low) to 10 (high) and further weighted relative to each other. The ability to measure delamination was given the highest weighting (40%).

At the end of the controlled laboratory and field evaluations of the NDT techniques, the research team met with the expert panel. The purposes of this meeting were to (a) present a summary of the findings of the controlled evaluations and (b) present recommendations for which NDT technologies should be given further consideration for equipment development and uncontrolled field evaluation.

In the meeting, the research team presented a summary of the evaluation for each NDT technology and vendor as listed below:

- GPR from GSSI, USA;
- GPR from MALA AB, Sweden;
- GPR from 3d-Radar AS, Norway;
- PSPA technique from Geomedia Research and Development, USA;
- Scanning IE/SASW technique from Olson, USA;
- IR cameras from FLIR and ICI, USA;
- FWD with equipment from the NCAT; and
- LWD with equipment from the ERDC.

Each summary included a sample of the data collected and the relative success of the technology to identify the delamination. The team presented the strengths and weaknesses of the equipment and software and the types of hardware and software improvements needed. Table 3.1 shows a summary of the evaluations. The evaluations showed that IR techniques were not able to detect delamination and were not considered for further evaluation. GPR techniques had good potential to detect severe delamination (stripping). Mechanical wave technologies (SASW and IE) had fair potential to detect debonded layers. LWD and FWD may have potential to detect delamination, but their deflection time histories need to be examined further.

On the basis of results of the evaluation, the panel agreed with the research team's recommendation that one GPR and one mechanical wave technique be selected for hardware and software improvement and uncontrolled evaluation. The research team would continue to examine LWD data by using equipment available to the team. Two vendors were selected on the basis of their ability and interest to make equipment improvements. The selected vendors, 3d-Radar and Olson Instruments, Inc., were then contacted to begin negotiations on hardware and software development required to receive research seed money and continued evaluation in the study.

Uncontrolled Field Evaluation

Description of Test Sites

Pavement sections with some delamination problems in four states were selected for uncontrolled field testing of the two NDT techniques. However, because of some delays in

Table 3.1. Summary of Findings from Controlled Laboratory and Field Evaluation

Factor	GPR			Mechanical Wave			Deflection Measurement	
	GSSI	3d-Radar	MALA	MISW	IE	PSPA	LWD	FWD
Detection of stripping	Good	Good	Good	Poor	Fair	Fair	Fair	Poor
Detection of debonding	Fair	Poor	Poor	Poor	Fair	Fair	Poor	Poor
Potential for implementing	Fair to good	Good	Good	Fair	Fair	Good	Good	Good
Equipment availability	Not multichannel	Not FCC-approved	Available	Limited	Limited	Available	Available	Available
Current application	Used in United States	Used outside United States	Used in United States	Limited use in United States	Limited use in United States	Used in United States	Used in United States	Used in United States
Cost ($)	~100,000	~250,000	~100,000	NA	NA	~30,000	~12,000	~200,000
Speed	TBD with multi-channel	3 to 45 mph; reso-lution varies	40 mph with 8 channels	Point-load	2 to 5 mph	Point-load	Point-load	Point-load
Effective depth	Good	Good	Good	Variety	4 to 6 in.	0 to 12 in.	Depends on structures	Good
Data analysis	Good for time slices	Good for time slices	Good for time slices	Poor	Poor	Poor	Fair	Fair
Results	2-D map	2-D map	2-D map	Point list	2-D map	Point list	Point list	Point list
Advantages	Noncontact; largest supplier	No development required	Minimum development; off-the-shelf	None	Full coverage: rolling	Low cost	Low cost	Availability
Limitations	Requires development	Price = not FCC-approved	Mechanical deploy-ment	Time-consuming	Walking speed	Point-load	Point-load	Point-load
Possible Modification	Implement multichannel	None	Mechanical deploy-ment	Equipment development	Equipment development	Software refinement	Analysis method	Analysis method

Note: FCC = U.S. Federal Communications Commission; 2-D = two-dimensional; NA = not available; TBD = to be determined.

equipment improvement, uncontrolled field testing did not begin until winter 2010 for the GPR technique and began in spring 2011 for the mechanical wave technique. Weather conditions were not suitable for field testing in Maine and Washington State. Therefore, the two NDT techniques were evaluated only on pavement sections in Florida and Kansas.

In Florida, the pavement sections selected for high-speed GPR testing were northbound and southbound segments between MP 413 and MP 409 on I-75. After the high-speed GPR testing was completed, results were reviewed, and a southbound section approximately 4,500 ft in length starting from MP 413 was selected for low-speed GPR testing. Core data in this area provided by the Florida DOT showed a total asphalt thickness of approximately 9 in. In 1996, the pavement was milled approximately 5.5 in. and replaced with a 0.5-in. layer of asphalt rubber membrane interlayer (ARMI), a 2-in. layer of 19-mm Superpave mix, a 1.25-in. layer of 12.5-mm Superpave mix, and a 0.75-in. layer of open-graded friction course (OGFC). On the basis of results of indirect tensile strength testing of field cores, moisture damage may be occurring either between the 12-mm mix and the 19-mm mix or between the 19-mm mix and the interlayer layer.

After reviewing results of the GPR testing and other information provided by the Florida DOT, the research team decided to conduct field testing of the mechanical wave technique on the same 2000-ft section starting from MP 413. In addition, locations where anomalies had been identified in the GPR results were selected for LWD testing and cutting cores to verify the pavement condition. More details on the core locations are in Volume 5, Chapter 1.

In Kansas, a westbound pavement section between MP 412 and MP 425.5 on US-400 was selected for high-speed GPR testing. Results of the high-speed GPR testing were then reviewed, and a pavement section of approximately 3,500 ft in length starting from MP 417.1 was selected for low-speed GPR testing. On the basis of core data provided by the Kansas DOT, the pavement thickness of the long section varied from 13.5 to 19 in., and the pavement thickness of the short section was approximately 13.5 in. This section was a full-depth asphalt pavement. In 1988, an 8-in. dense-graded asphalt base layer was built on top of subgrade and then surfaced with a 2-in. asphalt layer. In 1991, this section was overlaid with an asphalt layer 1 to 1.5 in. thick. Another surface layer approximately 2 in. thick was placed on top of this section in 1999. The data also showed that all the cores cut from the short section broke between 1.75 and 4.75 in. from the surface, and the base layer had a severe stripping problem.

After reviewing the GPR test results and other information provided by the Kansas DOT, the research team decided to conduct field testing of the mechanical wave technique on the same 3,500-ft section starting from MP 417.1. Locations where anomalies had been identified in the GPR results were selected for LWD testing and cutting cores to verify the delamination condition. More details on the core locations are in Volume 5, Chapter 3.

Uncontrolled Field Testing of 3d-Radar GPR System

Technology Improvements

Full Lane Width Antenna

The system provided by 3d-Radar for the uncontrolled field test sites used a wider antenna array than that used for the controlled testing at NCAT. The antenna array model B3231 has the ability to collect up to 31 parallel B-scans simultaneously, with a minimum spacing of 10 cm (approximately 4 in.). The array has an overall width of 3.2 m (approximately 10 ft 5 in.) and is controlled with a single cable connected to the Geoscope control unit. This antenna covers close to a complete lane width, and thus represents a wider swath of data than the data collected at the NCAT Pavement Test Track. With this survey width, field testing can be performed with a single pass, and it was not necessary to piece together parallel passes of data as was necessary for the controlled testing.

Antenna Deployment System

For these field tests, a special tower mount was designed to shift the antenna quickly between data acquisition and system transportation. The mount consists of a vertical cylinder fixed to the hitch receiver of the vehicle. The antenna array is attached to a sleeve that can be raised and lowered along the main tower by an electric power winch. During data acquisition, the antenna array is lowered down and perpendicular to the direction of travel, covering the largest part of a traffic lane. During transportation between survey sites, the array can be lifted and turned 90° to minimize possible issues of traffic safety and equipment damage.

Delamination Detection Algorithm

A prototype delamination detection algorithm was developed on the basis of data collected at the NCAT facility during 2009 and 2010. The algorithm was built to account for the fact that delamination can occur at a relatively wide range of depths and show a variety of amplitude characteristics in the recorded data. The chosen approach was based on isolating a subvolume (depth range) where delamination is most likely to happen and performing an energy-based study of frequency intervals. Advantages are that by considering frequencies, every sample will carry information about the whole depth range to be analyzed, while sorting the energy values takes care of the varying amplitudes of signatures due to delamination. Schematically, the time window of interest is extracted from every trace and converted to frequency

Figure 3.22. Red rectangles showing final output of algorithm, identifying locations with potential delamination.

domain, where the spectrum is divided into frequency intervals, or "bins." The algorithm computes the energy contained in every bin and then sorts the obtained values. The value that will be finally extracted is relative to only one bin, which is selected by the user. The user then defines a threshold value and the minimum size for an anomaly of interest to produce the final output (Figure 3.22). In that figure, red rectangles are the final output of the algorithm, the result of a statistical analysis based on parameters input by the user.

Uncontrolled Field Evaluation

At each site, tests were conducted at 3 speeds: high, medium, and low. It was understood that lower speeds could provide more detailed data, but higher speeds would be more representative of the overall objective of the project.

To determine the relationship between the speed of the survey and the level of data detail, the time required to perform a complete array scan together with the in-line sampling needs to be calculated. 3d-Radar provided an Excel-based utility to assist with these calculations to define the maximum surveying speed during the acquisition. As summarized in Table 3.2, three different system configurations were tested to allow for different maximum vehicle speeds.

In the Kansas testing, the high-speed and medium-speed tests were carried out in the westbound direction over the full length of the site, from milepost (MP) 412, west of the western county line, to the intersection between US-400 and K-7. The nominal antenna height for those tests was 11 in. above the pavement. A repeat of the westbound medium-speed test was conducted with an antenna height of 8 in. After the medium-speed tests, the data were analyzed by using the delamination detection algorithm described above. On the basis of results of this analysis, surface observations, and prior core data, a shorter section 3,500 ft in length was selected for evaluation by using the low-speed survey protocol. This section was located between two bridges, beginning directly after MP 417 and ending approximately at MP 417.78. The low-speed test was carried out with an antenna height of 8 in.

In the Florida tests, the high-speed and medium-speed tests were carried out over the full length of the site, from MP 408 to MP 413 in both the northbound and southbound directions. On the basis of visual observation of the data and the pavement surface, a shorter section, southbound from MP 413 to the rest area (approximately 4,500 ft), was selected for the low-speed testing.

Evaluation Results

The data analysis for the Florida and Kansas sites focused on the low-speed data because these data provide the greatest level of detail. In each case, the data were analyzed manually with the depth slice feature of 3d-Radar's Examiner program. This program provides a visual display of the raw data and allows the user to view horizontal slices of the data at different depths. The purpose of the initial data analysis was to identify locations for coring.

The analysis concentrated on the presence of anomalies in the GPR data, similar to anomalies that were detected at the delaminated areas in the NCAT test track. A series of anomalies were identified at each site, and the station, offset, and depth were recorded. Figure 3.23 shows a sample of this

Table 3.2. System Configuration for Uncontrolled Field Testing

Description	Slow Speed	Medium Speed	High Speed
Frequency range	200–3,000 MHz	200–3,000 MHz	200–3,000 MHz
Frequency step	2.5 MHz	2.5 MHz	2.5 MHz
Dwell time	1 μs	0.6 μs	0.5 μs
In-line sampling	10 cm (~4 in.)	20 cm (~8 in.)	30 cm (~12 in.)
Cross-line sampling	10 cm (~4 in.)	20 cm (~8 in.)	30 cm (~12 in.)
B-scans per swath	31	16	11
Maximum speed	~3.5 mph	~18 mph	~45 mph

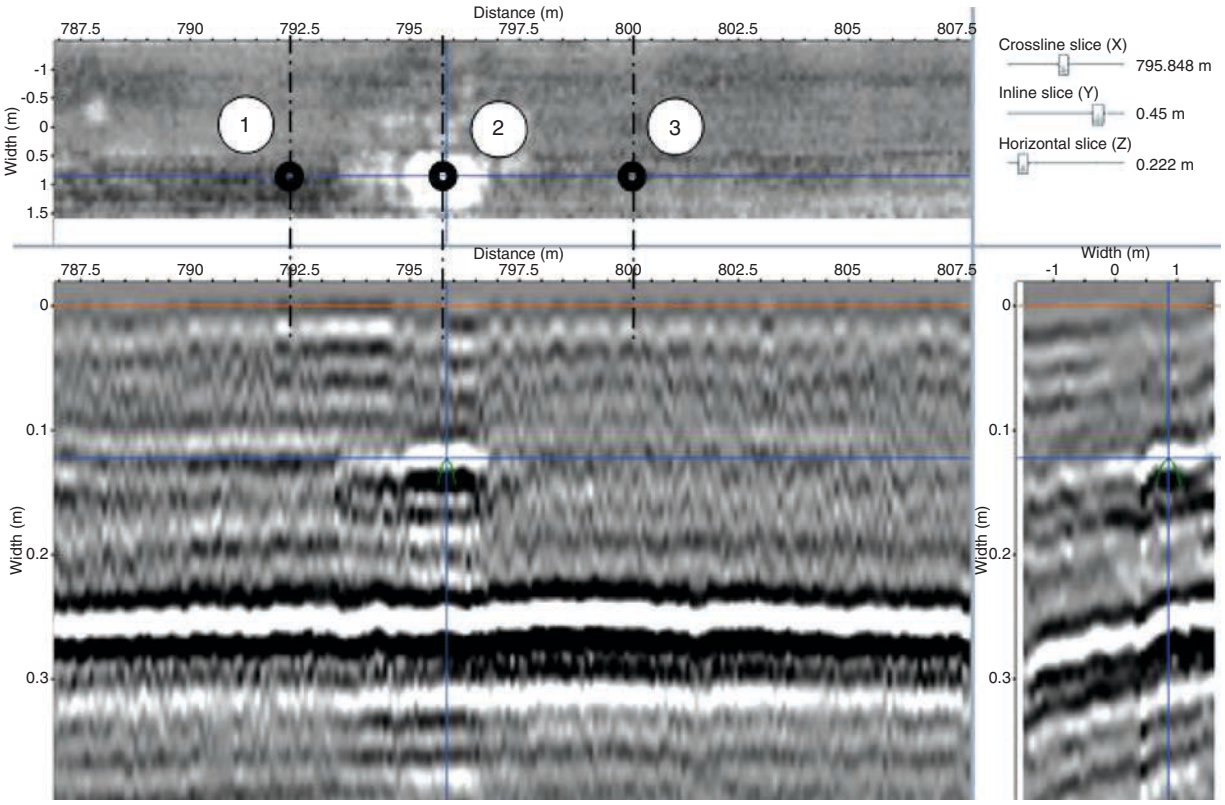

Figure 3.23. Sample of GPR data sections used to identify coring locations.

interpretation of the GPR data by using the depth slice at 4.7 in. (12 cm) (top), the longitudinal section at 31 in. (0.8 m) from the center of the lane (bottom left), and the transverse section at Station 795.8. These observations served as a basis for selecting the coring locations. Locations 1, 2, and 3 are shown in the figure. Note that Core 2 is located at a GPR anomaly, while Cores 1 and 3 are outside the anomaly area.

Coring locations and observed conditions for the Florida and Kansas sites are shown in Tables 3.3 and 3.4. Note that all of the Florida cores were extracted intact, but a detailed analysis of the individual core layers, including indirect tensile testing, revealed evidence of moisture damage. The Kansas cores, on the other hand, all fell apart when extracted and showed obvious evidence of moisture damage in between lifts.

An automated analysis method for quantifying the visual GPR data observations discussed above was explored by the project team using the 3-D volume of time domain data provided by the 3d-Radar system. This analysis is based on an activity analysis (Maser 2008). This analysis detects the intensity of GPR reflection activity at each location. Locations where there was more intense activity (i.e., anomalies) were more likely to be delaminated or damaged, because the damage created anomalous reflections in the GPR data.

The activity analysis was carried out on the Kansas and Florida data sets, to see whether the results would replicate the visual observations of the data. The complete activity analysis plots are shown in Volume 5, Chapters 2 and 4. A sample result from this analysis is shown in Figure 3.24. This result replicates the visual observation shown in Figure 3.23. The analysis, however, does not explain the significant overall differences observed between the cores taken at the two sites.

Technology Implementation Status

A technical brief on GPR is provided in Appendix A. The brief describes the required features of this NDT technology on the basis of the results of this study. The technical brief describes the basic principle of the technology, lists the NDT hardware and operating parameters, recommends data collection and analysis requirements, and lists advantages and limitations. As GPR technology advances, the technical brief will need to be revised to reflect those improvements.

From a traffic control point of view, it would be most desirable to collect data at a normal driving speed. From a pavement evaluation point of view, it would be desirable to collect a high density of data (lower travel speed). 3d-Radar is improving its system so that speeds can be increased by a factor of two or more.

The analysis of the data collected has also indicated that slow speed measurements are affected by movement of the

Table 3.3. GPR versus Core Information for Florida I-75 Site

Core	Distance (ft) from MP 413	Offset	GPR Observation	Core Condition for Layer 2[a]	
				Tensile Strength (psi)	Stripping Ranking
1	2,232	RWP	No anomaly	133.9	4
2	2,242	RWP	Anomaly	117.7	4
3	2,252	RWP	No anomaly	130.2	4
4	3,607	RWP	No anomaly	97.3	4
5	3,632	RWP	Anomaly	119.4	4
6	3,640	RWP	Anomaly	105.4	4
7	3,742	RWP	Anomaly	137.1	4
8	3,745	RWP	Anomaly	132.7	4
9	4,270	CL	No anomaly	132.2	4
10	4,286	CL	Anomaly	128.5	4

Note: CL = centerline; RWP = right wheelpath; LWP = left wheelpath.
[a] According to AASHTO T 283.

Table 3.4. GPR versus Core Information for Kansas US-400 Site

Core	Distance (ft) from South Deck Joint	Offset	GPR Observation	Core Condition
1	1,080.8	CL	Anomaly	Stripped
2	1,694.2	RWP	Anomaly	Stripped
3	2,271.5	CL	Anomaly	Stripped
4	2,996.3	RWP	Anomaly	Stripped
5	3,022.6	LWP	Anomaly	Stripped
6	3,224.6	RWP	Anomaly	Stripped
7	288.8	CL	Anomaly	Stripped
8	427.9	CL	No anomaly	Stripped

Note: CL = centerline; RWP = right wheelpath; LWP = left wheelpath.

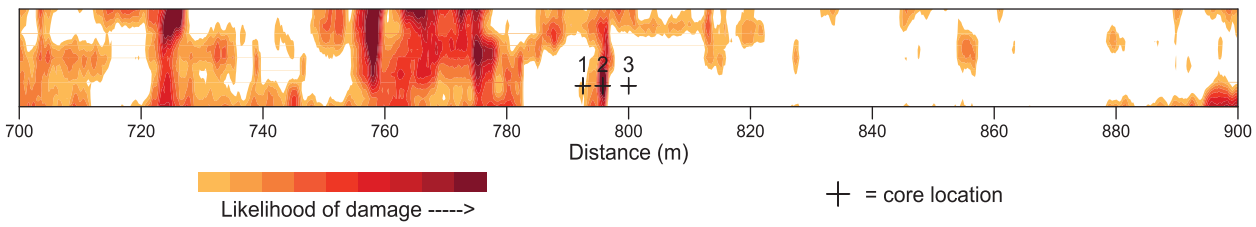

Figure 3.24. Sample result of activity analysis for Florida I-75 site.

antenna, particularly visible close to the surface. Suspicions are that this behavior is due to the resonant frequency of the vehicle suspension; that is, the antenna vibrates together with the vehicle and produces small undulations in the data. Cross-checking typical values for resonance frequency of the suspensions with the variations in the data showed that this seems to be the case. Future equipment development will need to address this issue, directly in the hardware if possible, either by modifying the antenna mount or by using an optional antenna trailer, or possibly by using postprocessing software.

The size of the generated files (5 to 10 gigabytes) was another issue encountered during this study. Storing files, transferring files, and postprocessing of data require an unusually large amount of time because of the large file size. Modification of the Examiner software package to support optional routines for semiautomatic partitioning, in order to allow fast processing and access of subsections, is being implemented. Future releases of Examiner will allow the data to be divided into smaller portions, an operation currently performed only manually by the user.

3d-Radar's delamination detection algorithm was developed on the basis of experience at the NCAT facility, where human-introduced simulated delamination provided solid and clean characteristics. Further study of the data collected in real situations, combined with ground truth, will help refine the signature given by an interesting delamination both qualitatively and quantitatively. The next step for the detection algorithm is to increase its robustness to detect a specific type of anomaly. Additionally, the algorithm will attempt to factor in characteristics of the road substructure, where variation in depth of targeted layers and eventual lateral discontinuities are present. Finally, this version of the algorithm requires multiple inputs from the user, which means that the data analyst must have a background in GPR data processing. A further refinement, which includes a more detailed and targeted analysis of the data and ground truths collected during this project, should minimize the input required in future revisions and make the algorithm a more user-friendly tool for nonspecialist operators.

Uncontrolled Field Testing of Olson Engineering Mechanical Wave Technique

Technology Improvements

A series of modifications of the Olson scanning IE/SASW system were made before the uncontrolled field testing. The objectives of the modifications were to improve the system's ability to detect shallow delaminations (a depth of approximately 2 in.) and to increase the test area coverage, thus reducing the required test time on a single pavement section.

The improvements included designing and constructing an expanded IE/SASW system from a single pair of wheels to three separate pairs of wheels. The decision to expand to six measurement wheels was made when the testing plan was designed to perform IE testing over five 2-ft. spacings to cover a 12-ft-wide lane. The improved system with three sets of paired wheels requires two passes of SASW testing to cover a full lane width. Additional expansion of the system could be accomplished in the future to eliminate the need for two passes per traffic lane. Currently, the system scans every 1.0 square feet (a nominal 2-ft lane width every 0.5 ft of lane length) at an approximate speed of 1 to 2 mph, or walking speed.

The additional four measurement wheels were constructed to be nearly identical to the original pair of transducer wheels. Each wheel includes (a) six IE/SASW transducers evenly spaced around the circumference at 6-in. intervals; (b) six impactor solenoids; and (c) electronic circuitry for signal conditioning, solenoid firing, and data acquisition initiation. As the additional four wheels were prepared, a few slight modifications were made to improve the design. A lip was added onto the high-density polyethylene wheel to secure the urethane tire, and a variable attenuator circuit was added to the signal conditioning to allow the signal to be reduced in voltage amplitude to avoid clipping during data acquisition. The spacing between each pair of transducer wheels was changed from 12 in. to 6 in. to allow for a more accurate result and to give more sensitivity for locating shallow delaminations (2 to 6 in.). Rubber couplings were used for the 6-in. spacing to avoid excessive vibration noise. The distance between the impactor and 6-in. transducer spacing remained at 1.75 in.

Another major modification was the addition of data acquisition initiation timing circuitry to synchronize the data collection of the three independent transducer wheel pairs. The timing circuitry collects data only when the wheel pairs test sequentially from left to right, thus allowing the data to be well organized in the software. The timing circuitry has two separate options, which allows the scanning system to be run as three sets of SASW testing wheel pairs or as six individual IE testing wheels.

The last major change was the addition of an independent distance wheel to record the distance from the start of the scan to each data collection point with any of the transducer wheels or pairs. The distance wheel outputs 128 pulses per revolution, thus resulting in a distance measurement resolution of approximately 0.1 in.

Additional miscellaneous modifications included a simplified and redesigned assembly of the wheel pair carriage to make it easier and quicker to assemble. The towing assembly mounted to the truck was also altered slightly by adding more pin connections to ease field assembly. The attachment of the wheel pairs to the towing assembly was

changed to a clamping attachment that can slide across the towing assembly bar, allowing endless measurement configuration possibilities. Lift bails were added to the towing assembly to allow the transducer wheels to be picked up off the pavement surface to back the system up or to reposition the truck with greater ease. Also, the wiring between the transducer wheels and the data acquisition computer was simplified.

The six-wheel scanning IE/SASW system was designed to perform IE testing on all six transducer wheels, or IE testing on the transducer wheel near the impactor solenoid and SASW testing by using the pair of transducer wheels. The six-wheel IE testing is best for assessing concrete bridge slabs or parking garage deck slabs without an asphalt overlay. The IE/SASW setup with three paired wheels is best for testing asphalt material, either full depth or as an overlay. For IE/SASW testing, sensor elements in both transducer wheels (within a pair) are aligned and locked with a pin to prevent slippage. The sensor elements are offset approximately 2 in. between each adjacent pair of transducer wheels. The solenoids are powered either with a 12-VDC battery or with an AC vehicle adapter.

For this study, the system was set so that only the solenoids of the left transducer wheel (of each pair) were used for generating impacts. The solenoids of the right transducer wheel were disabled for the duration of the testing. The impact sequence started with firing the single solenoid used for the left pair of transducer wheels followed by the solenoid for the middle pair of transducer wheels and then the solenoid for the right pair of transducer wheels. The sequence was then repeated. Once one of the solenoids fires, data for all three pairs of transducer wheels (six channels) are acquisitioned simultaneously. Only the data from the pair of wheels where the solenoid is fired and impacts are analyzed. At each acquisition, two channels (one wheel pair) actually have valid surface wave data. The other four channels (two pairs) acquire background noise. The postanalysis software scanned through all the acquired data and pulled out only valid SASW data for further analysis.

The system is operated with the Olson Freedom Data PC, which runs the acquisition software and receives all data. Features of the postanalysis software include auto windowing, dynamic masking/dispersion curve display, and composite velocity calculations. The plotting of the test results is performed in Surfer software. Figure 3.25 shows a photograph of the current scanning IE/SASW system.

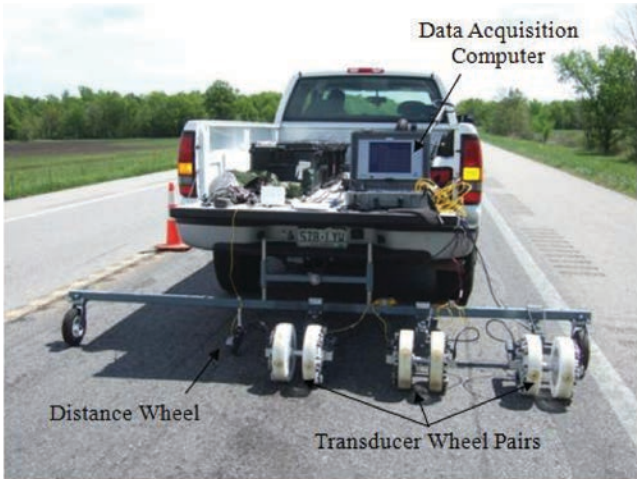

Figure 3.25. Olson Engineering IE/SASW scanning system.

Uncontrolled Field Evaluation

Before the uncontrolled field testing, Olson Engineering performed additional controlled field testing of the improved scanning IE/SASW system at the NCAT Pavement Test Track. The scanning IE/SASW test was performed on the 10 test sections on the test track in two runs.

The field evaluation of the scanning IE/SASW system took place in Gainesville, Florida, on March 1, 2011, and in Pittsburg, Kansas, on April 26, 2011. During testing, the temperature ranged from approximately 65°F to 70°F in Florida and from approximately 50°F to 60°F in Kansas. A 2,000-ft-long area in the right lane along I-75 was selected for testing in Florida, and a 3,500-ft-long area in the right lane along US-400 was selected for testing in Kansas. The test sites were selected on the basis of results of previous GPR testing.

At each site, two passes of the scanning IE/SASW system were required to cover the traffic lane. The three pairs of wheels were positioned on the right side of the lane for the first pass and on the left side of the lane for the second pass. More details of the uncontrolled evaluation are in Volume 4, Chapter 2.

Evaluation Results

NCAT Pavement Test Track

The scanning IE/SASW test results from the test track are presented as surface wave velocity plots at different depths from 0.1 to 0.8 ft (1.2 to 9.6 in.) from the surface. Figure 3.26 presents the surface wave velocity profile from Section 1 on the test track. Surface wave velocities are presented in grayscale, and they range from 3,000 (light gray) to 5,000 ft/sec. (black). The higher the surface wave velocity, the better the condition of the pavement. Anomalies can be seen as a light spot where the velocities are lower.

Figure 3.26 shows a drop of surface wave velocity between the depths of 0.4 and 0.5 ft (4.8 and 6 in.). Thus, the results show the likelihood of debonding between depths of 0.4 and

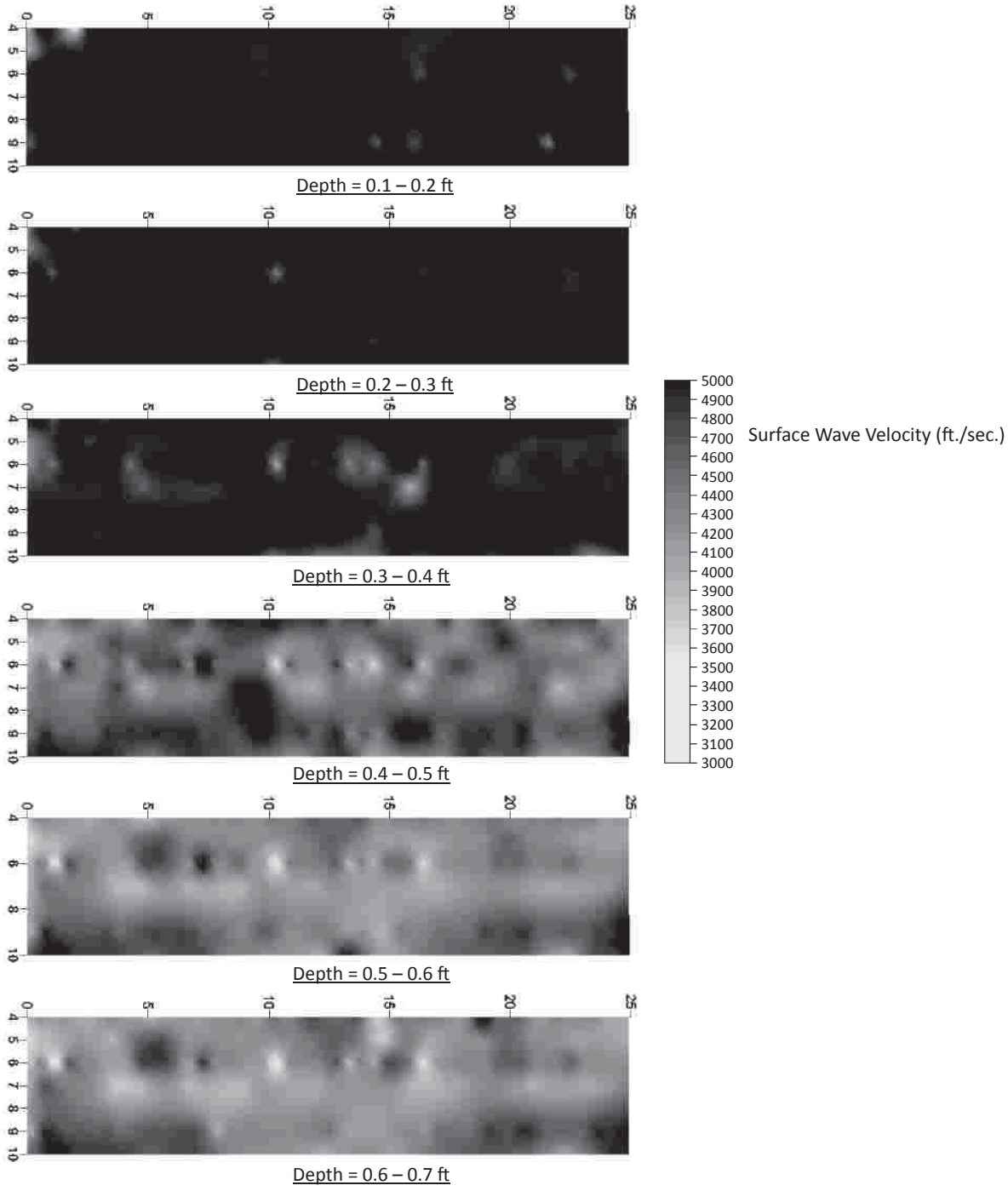

Note: Section 1 = 0 to 25 ft.

Figure 3.26. Profile plots of surface wave velocity.

0.5 ft. The interpretation of the scanning SASW results agrees well with the as-built condition, which is delamination at a 5-in. depth simulated with baghouse dust and paper.

The same surface wave velocity plots were generated for the other nine test sections on the test track. The results show that the scanning SASW was good at detecting intact pavement and RAP materials at a 2-in. depth. The scanning SASW was less accurate at detecting the deeper delaminations (5 in.) of the other sections simulated with RAP materials, baghouse dust, and paper. The scanning SASW did a fair to poor job of detecting the 2-in.-deep delaminations simulated with baghouse dust.

The scanning IE data collected on the test track were also analyzed. The results indicated that the scanning

IE/SASW system was able to detect the 5-in.-deep delaminations but not the shallower 2-in.-deep delaminations. This was most likely a result of the current system's difficulty in exciting high frequencies in asphalt mixtures at higher temperatures; this was due to asphalt's temperature-dependent elastic moduli.

Gainesville, Florida, Testing

The scanning SASW results from the Florida Interstate are presented graphically in Volume 3, Chapter 3 in 50-ft-long sections. The results are presented as surface wave velocity plots at depths from 0.1 to 0.7 ft (1.2 to 8.4 in.) from the surface. The surface wave velocities are illustrated by using a color scale ranging from 1,000 to 3,500 ft/s. In general, the higher the surface wave velocity, the better the condition of the asphalt pavement. The surface wave velocities from data measured on the NCAT Pavement Test Track were higher because the pavement was cooler and less distressed.

Overall, there were three categories of test results observed from the Florida test site, as follows:

- Two percent of the test locations evaluated had a relatively constant and high (≥3,500 ft/s) surface wave velocity from depths of 0.1 to 0.7 ft (1.2 to 8.4 in.). This condition indicates sound pavement.
- The majority (about 93%) of the test locations evaluated had a sharp drop (>500 ft/sec) of surface wave velocity between 0.2 and 0.4 ft (2.4 and 4.8 in.). The location of the drop is likely the depth of debonding or a thin layer of low-velocity (low-strength) material.
- Approximately 5% of the test locations evaluated had a slow drop of surface wave velocity, indicating degradation of the pavement at greater depths.

Significant amounts of surface distress were observed on the test pavement, but the majority of the data had relatively high surface wave velocities (>3,500 ft/s) near the pavement surface.

In general, the conditions of all locations within the 2,000-ft-long section along I-75 were similar, with the majority of the scanning SASW data indicating either possible debonding or an existence of a thin layer of low-strength material at depths between 0.2 and 0.4 ft (2.4 and 4.8 in.). In addition, the pavement along the center of the lane seemed to be in better condition than that of the wheelpaths. The general condition of the pavement in the right wheelpath (RWP) appeared to be in worse condition when compared to the left wheelpath (LWP). It should be noted that the Florida pavement was rough with exposed aggregate when compared to the smooth experimental sections of the NCAT Pavement Test Track.

Pittsburg, Kansas, Testing

The scanning SASW test results from the Kansas test site are presented graphically in Volume 4, Chapter 4, in 50-ft-long sections. The surface wave velocities are illustrated with a color scale ranging from 1,000 to 3,000 ft/s.

Overall, the majority of the measured data along the US-400 test site had relatively high surface wave velocities (>3,000 ft/s) near the pavement surface (<0.3 ft deep) and decreasing velocities with depth, thus indicating weaker underlying materials. The overall data interpretation is that the pavement likely had a relatively new asphalt overlay in good condition with older underlying pavement composed of weaker materials with a widely variable condition. In some areas, the velocity decrease with depth was gradual and interpreted as an expected result of newer materials overlying older material. The drop in the surface wave velocity was typically steady, indicating a more gradual change in material strength with depth. However, in some areas, the velocity decrease was sharp and severe, indicating poor condition of the underlying materials. The degree of change appeared severe with velocities at depths of 0.4 to 0.7 ft (4.8 to 8.4 in.), or less than half of the velocity at the pavement's surface.

More detailed analysis along the Kansas test site is described as follows:

- 0 to 160 ft. The pavement was a concrete bridge deck, which had velocities far above the color scale maximum of 3,000 ft/s.
- 160 to 210 ft. This section had relatively high velocities throughout the pavement and exhibited less of a velocity decrease with depth. This outcome may indicate a stiffer subbase preparation for the bridge approach slabs.
- 210 to 350 ft. In relation to much of the Kansas test segment, this area appeared to be in fair condition with slightly lower velocities and velocity values decreasing with depth.
- 350 to 1,000 ft. This section showed significant degradation with depth in the left half of the lane. As noted previously, the surface layer had reasonably sound velocities, and the lower layers had significantly lower velocities.
- 1,000 to 2,200 ft. The degradation in this section was similar to that in the previous section but extended across the full lane width. The surface layer had reasonable surface wave velocities, which then drastically decreased with depth.
- 2,200 to 2,500 ft. This section measured relatively high velocities throughout the cross section and was considered one of the best areas of the test site.
- 2,500 to 3,100 ft. The degradation in this section extended across the full lane width. The surface wave velocities decreased with depth.

- 3,100 to 3,285 ft. This section had relatively high surface wave velocities throughout the cross section and was considered one of the best areas of the test site.
- 3,285 to 3,495 ft. The surface wave velocities decreased with depth, showing degradation extending across the full lane width.
- 3,495 to 3,600 ft. This section also had relatively high surface wave velocities throughout the cross section and was considered one of the best areas of the test site.

Technology Implementation Status

Technical briefs on SASW and IE are provided in Appendices B and C, respectively. The briefs describe the required features of these NDT technologies on the basis of results of this study. Each technical brief describes the basic principle of the technology, lists the NDT hardware and operating parameters, recommends data collection and analysis requirements, and lists advantages and limitations. As SASW and IE technologies advance, these technical briefs will need to be revised to reflect those improvements.

The field testing results indicate that the Olson Engineering scanning IE/SASW system is able to locate delaminations or stripping or both at a variety of depths. The device can complete lane-width testing in two passes while operating at a walking speed. One lane mile of pavement can be scanned in 1 to 2 h.

The IE/SASW scanning system is a prototype device and is not ready for commercial use. There have been only a limited number of trials of the improved system in the field. Hardware components should be consolidated to simplify assembly. The data interpretation and analysis software requires technical expertise and experience to operate. Additional software is needed to automate the data interpretation to reduce the data analysis time.

The testing speed is a significant improvement over manual point testing but still needs to be improved to meet the SHRP 2 project objective. The system can determine the depth of the pavement material discontinuity but cannot measure the condition of the pavement below the discontinuity.

Uncontrolled Field Testing of the LWD

Technology Improvements

There were no modifications or technology improvements to the LWD for the field testing in Florida and Kansas. The drop weight used for the LWD during testing was 22 lb, and the spacing of the accelerometers was 6 in. The LWD was tested in the field because the equipment was readily available, relatively simple to operate, and added no cost to the project. Also, the LWD had shown some promise for at least being able to help identify areas of delamination and stripping at point locations. Measured deflections from accelerometers D1, D2, and D3 were used for the analysis.

Uncontrolled Field Evaluation

Testing in Gainesville, Florida, took place on March 1, 2011. The air temperature ranged from approximately 65°F to 75°F throughout the testing time. The locations of 10 core samples were determined within the predetermined 2,000-ft test lane on the basis of results of the GPR testing conducted previously. The LWD was tested at each core location before the samples were cut and removed. The testing procedure included operating the LWD on top of the core hole area, moving and testing the LWD approximately 3 ft behind the core hole area, moving and testing the LWD approximately 3 ft to the left or right of the core hole area (depending on whether the core area was in the right or left wheelpath), and moving and testing the LWD approximately 3 ft in front of the core hole area. Each test location had a minimum of three test repeats to obtain a representative average.

The testing in Pittsburg, Kansas, took place on April 26, 2011, when the air temperature ranged from approximately 50°F to 60°F. Previous GPR testing and analysis recommended six locations for extracting core samples within the predetermined 3,600-ft test lane. The same basic procedure of testing the LWD on and around a 3-ft perimeter of each core hole area, as conducted in Florida, was performed in Kansas.

Evaluation Results

The LWD was operated at and around each predetermined core hole area at each test site before the core samples were removed from the pavement. Ten cores were extracted from the test site in Florida. Each of the 10 core samples was intact when removed from the pavement, indicating full bond. Figure 3.27 gives the deflection results of the LWD tests at and around each core hole area. The tests labeled with a 1 after the core hole number (e.g., 1-1, 2-1, 3-1) are the results of the LWD being tested directly on top of where the core sample was to be removed. The red horizontal lines seen on Figure 3.27 are the averages of D1 (the accelerometer directly under the center of loading) with each core location. It was difficult to analyze the results since none of the core samples showed signs of stripping or delamination.

Six core sample locations were identified for removal in Kansas. Every core sample crumbled when removed from the pavement, thus indicating stripping. Figure 3.28 gives the deflection results of the LWD at and around each of the six core hole areas. An attempt to obtain good pavement baseline data was made inside the 3,600-ft-long test area; however,

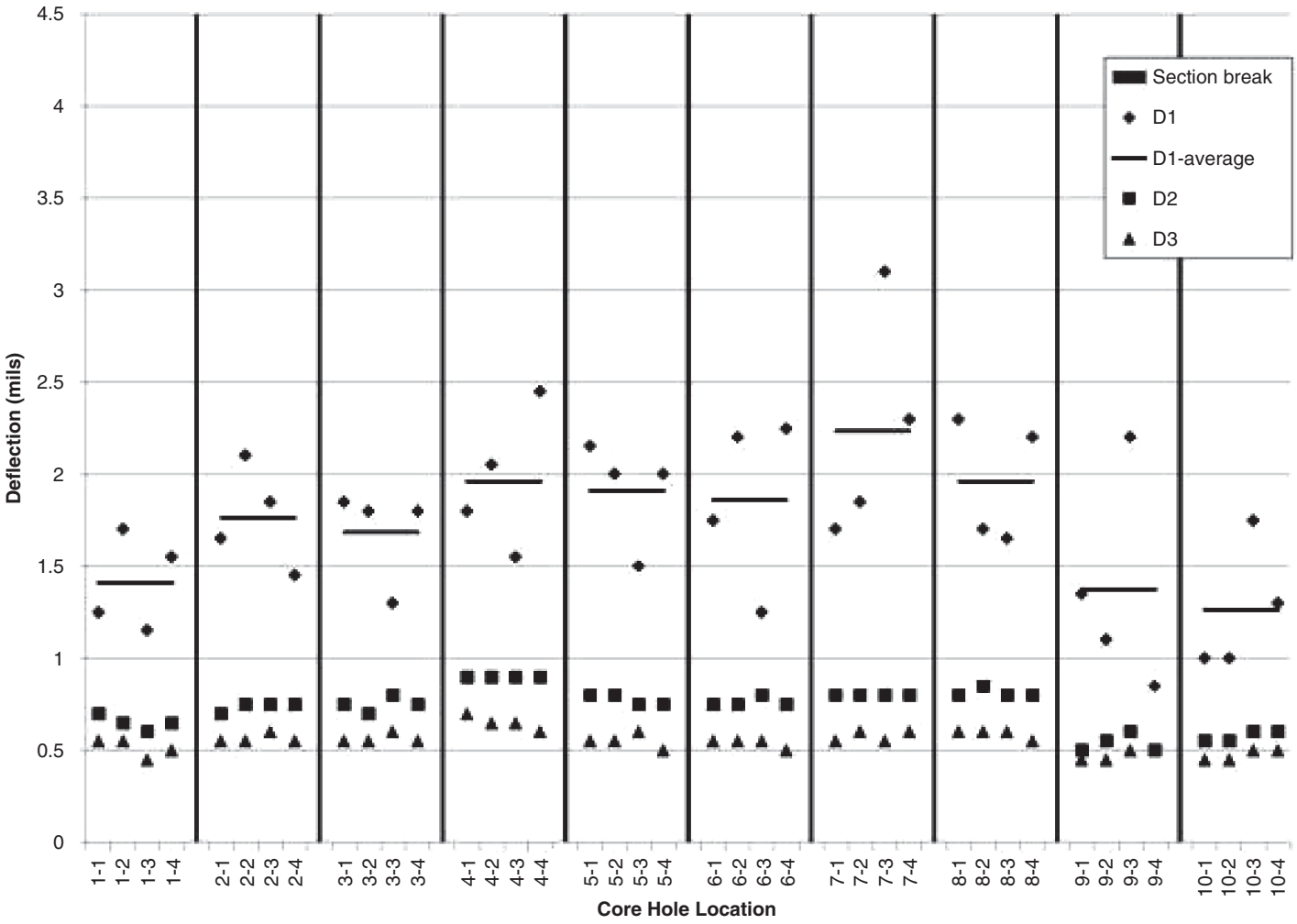

Figure 3.27. LWD deflection results on I-75 in Florida.

the core samples that were removed from the pavement all showed signs of delamination. Thus, there was no comparison for data measured with the LWD.

Both the Florida and Kansas sites consisted of thick asphalt pavement. The thickness of the Kansas pavement (13.5 in.) would typically result in lower LWD deflection values in comparison to the Florida pavement (9.0 in.). The higher deflections on the Kansas pavement demonstrate the ability of LWD to identify the presence of a severe discontinuity. Unfortunately, a sound pavement section was not tested on the Kansas site to verify the difference between sound and delaminated pavement for a typical site specific evaluation.

Technology Implementation Status

The LWD is easily portable, commercially available, and widely used. However, the device is a point-load system and did not meet the SHRP 2 project objective. The LWD is capable of determining changes in pavement stiffness but is not able to determine the causes of stiffness changes or the depth of stiffness changes.

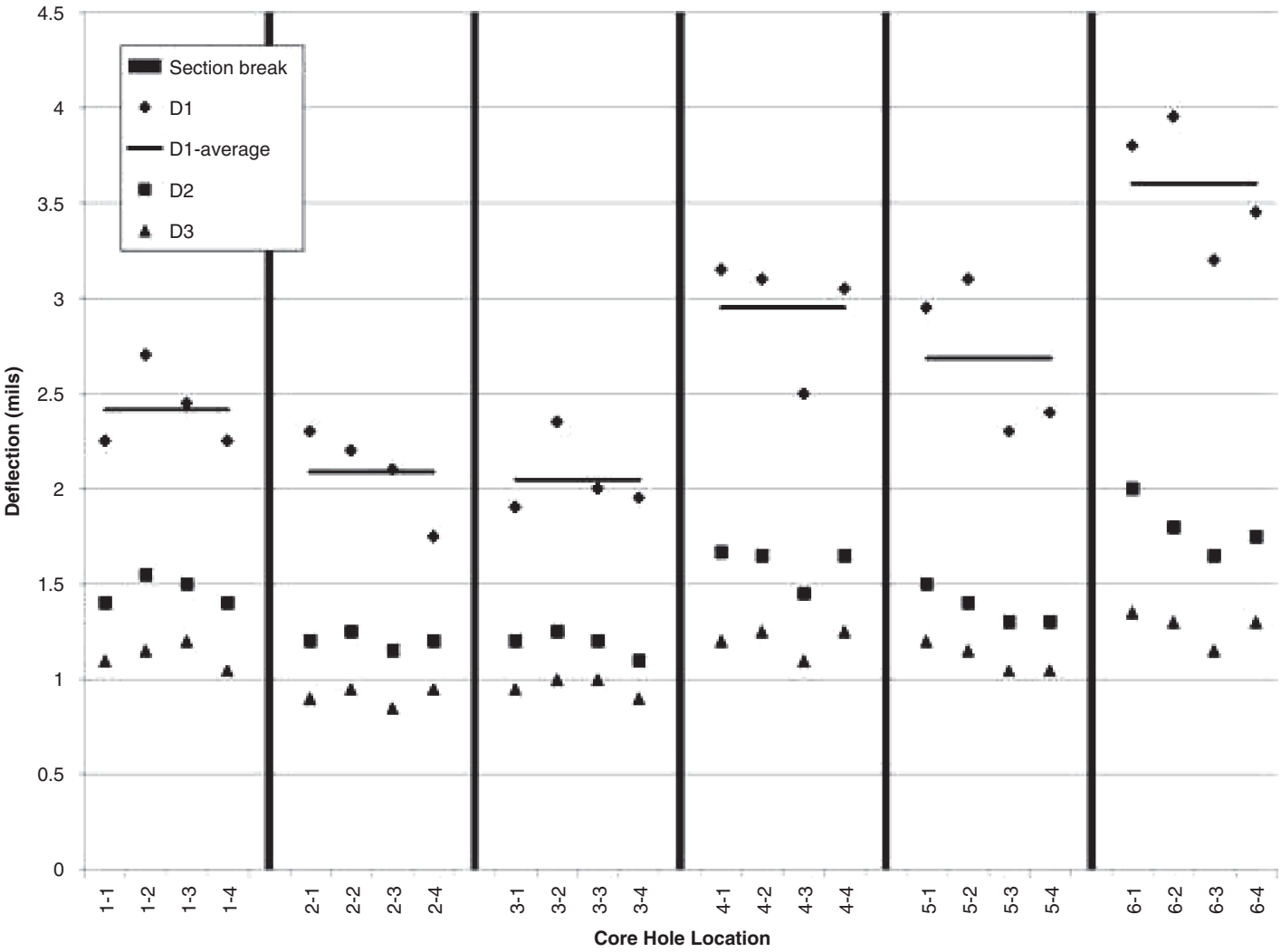

Figure 3.28. LWD deflection results on US-400 in Kansas.

CHAPTER 4

Conclusions and Recommendations

Conclusions

NDT hardware to measure changes in pavement response is available. GPR is the only NDT technology that is currently capable of testing full lane width and at moderate testing speed. Advances in mechanical wave NDT equipment significantly reduce the testing time but are limited to testing at speeds of less than 5 mph.

Software to analyze the data is available and requires a highly trained technician. The level of automated data analysis must be improved to reduce the manual time required to obtain results.

None of the NDT technologies can conclusively distinguish between types of pavement discontinuities. The measurement identifies a discontinuity, or change, in the pavement condition, but cannot determine from the measurement why the change occurred. GPR, IE, and SASW each use a unique signal measurement that is influenced by the pavement condition. The technician will need to understand how the pavement condition influences the signal. Coring will still be required to confirm the nature of the discontinuity. None of the NDT technologies is capable of identifying partial or no bond due to inadequate tack coat during construction.

GPR can identify variations in the pavement, isolate the depth of a discontinuity in the pavement, and provide a relative degree of severity. Severe conditions, such as stripping, can be observed with conventional analysis software. Detecting debonding between asphalt layers is only possible when there is moisture trapped in the debonded area between the layers using current analysis methodology. Software to quantify the extent of discontinuities over a large survey area is needed.

IE can identify variations in the pavement below a 4-in. depth, but confident analysis requires the HMA to be cool and stiff. The measurement has limited ability to provide the degree of severity and cannot measure pavement condition below the top of the discontinuity.

SASW can identify variations in the top 7 in. of the pavement, provided the analysis uses a reasonable value for the stiffness of the pavement. Like IE, the SASW measurement has limited ability to provide the degree of severity and cannot measure pavement condition below the top of the discontinuity.

GPR, IE, and SASW can be valuable project-level tools used independently or in series. Table 4.1 provides a summary of the features of the NDT technologies that were further developed as a part of this study. As the NDT industry continues to improve the hardware and software, these NDT tools will become more effective tools for pavement evaluation. For example, data analysis software development is needed to make NDT a network-level tool for detecting delamination in HMA pavements.

Recommendations

On the basis of results of this study, the following recommendations can be made. These recommendations are based solely on the NDT technologies available but should not preclude other innovative approaches as they develop.

1. GPR demonstrated full lane-width testing and IE/SASW improved its lane width capability from a width of 2 ft to a width of 6 ft. NDT manufacturers should continue to develop their equipment to provide testing hardware that can measure full-lane width. The hardware development must include the ability to narrow the width of the equipment during transport from site to site for the safety of both equipment and other vehicles.
2. GPR and SASW technologies require an extensive amount of manual data analysis. NDT manufacturers should continue to improve the data analysis software with the goal of providing real-time results that would be valuable for project- and network-level pavement

Table 4.1. Summary of Improved NDT Technologies

Technology	GPR	SASW	IE
Measurement width	Full-lane width	Half-lane width	Half-lane width
Measurement speed	Up to 40 mph	Less than 5 mph	Less than 5 mph
Effective measurement depth	Lower than top 2 in.	0 to 7 in.	4 to 12 in. (for cold-stiff HMA)
Analysis software	Manual = complicated; some automated features	Manual = complicated	Automated = real time

assessment. Software to provide real-time IE results is available.

3. If highway agencies expressed an interest in applying NDT for pavement evaluation, the NDT industry would see market potential and continue to develop its equipment.
4. GPR equipment should have an array of antennae and frequency sweep pattern ranging up to 3 GHz. Use GPR without a lane closure to locate discontinuities in a pavement. Operate the GPR equipment full-lane width at moderate travel speed to perform a preliminary assessment of HMA pavement condition. The results of the GPR analysis will assist engineers in identifying pavement sections that require a more intensive evaluation.
5. IE/SASW equipment can be built as multiple unit pairs in a towing package. Use IE and SASW within a lane closure to locate the depth of pavement discontinuities. This equipment costs less than a lane-width GPR antenna full package does, but the data collected are also less comprehensive. IE and SASW can be used to supplement GPR analysis.
6. Highway agencies might consider research funding to support development of software for project-level and network-level analysis.
7. Many highway agencies operate FWD equipment. Research funding should be considered to explore further the use of FWD time history data as an NDT tool for identifying pavement discontinuities.

References

Al Hakim, B., R. Armitage, and N. Thom. 1998. Pavement Assessment Including Bonding Condition: Case Studies. *Proc., 5th International Conference on Bearing Capacity of Roads and Airfields,* University of Trondheim, Trondheim, Norway, pp. 439–448.

Al-Qadi, I. L., S. Lahouar, K. Jiang, K. McGhee, and D. Mokarem. 2005. Validation of Ground Penetration Radar Accuracy for Estimating Pavement Layer Thicknesses. Presented at 84th Annual Meeting of the Transportation Research Board, Washington, D.C.

Armitage, R. J., M. R. Kruntcheva, and M. R. Willett. 2000. Trials of the Portable Seismic Pavement Analyzer (PSPA). *Report Prepared for Highways Agency, Pavement Engineering Group.* Scott Wilson Pavement Engineering, Nottingham, United Kingdom.

Armitage, R., M. Kruntcheva, and M. Willett. 2000. Trials of the Portable Seismic Pavement Analyzer. *Report Prepared for Highways Agency, Pavement Engineering Group.* Scott Wilson Pavement Engineering, Nottingham, United Kingdom.

Baker, M., K. Crain, and S. Nazarian. 1995. *Determination of Pavement Thickness with a New Ultrasonic Device.* Research report, 1966-1, Center for Highway Materials Research, University of Texas at El Paso.

Balasundaram, A., Z. Ahmed, R. Kohlberger, and D. Hoffman. 2006. The Integrated Use of GPR and Conventional Methods for Continuous Pavement Condition Investigations: A Case Study of the QEW Rehabilitation and Widening Project. *Proc., 2006 Annual Conference of the Transportation Association of Canada,* Charlottetown, Prince Edward Island.

Bognacki, C. J., A. Frisvold, and T. Bennert. 2007. Investigation of Asphalt Pavement Slippage Failures on Runway 4R-22L, Newark International Airport. Presented at FAA Worldwide Airport Technology Transfer Conference, Atlantic City, N.J.

Canestrari, F., G. Gerrotti, M. N. Portl, and E. Santagata. 2005. Advanced Testing and Characterization of Interface Shear Resistance. In *Transportation Research Record: Journal of the Transportation Research Board, No. 1929,* Transportation Research Board of the National Academies, Washington, D.C., pp. 69–78.

Carino, N. J. The Impact-Echo Method: An Overview. 2001. *Proc., Structures Congress and Exposition,* Reston, Va.

Carino, N. J., and M. Sansalone. 1992. Detecting Voids in Metal Tendon Ducts Using the Impact-Echo Method. *ACI Materials Journal,* Vol. 89, No. 3, pp. 296–303.

Celaya, M., and S. Mazarian. 2007. Stripping Detection in Asphalt Pavements with Seismic Methods. Presented at 86th Annual Meeting of the Transportation Research Board, Washington, D.C.

Celaya, M., P. Shokouhi, and S. Mazarian. 2007. Assessment of Debonding in Concrete Slabs Using Seismic Methods. Presented at 86th Annual Meeting of the Transportation Research Board, Washington, D.C.

DeJong, D. L. 1973. *Computer Program: BISAR.* Royal/Shell Laboratory, External Report AMSR 0006.73, Amsterdam, Netherlands.

Federal Highway Administration, U.S. Department of Transportation. 2008. FOCUS: Rolling Wheel Deflectometer: A High-Speed Deflection Device to Improve Asset Management. Website: www.tfhrc.gov/FOCUS/may08/02.htm. Accessed August 30, 2008.

Gomba, S. M. 2004. *Evaluation of Interlayer Bonding in Hot Mix Asphalt Pavements.* MS thesis, Rowan University, Glassboro, N.J.

Grote, K., S. Hubbard, J. Harvey, and Y. Rubin. 2004. Evaluation of Infiltration in Layered Pavements Using Surface GPR Reflection Techniques. *Journal of Applied Geophysics* 57, October 26, pp. 129–153.

Gucunski, N., and A. Maher. 2000. Final Report FHWA NJ 2000-05. Rutgers University, Piscataway, N.J.

Gucunski, N., C. Rascoe, and A. Maher. 2008. 3-D GPR in Transportation Infrastructure Evaluation. Presented at 21st Symposium on the Application of Geophysics to Engineering and Environmental Problems (SAGEEP 2008), Philadelphia, Pa.

Hachiya, Y., and K. Sato. 1997. Effect of Tack Coat on Bonding Characteristics at Interface between Asphalt Concrete Layers. *Proc., 8th International Conference on Asphalt Pavements,* pp. 349–362.

Hammons, M. I., H. Von Quintus, K. Maser, and S. Nazarian. 2005. *Detection of Stripping in Hot Mix Asphalt.* Final Report. Applied Research Associates, Gainesville, Fla.

Hammons, M. I., H. Von Quintus, G. M. Geary, P. Y. Wu, and D. M. Jared. 2006. Detection of Stripping in Hot Mix Asphalt. Presented at 85th Annual Meeting of the Transportation Research, Board, Washington, D.C.

Holt, F., and R. Eckrose. 1989. Application of Ground Penetrating Radar and Infrared Thermography to Pavement Evaluation. *Nondestructive Testing of Pavements and Backcalculation of Moduli.* ASTM STP 1026. American Society for Testing and Materials, pp. 105–115.

Kennedy, C., and N. Lister. 1980. The Development of Slip-Planes in Rolled Asphalt Surfacings. In *Experimental studies of slippage,* Institution of Civil Engineers, London, pp. 31–56.

Khandal, P., and I. Rickards. 2001. *Premature Failure of Asphalt Overlays from Stripping: Case Histories.* NCAT Report 01-01, p. 40.

Kim, Y., J. S. Lutif, A. Bhasin, and D. N. Little. 2008. Evaluation of Moisture Damage Mechanisms and Effects of Hydrated Lime in Asphalt Mixtures through Measurements of Mixture Component Properties and Performance Testing. *Journal of Materials in Civil Engineering,* Vol. 20, No. 10, pp. 659–667.

Kruntcheva, M., A. Collop, and N. Thom. 2005. Effect of Bond Condition on Flexible Pavement Performance. *Journal of Transportation Engineering,* Vol. 131, No. 11, pp. 880–888.

Kruntcheva, M., A. Collop, and N. Thom. 2004. Feasibility of Assessing Bond Condition of Asphalt Concrete Layers with Dynamic Nondestructive Testing. *Journal of Transportation Engineering,* Vol. 130, No. 4, pp. 510–518.

Kruntcheva, M., A. Collop, and N. Thom. 2000. *The Portable Seismic Pavement Analyzer: Laboratory Trials.* Project Report PGR 2000-02, School of Civil Engineering, University of Nottingham, United Kingdom.

Kullkarni, M. B. 2004. *Effect of Tack and Prime Coats, and Bag-house Fines on Composite Asphalt Pavements.* PhD dissertation, North Carolina State University, Raleigh.

Leng, Z., H. Ozer, I. L. Al-Qadi, and S. H. Carpenter. 2008. Interface Bonding between Hot-Mix Asphalt and Various Portland Cement Concrete Surfaces: Laboratory Assessment. In *Transportation Research Record: Journal of the Transportation Research Board, No. 2057,* Transportation Research Board of the National Academies, Washington, D.C., pp. 46–53.

Lepert, P., J. Poilane, and M. Villard-Bats. 1992. Evaluation of Various Field Measurement Techniques for the Assessment of Pavement Interface Condition. *Proc., 7th International Conference on Asphalt Pavements,* Vol. 3, pp. 224–237.

Liu, J., D. G. Zollinger, and R. L. Lytton. 2008. Detection of Delamination in Concrete Pavements Using Ground-Coupled GPR Technique. Presented at 87th Annual Meeting of the Transportation Research Board, Washington, D.C.

Maina, J. W., and K. Matsui. 2004. Developing Software for Elastic Analysis of Pavement Structure Responses to Vertical and Horizontal Surface Loading. In *Transportation Research Record: Journal of the Transportation Research Board, No. 1896,* Transportation Research Board of the National Academies, Washington, D.C., pp. 107–118.

Manning, D., and F. Holt. 1987. Detecting Deterioration in Asphalt Covered Bridge Decks. In *Transportation Research Record 899,* TRB, National Research Council, Washington, D.C., pp. 10–21.

Maser, K. R. 2005. *Feasibility of Using Ground Penetrating Radar (GPR) for Pavements, Utilities, and Bridge.* Technical Report SD2005-05-F, South Dakota Department of Transportation, Pierre.

Maser, K. R. 2008. Integration of Ground Penetrating Radar and Infrared Thermography for Bridge Deck Condition Evaluation. *Proc., NDE/NDT for Highways and Bridges,* Oakland, Calif., pp. 67–74.

Maser, K. R. 2003. Non-Destructive Measurement of Pavement Layer Thickness. Report FHWA/CA/OR-2003/03 prepared for the California Department of Transportation, Sacramento.

Maser, K. R. 1999. Pavement Characterization Using Ground Penetrating Radar: State of the Art and Current Practice. In *Nondestructive Testing of Pavements and Backcalculation of Moduli,* Vol. III. ASTM STP 1375, American Society for Testing and Materials, pp. 313–326.

Maser, K., and I. Sande. 1999. Application of Ground Penetrating Radar for Evaluation of Subsurface Airfield Pavement Conditions in Denmark and Norway. *Proc., 1999 FAA Airport Technology Transfer Conference,* Atlantic City, N.J.

Maser, K. R., and J. Puccinelli. 2009. *Ground Penetrating Radar (GPR) Analysis.* Technical Report FHWA/MT-09-005/8201, Montana Department of Transportation, Helena.

Meggers, D., and N. Worley. 2000. *Comparison of Ground Penetrating Radar Bridge Deck Evaluation and Repair: Polk-Quincy Viaduct I-70, Topeka, Kansas.* Kansas Department of Transportation, Topeka.

Mejia, D., M. Celaya, S. Iyer, C. Rao, P. Shokouhi, and S. Nazarian. 2008. *A Work Plan toward Evaluation of Technologies to Assess Presence and Extent of Delamination of HMA Airfield Pavements.* AAPTP Project 06-04, Center for Transportation Infrastructure Systems, El Paso, Texas.

Mohammad, L., M. A. Raqib, and B. Huang. 2002. Influence of Asphaltic Tack Coat Materials on Interface Shear Strength. In *Transportation Research Record: Journal of the Transportation Research Board, No. 1789,* Transportation Research Board of the National Academies, Washington, D.C., pp. 56–65.

Monem, T. A., A. A. Oloufa, and H. Mahgoub. 2005. *Asphalt Crack Detection Using Thermography.* University of Central Florida-Center for Advanced Transportation Systems Simulation (CATSS). Report No. ITC 108 A 2005-06-01.

Moropoulou, A., N. Avdelidis, M. Koui, and K. Kakaras. 2002. Flaw Detection and Evaluation of Airport Pavements by Means of Infrared Thermography. Website: www.flirthermography.com/media/Detection_Evaluation_Airport_Paving.pdf. Accessed October 31, 2007.

Moropoulou, A., N. P. Avdelidis, M. Koui, and K. Kakaras. 2000. *Flaw Detection and Evaluation or Airport Pavements by Means of Infrared Thermography.* National Technical University of Athens, Department of Chemical Engineering, Section of Materials Science and Engineering, Athens, Greece.

Munoz, D. 2009. *Finite Element Modeling of Nondestructive Test Methods Used for Detection of Delamination in Hot Mix Asphalt Pavements.* MS thesis, University of Texas at El Paso.

National Highway Institute (NHI). 2013. Hot-Mix Asphalt Pavement Evaluation and Rehabilitation. Training Course FHWA-NHI-131063, NHI, FHWA, Arlington, Va.

Nazarian, S. 2006. *Implementation of Seismic-Based Quality Management of Flexible Pavement.* Report FHWA/TX-05/5-1735-01-1. Center for Transportation Infrastructure Systems, El Paso, Texas.

Nazarian, S., M. Baker, and K. Crain. 1997. Assessing Quality of Concrete with Wave Propagation Techniques. *Materials Journal,* American Concrete Institute, Farmington Hills, Mich., Vol. 94, No. 4, pp. 296–306.

Nazarian, S., M. R. Baker, and K. Crain. 2003. Development and Testing of a Seismic Pavement Analyzer. SHRP-H-375, Strategic Highway Research Program, National Research Council, Washington, D.C.

Nazarian, S., V. Tandon, and D. Yuan. 2006. Mechanistic Quality Management of Asphalt Concrete Layers with Seismic Methods. *Journal of ASTM International,* Vol. II, No. 8, pp. 88–99.

Rister, B., C. Graves, and J. Creech. 2008. *Investigation of the Extended Use of Ground Penetrating Radar (GPR) for Measuring In-Situ Material Quality Characteristics.* University of Kentucky Transportation Center Report, No. KTC-08-31/SPR307-05-1F, Lexington.

Roberts, R., and F. Romero. 1998. High Resolution GPR Bridge Deck Evaluation Surveys. *Proc., International Conference on Corrosion and Rehabilitation of Reinforced Concrete Structures,* Orlando, Fla.

Romanoschi, S. A., and J. B. Metcalf. 2001a. Characterization of Asphalt Concrete Layer Interfaces. In *Transportation Research Record: Journal of the Transportation Research Board, No. 1778,* TRB, National Research Council, pp. 132–139.

Romanoschi, S. A., and J. B. Metcalf. 2001b. Effects of Interface Condition and Heavy Wheel Loads on Life of Flexible Pavement Structures. In *Transportation Research Record: Journal of the Transportation Research Board, No. 1778,* TRB, National Research Council, Washington, D.C., pp. 123–131.

Sangiorgi, C., A. Collop, and N. Thom. 2003. A Non-Destructive Impulse Hammer for Evaluating the Bond between Asphalt Layers in a Road Pavement. Presented at International Symposium (NDT-CE 2003) of Non-Destructive Testing in Civil Engineering, Berlin, Germany.

Sansalone, M., and W. Street. 1997. *Impact-Echo: Non Destructive Evaluation of Concrete and Masonry.* Bullbrier Press, Ithaca, N.Y.

Sansalone, M., and N. Carino. 1986. *Impact Echo: A Method for Flaw Detection in Concrete Using Transient Stress Waves.* Report NBSIR 86-3452. National Bureau of Standards, Gaithersburg, Md.

Sansalone, M. 1993. Detecting Delamination in Concrete Bridge Decks With and Without Asphalt Overlays Using an Automated Impact-Echo Field System. *Proc., International Conference on Nondestructive Testing in Civil Engineering,* British Institute of Nondestructive Testing, United Kingdom.

Scullion, T., and E. Rmeili. 1997. *Detecting Stripping In Asphalt Concrete Layers Using Ground Penetrating Radar.* Texas Transportation Institute Research Report 2964-S, College Station.

Sebally, P. E., D. Little, E. Y. Hajj, and A. Bhasin. 2007. Impact of Lime and Liquid Antistrip Agents on Properties of Idaho Hot-Mix Asphalt Mixture. In *Transportation Research Record: Journal of the Transportation Research Board, No. 1998,* Transportation Research Board of the National Academies, Washington, D.C., pp. 65–74.

Sebesta, S., and T. Scullion. 2003. Application of Infrared Imaging and Ground Penetrating Radar for Detecting Segregation in HMA Overlays. Presented at 82nd Annual Meeting of the Transportation Research Board, Washington, D.C.

Stroup-Gardiner, M., and E. R. Brown. 2000. *Segregation in Hot Mix Asphalt Pavements.* NCHRP Report 441. TRB, National Research Council, Washington, D.C.

Tashman, L., K. Nam, T. Papagiannakas, K. Willoughby, L. Pierre, and T. Baker. 2008. Evaluation of Construction Practices that Influence the Bond Strength at the Interface between Pavement Layers. *Journal of Performance of Constructed Facilities,* Vol. 22, No. 3, pp. 154–161.

Tschegg, K., G. Kroyer, D. Tan, S. Stanzl-Tschegg, and J. Litzka. 1995. Investigation of Bonding between Asphalt Layers on Road Construction. *Journal of Transportation Engineering,* Vol. 121, No. 4, pp. 309–316.

Tsubokawa, Y., J. Mizukami, and T. Esaki. 2007. Study on Infrared Thermographic Inspection of De-bonded layer of Airport Flexible Pavement. Presented at 2007 Worldwide Airport Technology Transfer Conference, Atlantic City, N.J.

Uzan, J., M. Livneh, and Y. Eshed. 1978. Investigation of Adhesion Properties Between Asphaltic Concrete Layers. *Proc., Association of Asphalt Paving Technologists,* Vol. 47, Lake Buena Vista, Fla., pp. 495–521.

Van Dam, T., K. Kirchner, M. Shahin, and E. Blackmon. 1987. *Consequence of Layer Separation on Pavement Performance.* Report DOT/FAA/PM-86/48. U.S. Department of Transportation, Federal Aviation Administration.

Washer, G., R. Fenwick, B. Naveen, and J. Harper. 2009. Effects of Environmental Variables on the Infrared Imaging of Subsurface Features in Concrete Bridges. Presented at 88th Annual Meeting of the Transportation Research Board, Washington, D.C.

West, R. C., J. Zhang, and J. Moore. 2005. *Evaluation of Bond Strength between Pavement Layers.* NCAT Report 05-08, National Center for Asphalt Technology, Auburn University, Auburn, Ala.

Willis, J. R., and D. H. Timm. 2007. Forensic Investigation of Debonding in a Rich-Bottom Pavement. In *Transportation Research Record: Journal of the Transportation Research Board, No. 2040,* Transportation Research Board of the National Academies, Washington, D.C., pp. 107–114.

Willoughby, K., J. Mahoney, L. Pierce, J. Uhlmeyer, K. Anderson, S. Read, S. Muench, T. Thompson, and R. Moore. 2001. *Construction-Related Asphalt Concrete Pavement Temperature Differentials and the Corresponding Density Differentials.* Research Report, Washington State Transportation Center (TRAC), Pullman.

Ziari, H. and M. Khabiri. 2007. Interface Condition Influence on Prediction of Flexible Pavement Life. *Journal of Civil Engineering and Management*, Vol. 13, No. 1, 2007, pp. 71–76.

APPENDIX A

Technical Brief: Ground-Penetrating Radar

Basic Principle

Ground-penetrating radar (GPR) sends high-frequency radio waves into the pavement from a moving antenna attached to a survey vehicle. The equipment can collect data at up to normal driving speeds. The GPR waves reflect back from layer boundaries and discontinuities within the pavement. Testing has shown that stripped asphalt concrete (AC) layers and debonded AC layers with trapped moisture will produce detectable reflections that are not normally seen with intact pavement layers. Semiautomated software to detect these reflections and map the areas of potential damage has been developed.

Equipment and Operation

The GPR system is implemented by using a multiantenna array. The purpose of the array is to collect equally spaced parallel lines of data simultaneously so that coherent areas of delamination can be identified and mapped. Figure A.1 shows an example of such equipment. Data is collected continuously while the system is driven along the surface of the pavement. The data collection is typically triggered by using a distance measuring instrument (DMI) mounted to the vehicle wheel or to an external distance wheel.

Equipment Specifications

Table A.1 lists equipment specifications for GPR systems.

Data Output and Display

The field operation and playback software should be capable of the following displays, as shown in Figure A.2:

- Direct time domain waveform (A-scan);
- Longitudinal profile for a given transverse offset (B-scan);
- Time/depth slice for a given time range;
- Transverse profile for a given location or station; and
- Output format should be a volume of data with amplitude as a function of x (longitudinal distance), y (transverse offset), and z (wave response time).

Data Collection Protocol

Because of the number of antennas and the data collection rate, this type of GPR system collects large volumes of data. For example, a 7-mi test section with data collected at 8 in., longitudinally and transversely, resulted in an 11-gigabyte file. For project-level work, it is recommended that the project be divided into 1- to 2-mi sections for data collection. The start and end points of data collection should be referenced with mile markers or other fixed reference points. Roadway features encountered during the survey (intersections, bridge decks, etc.) should be annotated with some type of manual markers in the data. The data should be observed visually during collection to ensure that the system is operating properly and that the expected features (e.g., AC layers) are appearing in the data. For network-level work, it would be desirable to relax the data density so that more area can be covered without generating overwhelming quantities of data. For example, if data were collected every 2 ft longitudinally and transversely, the coverage would be roughly 42 lane miles for an 11-gigabyte file.

Data Analysis

The objective of the analysis is to identify anomalous reflection activity within AC layers or at AC layer boundaries, or both, that may be associated with asphalt mixture stripping or moisture infiltration into debonded areas. This evaluation can be carried out qualitatively by looking at cross sections and depth slices of the GPR data, as shown in Figure A.2. To handle large volumes of data, as required for a typical project or network-level application, the analysis needs to be

Figure A.1. Example of full lane width GPR antenna array.

automated but may require some user interaction to identify the AC layers of interest in the GPR data. Once identified, these layers will be automatically tracked by the software. The results of the analysis should be a display of areas of potential delamination and stripping versus milepost or roadway station. A sample of this type of output is shown in Figure A.3.

Equipment Availability and Cost

Currently, one manufacturer (3d-Radar) makes a complete GPR system of the type outlined in the specifications. The 3d-Radar system has a provisional license for selected use, but has not yet received full approval by the FCC for sale in the United States. Two other manufacturers—Geophysical Survey Systems, Inc. (GSSI) and MALA—deliver a multichannel

Table A.1. GPR System Equipment Specifications

System Type	Array of Multiple, Air-Launched Antenna Elements Lined Up Transverse to the Direction of Travel
Frequency Range	
Impulse radar systems	Center frequency of pulse: 2.0 GHz (minimum); 10 db limits: 1.0–3.0 GHz
Frequency sweep radar systems	Frequency range: up to 3.0 GHz
Lateral spacing of antenna elements	1.5 ft (maximum)
Lateral coverage per pass	12 ft (full lane width)
Longitudinal data collection rate	1 scan per foot per antenna element (minimum)
Travel speed during data collection	20 mph (minimum)
Travel speed during mobilization	Posted speed limit
Real-time display	B-scan for selected antenna elements
System monitoring and control	Within survey vehicle
Data collection rate	Data collection triggered on distance when a DMI is used
Spatial reference	Vehicle DMI or GPS, or both

Note: GPS = Global Positioning System.

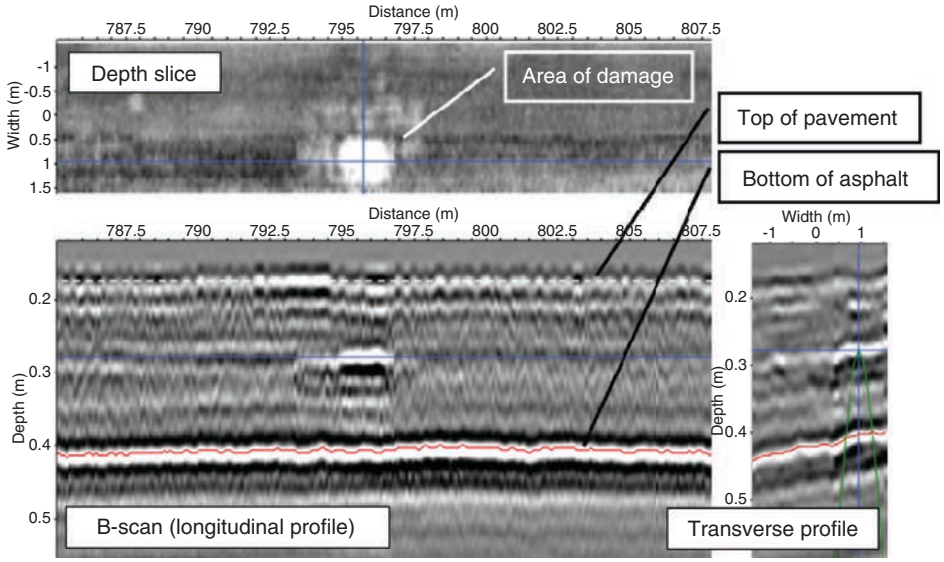

Figure A.2. Sample display of data.

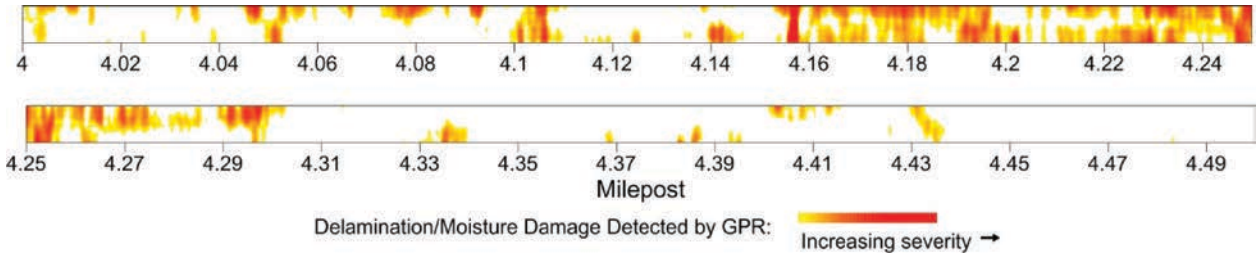

Figure A.3. Sample output of data processing.

GPR system that can meet the specifications. However, neither GSSI nor MALA offers the full lane-width configuration, with antenna array and mechanical support, as a standard product at this time. It is possible, however, for a potential user to purchase the necessary components and configure a system. The estimated cost of each of these GPR systems is approximately $200,000.

Advantages and Limitations

The primary advantage of a GPR system is its ability to collect three-dimensional (3-D) subsurface condition information while moving at speeds that do not require lane closures. GPR is particularly sensitive to moisture, so a GPR system can pick up areas of moisture infiltration and damage. A second advantage of a GPR system is its multifunctional capability. The system can collect data relative to the entire pavement structure, including base, subgrade, shallow drainage structures, utilities, and bridge approaches.

The principal limitation of GPR is that it is not capable of detecting physical debonding between pavement layers. GPR detects electromagnetic properties, not mechanical properties. A second limitation is the complexity of the data analysis. More automated software analysis tools are needed to examine the large 3-D data files.

APPENDIX B

Technical Brief: Spectral Analysis of Surface Waves

Basic Principle

In the spectral analysis of surface waves (SASW) test, the pavement is struck with a short, high-frequency source, thus creating a surface wave that propagates away from the source. Two receivers spaced near the source, but at different distances, detect the arriving surface wave, and data from these two locations are used to calculate the curve of wavelength versus frequency (dispersion curve) for the surface wave. Because wavelength is related to depth of penetration, this dispersion curve is interpreted as a relationship between surface wave velocity and depth. A sharp drop in velocity at a particular depth is indicative of a discontinuity in the pavement structure, which would be associated with delamination (debonding) and stripping. Automated equipment has been developed to carry out this test continuously at a slow walking speed. Software to analyze the data is partially automated but still requires considerable user interaction.

Equipment and Operation

The SASW system consists of an array of rotating sensor wheel pairs, with each pair of wheels spaced approximately 2 ft laterally from the adjacent pair. The purpose of the array is to collect equally spaced parallel lines of data simultaneously so that coherent areas of delamination can be identified and mapped. Figure B.1 shows an example of such equipment. In that example, each wheel is approximately 1 ft in diameter and is mounted with six displacement sensors and impactor pairs. Each sensor/impactor pair is spaced at 6 in. intervals around the circumference of the wheel. Each sensor wheel pair is coupled with a rubber isolated axle. Data are collected continuously at 6-in. intervals while the system rolls along the surface of the pavement. The data collection for each wheel is independently triggered, and the position of the collected data is obtained by using a distance measuring instrument (DMI) mounted to the vehicle wheel or to an external distance wheel. Equipment specifications are listed in Table B.1.

Data Output and Display

The field operation and playback software should be capable of the following displays:

- Direct time domain waveforms from each of the two receivers (Figure B.2);
- Dispersion curve for each wheel pair (Figure B.3);
- Waterfall plot of dispersion curves collected versus distance covered for each wheel pair; and
- Output format should be a volume of data with surface wave velocity as a function of x (longitudinal distance), y (transverse offset), and z (depth).

Data Collection Protocol

Due to the relatively low collection speed, this system should be used exclusively for project-level work, with a focus on specific locations and areas of concern. The start and end points of data collection should be referenced with mile markers or other fixed reference points. Landmarks encountered during the survey (e.g., intersections, bridge decks) should be annotated with some type of manual marker in the data. The data should be observed visually during collection to ensure that the system is operating properly and that the expected features are appearing in the data.

Data Analysis

The objective of the analysis is to identify locations where a sharp drop in surface velocity with depth is associated with delamination (debonding) of an asphalt layer from the layer

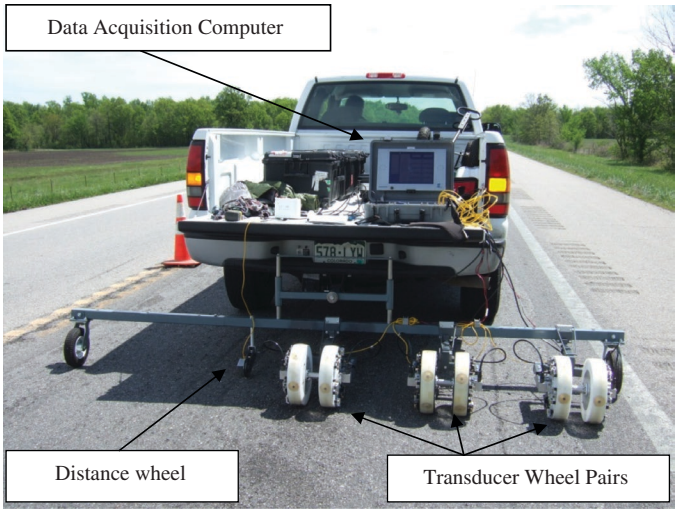

(a)

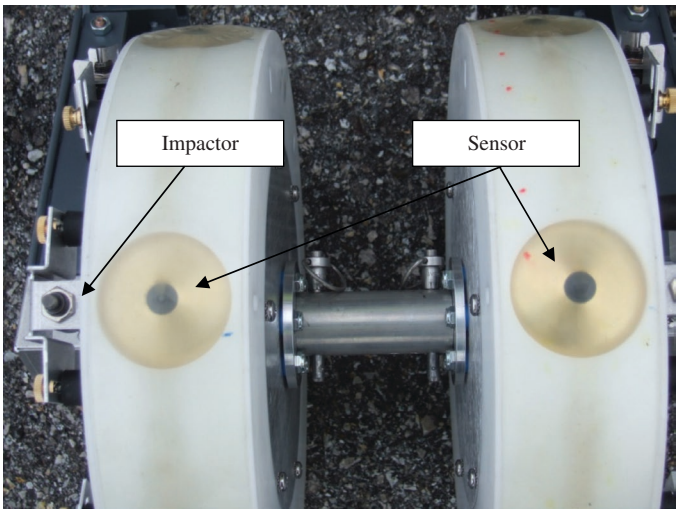

(b)

Figure B.1. IE/SASW scanning system (test setup of 6-in. transducer spacing and 2 ft between pairs): (a) layout of sensor wheel array and (b) detail of sensor wheel pair.

below. To accomplish this task, the surface wave profiles at each location (Figure B.3) are assembled as a full volume of data, where x and y are the coordinates of the test point, z is the wavelength (or depth), and the value at point (x, y, z) is the surface wave velocity. Surface wave velocities can be presented for each selected depth range (or "depth slice"), and the velocity values within the slice are presented in grayscale. In the example in Figure B.4, velocities range from 3,000 ft/s (light gray) to 5,000 ft/s (black). The higher the surface wave velocity, the better the condition of the pavement. Anomalies can be seen as light spots where the velocities are lower. It is clear in this example that there is a sharp drop in velocity at

Table B.1. SASW Equipment Specifications

System Type	Array of Pairs of Rotating Sensor Wheels, Lined Up Transverse to the Direction of Travel
Sensor frequency response	Up to 50,000 Hz
Impact source input frequency	Up to 50,000 Hz
Lateral spacing between wheel pairs	Variable (2.0 ft typical)
Lateral coverage per pass	6 ft with three wheel pairs (half-lane width)
Longitudinal data collection rate	1 test per ft (minimum)
Travel speed during data collection	1 to 2 mph
Travel speed during mobilization	Posted speed limit
Real time display	Single wheel pair waveforms at reduced display rate
System monitoring and control	Within or outside survey vehicle
Data collection rate	Based on speed and sensor spacing on sensor wheel
Spatial reference	Vehicle DMI or external distance wheel

a depth of approximately 0.4 ft, suggesting a delamination at that depth.

Analysis of the depth slices shown in Figure B.4 can be labor-intensive. It would be desirable to have data analysis software that can automatically search through the volume of data, detect locations where there is a sharp drop in the velocity with depth, and report those locations and depths in a plan area map that can be readily interpreted by a highway engineer.

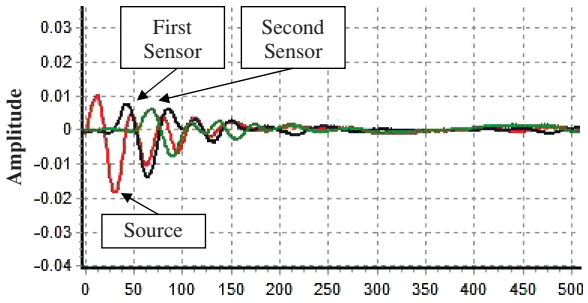

Figure B.2. Detected waveforms.

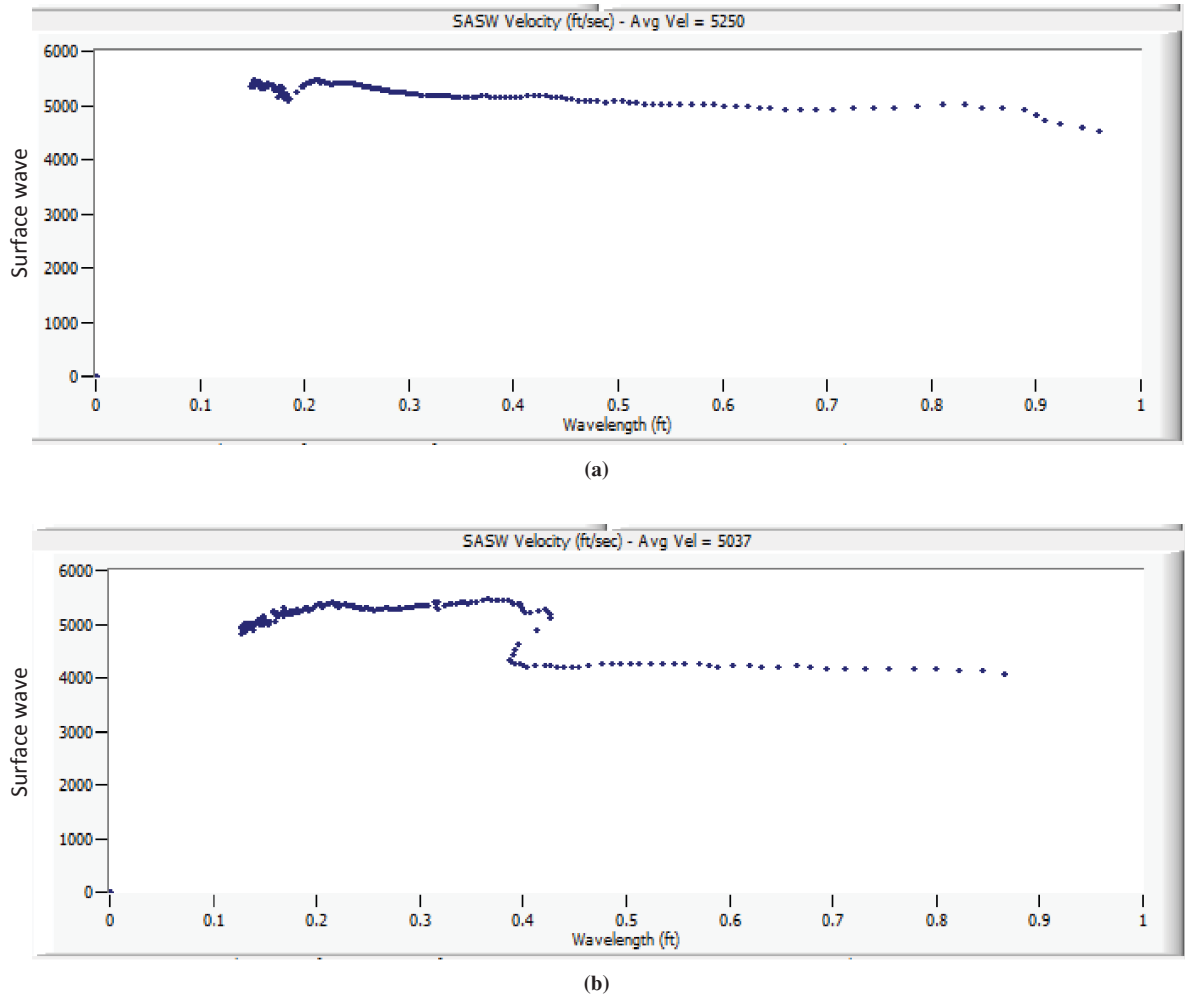

Figure B.3. Dispersion curves calculated from SASW data: (a) dispersion curve from sound pavement and (b) dispersion curve from pavement with debonding at depth of 5 in.

Equipment Availability and Cost

The SASW continuous scanning system discussed in this brief is not available commercially. A prototype system has been developed and tested by Olson Engineering. Also, the data interpretation and use of the analysis software in its current state require a fair amount of experience. An estimated cost of a fully operational system is not available.

Advantages and Limitations

The primary advantage of an SASW system is its ability to detect delamination (debonding) within asphalt pavement layers directly. The principal limitation is speed. The system is restricted to testing at walking speed and, thus, its application is limited to project-level analysis and diagnostic investigations.

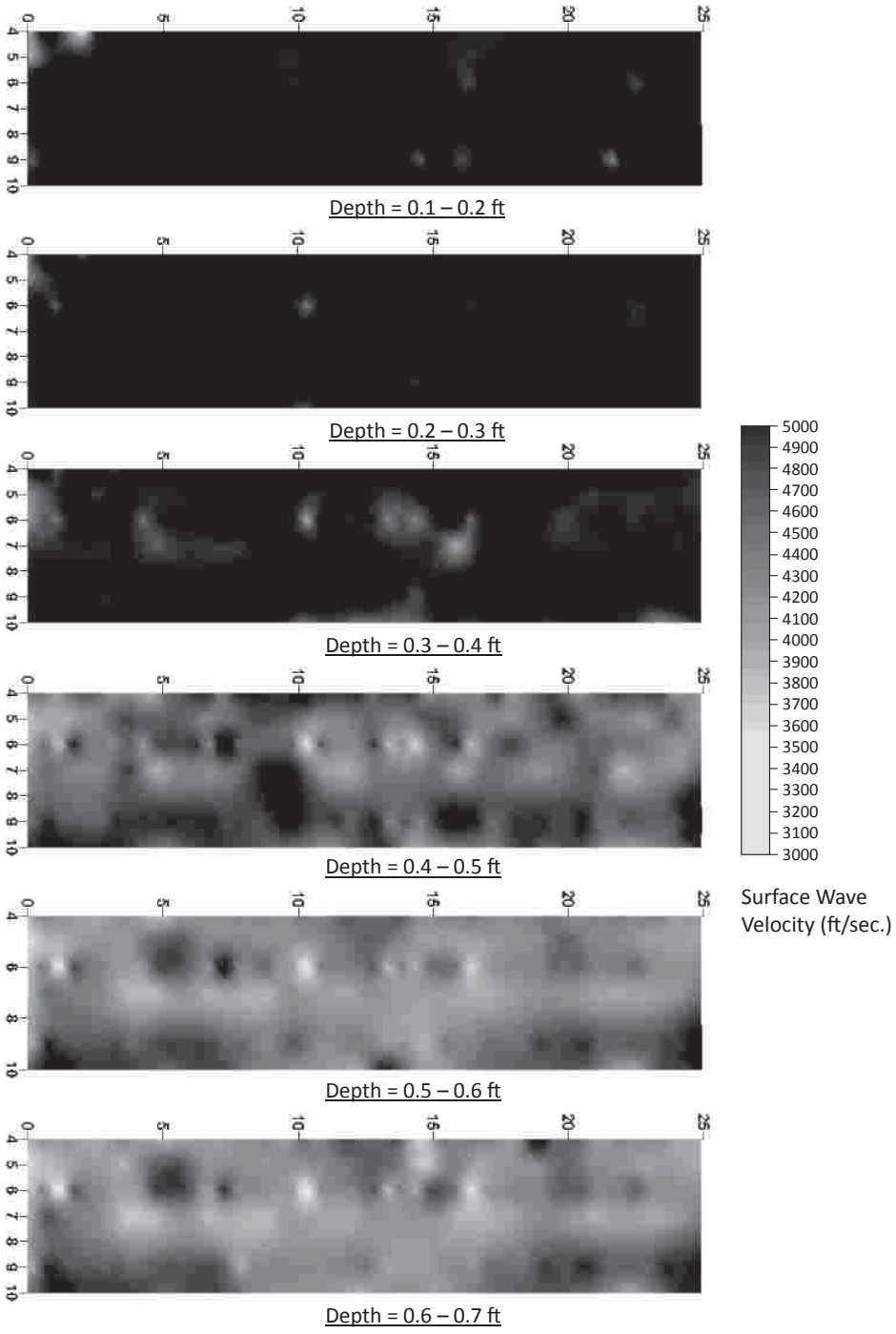

Figure B.4. Depth slices of SASW velocity versus depth data.

APPENDIX C

Technical Brief: Impact Echo

Basic Principle

Impact echo (IE) is a point test method that transmits a high-frequency mechanical (sound) wave into the pavement and measures the P-wave reverberation (echo) between the top and bottom surfaces. An impact source and receiver are placed adjacent to each other on the pavement surface. The amplitude of the reverberation detected by the receiver is converted into the frequency domain as amplitude versus frequency. For a homogeneous pavement layer, there is a resonant or dominant frequency directly proportional to the thickness of the pavement layer, according to the equation below. This resonant frequency is referred to as the "thickness resonance." The frequency data are typically converted into thickness by using the following equation with an assumed P-wave velocity.

$$T = V/2f$$

where

T = thickness,
V = P-wave velocity in pavement, and
f = frequency.

For a uniform pavement with no delaminations, the calculated thickness resonance will be relatively uniform. However, when there is delamination, the reverberation will be disrupted and other, lower frequency modes of vibration will occur. This lower frequency will lead to abnormally high calculated thickness values at delamination locations. For a series of IE tests conducted over an area, the calculated thickness can be plotted, and areas where the thickness is unreasonably high (i.e., not expected in the pavement structure) are interpreted as delaminated. Automated equipment has been developed to carry out this test continuously at a slow walking speed. Software to analyze the data is partially automated.

Equipment and Operation

A typical hand-held portable IE device consists of a source and a receiver, and it requires about 15 to 30 s to place the device, conduct the test, and move to the next location. The actual IE measurement occurs in milliseconds. For the purposes of scanning a larger area of pavement, an automated system is preferred. The system consists of an array of rotating sensor wheels, each equipped with impact sources and motion sensors around the perimeter. The purpose of the sensor wheel is to carry out IE tests while the wheel is continuously rolling. Use of multiple sensor wheels spaced transversely across the width of the pavement allows coverage of an area of pavement while traveling at a slow walking speed. The purpose of the wheel array is to collect equally spaced parallel lines of data simultaneously so that coherent areas of delamination can be identified and mapped.

Figure C.1 shows two examples of IE equipment. In those examples, each wheel is approximately 1 ft in diameter, and is mounted with six pairs of a displacement sensor and an impact source. Each sensor/source pair is spaced at 6-in. intervals around the circumference of the wheel. Every two sensor wheels are coupled together with a rubber isolated axle. Data are collected continuously at 6-in. intervals while the system rolls along the surface of the pavement. The data collection for each wheel is independently triggered, and the position of the collected data is obtained by using a distance measuring instrument (DMI) mounted to the vehicle wheel or to an external distance wheel. Table C.1 lists equipment specifications for IE.

Data Output and Display

The field operation and playback software should be capable of the following displays:

- Direct time domain waveforms from each source-receiver pair;

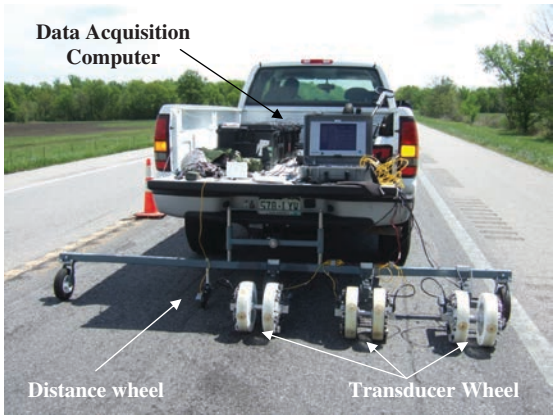

(a)

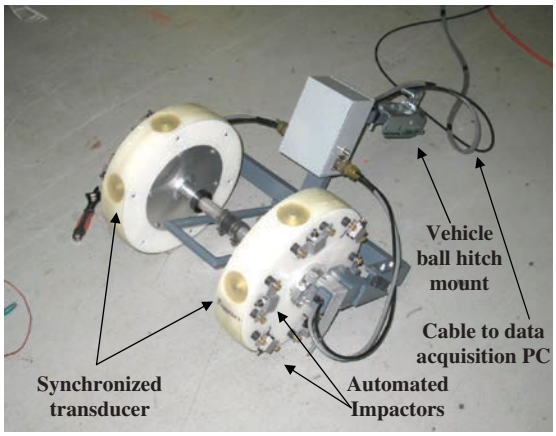

(b)

Figure C.1. Current IE/SASW scanning systems: (a) six-sensor wheel array and (b) two-sensor wheel unit.

- Running amplitude/thickness plot, or equivalent b-scan, for each sensor wheel; and
- Output format should be a two-dimensional (2-D) array of data with thickness as a function of *x* (longitudinal distance) and *y* (transverse offset).

Data Collection Protocol

Because of this system's relatively low collection speed, this system should be used exclusively for project-level evaluation, with a focus on specific locations and areas of concern. The start and end points of data collection should be referenced with mile markers or other fixed reference points. Roadway features encountered during the survey (e.g., intersections, bridge decks) should be annotated with some type of manual markers in the data. The data should be observed visually during collection to ensure that the system is operating properly and that the expected features are appearing in the data.

Table C.1. IE Equipment Specifications

System Type	Array of Six Rotating Sensor Wheels, Lined Up Transverse to the Direction of Travel
Sensor frequency response	Up to 50,000 Hz
Impact source input frequency	Up to 50,000 Hz
Lateral spacing of sensor wheels	2.0 ft (typical)
Lateral coverage per pass	12 ft (full lane width)
Longitudinal data collection rate	One test per foot (minimum)
Travel speed during data collection	1 to 2 mph
Travel speed during mobilization	Posted speed limit
Real time display	Resonant frequency
System monitoring and control	From within or outside survey vehicle
Data collection rate	Based on speed and sensor spacing on sensor wheel
Spatial reference	Vehicle DMI or external distance wheel

Data Analysis

The objective of the analysis is to identify locations where a significant increase in computed thickness is associated with debonding or delamination of an asphalt layer from the layer below. To accomplish this task, the amplitude/thickness plots created at each location are assembled as a 2-D array of data, where *x* and *y* are the coordinates of the test point, and *z* is the resonant thickness value. These thickness values can be contour plotted, and thickness values exceeding a specified threshold can be highlighted as those associated with debonding and delamination. An example of such a plot is shown in Figure C.2.

Equipment Availability and Cost

The IE scanning system discussed in this technical brief is not available commercially. A prototype system has been developed and tested by Olson Engineering. Also, the data interpretation procedures and analysis software are reasonably well developed. An estimated cost of a fully operational system is not available.

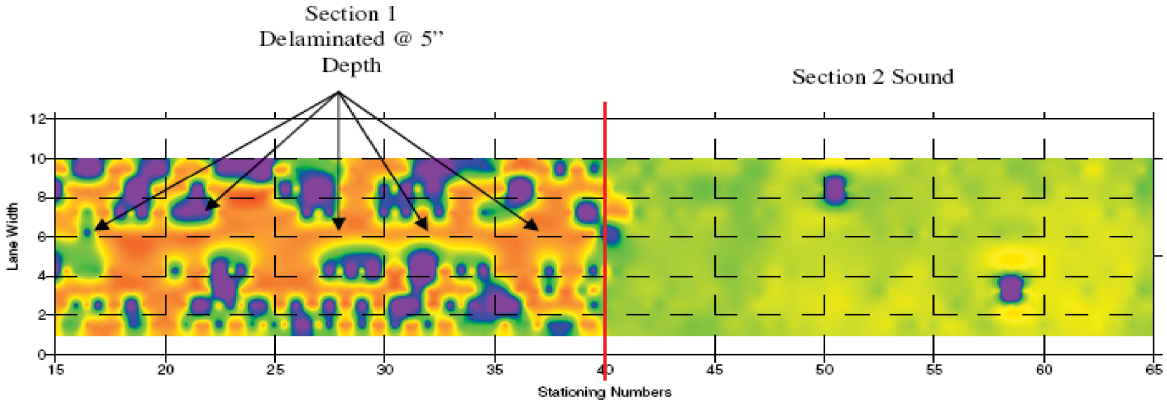

Note: dark blue/cyan areas = anomalously high thicknesses; light green = expected AC thickness.

Figure C.2. Contour plot of resonant thickness.

Advantages and Limitations

The primary advantage of an IE system is its ability to directly detect debonding and delamination within asphalt pavement layers. The principal limitations are temperature and speed. The detection capability is limited to periods of colder temperatures, where the asphalt has a high enough stiffness to generate the reverberations detected by this method. The system can operate only at slow walking speed and its application is thus limited to project-level analysis and diagnostic investigations.

APPENDIX D

List of Topics for Volumes 2 Through 5

This SHRP 2 study generated a sizable amount of documentation that contains more details regarding the findings of evaluations and equipment development. Because of the quantity of detailed documentation on specific topics, these topic-specific documents are contained in Volumes 2, 3, 4, and 5. The topics covered in these volumes are listed below. Some of the topic-specific documents were prepared by groups associated with the study. Authorship of each paper is noted in each chapter in Volumes 2 through 5.

Volume 2: Theoretical Models

- Theoretical Models for Ground-Penetrating Radar
- Theoretical Models for Infrared Thermography Technology
- Theoretical Models for Mechanical Wave Technology—Impact Echo, Impulse Response, and Ultrasonic Surface Waves
- Theoretical Models for Mechanical Wave Technology—Deflection-Based Approach

Volume 3: Controlled Evaluation Reports

- Control Laboratory and Field Evaluations: Construction Report
- Laboratory and Field Evaluation of Ground-Penetrating Radar Systems
- Laboratory and Field Evaluation of Infrared Thermography Systems
- Controlled Evaluation of Mechanical Wave Technologies: Portable Seismic Pavement Analyzer, Scanning Impact Echo, and Multiple Impact Surface Waves
- Ultrasonic Tomography Testing at NCAT Pavement Test Track
- Controlled Evaluation of Lightweight Deflectometer
- Controlled Evaluation of Falling Weight Deflectometer

Volume 4: Uncontrolled Evaluation Reports

- 3d-Radar Report
- Olson Engineering, Inc. Results
- Olson Engineering, Inc., SASW Test Results from Florida Test Section
- Olson Engineering, Inc., SASW Test Results from Kansas Test Section

Volume 5: Field Core Verification

- 3d-Radar Ground-Penetrating Radar Field Testing Results for Locating Cores—Florida
- Florida Cores Analysis
- 3d-Radar Ground-Penetrating Radar Field Testing Results for Locating Cores—Kansas
- Kansas Cores Analysis

Related SHRP 2 Research

Nondestructive Testing to Identify Concrete Bridge Deck Deterioration (R06A)

Evaluating Applications of Field Spectroscopy Devices to Fingerprint Commonly Used Construction Materials (R06B)

Using Infrared and High-Speed Ground-Penetrating Radar for Uniformity Measurements on New HMA Layers (R06C)

Real-Time Smoothness Measurements on Portland Cement Concrete Pavements During Construction (R06E)

Assessment of Continuous Pavement Deflection Measuring Technologies (R06F)

High-Speed Nondestructive Testing Methods for Mapping Voids, Debonding, Delaminations, Moisture, and Other Defects Behind or Within Tunnel Linings (R06G)